ISSN 1007-9327 (print)
ISSN 2219-2840 (online)

World Journal of *Gastroenterology*

World J Gastroenterol 2022 November 14; 28(42): 6002-6077

Published by Baishideng Publishing Group Inc

World Journal of Gastroenterology

Contents

Weekly Volume 28 Number 42 November 14, 2022

REVIEW

MINIREVIEWS

ORIGINAL ARTICLE

Retrospective Cohort Study

Retrospective Study

Clinical Trials Study

ABOUT COVER

Editorial Board of *World Journal of Gastroenterology*, Andrada Seicean, MD, PhD, Professor, Regional Institute of Gastroenterology and Hepatology, University of Medicine and Pharmacy, 19-21 Croitorilor Street, Cluj-Napoca 400192, Romania. andrada.seicean@umfcluj.ro

AIMS AND SCOPE

The primary aim of *World Journal of Gastroenterology* (*WJG*, *World J Gastroenterol*) is to provide scholars and readers from various fields of gastroenterology and hepatology with a platform to publish high-quality basic and clinical research articles and communicate their research findings online. *WJG* mainly publishes articles reporting research results and findings obtained in the field of gastroenterology and hepatology and covering a wide range of topics including gastroenterology, hepatology, gastrointestinal endoscopy, gastrointestinal surgery, gastrointestinal oncology, and pediatric gastroenterology.

INDEXING/ABSTRACTING

The *WJG* is now abstracted and indexed in Science Citation Index Expanded (SCIE, also known as SciSearch®), Current Contents/Clinical Medicine, Journal Citation Reports, Index Medicus, MEDLINE, PubMed, PubMed Central, Scopus, Reference Citation Analysis, China National Knowledge Infrastructure, China Science and Technology Journal Database, and Superstar Journals Database. The 2022 edition of Journal Citation Reports® cites the 2021 impact factor (IF) for *WJG* as 5.374; IF without journal self cites: 5.187; 5-year IF: 5.715; Journal Citation Indicator: 0.84; Ranking: 31 among 93 journals in gastroenterology and hepatology; and Quartile category: Q2. The *WJG*'s CiteScore for 2021 is 8.1 and Scopus CiteScore rank 2021: Gastroenterology is 18/149.

RESPONSIBLE EDITORS FOR THIS ISSUE

Production Editor: *Hua-Ge Yu*; **Production Department Director:** *Xu Guo*; **Editorial Office Director:** *Jia-Ru Fan*.

NAME OF JOURNAL
World Journal of Gastroenterology

ISSN
ISSN 1007-9327 (print) ISSN 2219-2840 (online)

LAUNCH DATE
October 1, 1995

FREQUENCY
Weekly

EDITORS-IN-CHIEF
Andrzej S Tarnawski

EDITORIAL BOARD MEMBERS
http://www.wjgnet.com/1007-9327/editorialboard.htm

PUBLICATION DATE
November 14, 2022

INSTRUCTIONS TO AUTHORS
https://www.wjgnet.com/bpg/gerinfo/204

GUIDELINES FOR ETHICS DOCUMENTS
https://www.wjgnet.com/bpg/GerInfo/287

GUIDELINES FOR NON-NATIVE SPEAKERS OF ENGLISH
https://www.wjgnet.com/bpg/gerinfo/240

PUBLICATION ETHICS
https://www.wjgnet.com/bpg/GerInfo/288

PUBLICATION MISCONDUCT
https://www.wjgnet.com/bpg/gerinfo/208

ARTICLE PROCESSING CHARGE
https://www.wjgnet.com/bpg/gerinfo/242

STEPS FOR SUBMITTING MANUSCRIPTS
https://www.wjgnet.com/bpg/GerInfo/239

ONLINE SUBMISSION
https://www.f6publishing.com

World Journal of Gastroenterology

Submit a Manuscript: https://www.f6publishing.com

World J Gastroenterol 2022 November 14; 28(42): 6002-6016

DOI: 10.3748/wjg.v28.i42.6002

ISSN 1007-9327 (print) ISSN 2219-2840 (online)

REVIEW

Role of radiomics in the diagnosis and treatment of gastrointestinal cancer

Qi Mao, Mao-Ting Zhou, Zhang-Ping Zhao, Ning Liu, Lin Yang, Xiao-Ming Zhang

Specialty type: Radiology, nuclear medicine and medical imaging

Provenance and peer review: Invited article; Externally peer reviewed.

Peer-review model: Single blind

Peer-review report's scientific quality classification

Grade A (Excellent): 0
Grade B (Very good): B
Grade C (Good): C
Grade D (Fair): 0
Grade E (Poor): 0

P-Reviewer: Cannella R, Italy; Stabellini N, United States

Received: August 25, 2022
Peer-review started: August 25, 2022
First decision: September 2, 2022
Revised: September 24, 2022
Accepted: October 27, 2022
Article in press: October 27, 2022
Published online: November 14, 2022

Qi Mao, Mao-Ting Zhou, Ning Liu, Lin Yang, Xiao-Ming Zhang, Department of Radiology, Affiliated Hospital of North Sichuan Medical College, Nanchong 637000, Sichuan Province, China

Zhang-Ping Zhao, Department of Radiology, Panzhihua Central Hospital, Panzhihua 617000, Sichuan Province, China

Corresponding author: Lin Yang, MD, Professor, Department of Radiology, Affiliated Hospital of North Sichuan Medical College, No. 63 Wenhua Road, Nanchong 637000, Sichuan Province, China. linyangmd@163.com

Abstract

Gastrointestinal cancer (GIC) has high morbidity and mortality as one of the main causes of cancer death. Preoperative risk stratification is critical to guide patient management, but traditional imaging studies have difficulty predicting its biological behavior. The emerging field of radiomics allows the conversion of potential pathophysiological information in existing medical images that cannot be visually recognized into high-dimensional quantitative image features. Tumor lesion characterization, therapeutic response evaluation, and survival prediction can be achieved by analyzing the relationships between these features and clinical and genetic data. In recent years, the clinical application of radiomics to GIC has increased dramatically. In this editorial, we describe the latest progress in the application of radiomics to GIC and discuss the value of its potential clinical applications, as well as its limitations and future directions.

Key Words: Gastrointestinal cancer; Diagnosis; Treatment; Radiomics; Therapeutic response; Hepatocellular carcinoma

Core Tip: In this editorial, we summarize the latest advances of radiomics in the field of gastrointestinal cancer diagnosis and treatment. Radiomics has great potential in precision treatment decision-making for gastrointestinal cancer. However, radiomics studies have had relatively marked heterogeneity in their workflow. In the future, it will be necessary to establish and promote an imaging data acquisition protocol, standardize the research workflow, and conduct multicenter prospective studies on quality control.

Citation: Mao Q, Zhou MT, Zhao ZP, Liu N, Yang L, Zhang XM. Role of radiomics in the diagnosis and treatment of gastrointestinal cancer. *World J Gastroenterol* 2022; 28(42): 6002-6016
URL: https://www.wjgnet.com/1007-9327/full/v28/i42/6002.htm
DOI: https://dx.doi.org/10.3748/wjg.v28.i42.6002

INTRODUCTION

Gastrointestinal cancer (GIC) has high morbidity and mortality rates[1]. It causes approximately 5000000 new cases and 3540000 deaths worldwide each year, making it one of the main causes of cancer death[1]. Because of the high heterogeneity of these tumors, it is difficult to implement precision treatment[2]. Lambin *et al*[3] proposed the concept of radiomics in 2012. The emerging field of radiomics can convert potential pathophysiological information in existing medical images that cannot be recognized by the human eye into high-dimensional quantitative image features[2-4]. By analyzing the relationships between these features and clinical and genetic data, we can characterize tumor lesions, evaluate therapeutic responses, and predict survival. In recent years, research on the application of radiomics to GIC has grown dramatically. With this editorial, we aim to describe the latest advances of radiomics in the assessment of GIC and to explore the value of its potential clinical applications, its limitations, and its future directions.

RADIOMICS WORKFLOW

Imaging modalities that can be used for radiomics analysis include computed tomography (CT), magnetic resonance imaging (MRI), and positron-emission tomography (PET). Since CT is the most commonly used staging method for esophageal cancer (EC) and gastric cancer (GC), most radiomics studies on EC and GC are based on CT images[5-9]. In contrast, as MRI is widely used for colorectal cancer (CRC) staging, most radiomics studies on CRC are based on MRI features[10-13].

The workflow of radiomics usually includes image acquisition, lesion segmentation, feature extraction and selection, model building, and validation[14]. Lesion segmentation and feature extraction are the most essential steps. Manual, automatic, and semiautomatic segmentation methods are often used to segment the region of interest (ROI) or volume OI (VOI) (2D or 3D) in a target lesion, and manual segmentation is the most commonly used method (gold standard)[15]. After lesion segmentation, hundreds of radiomic features (shape, first-order, second-order, and higher-order radiomic features) can be extracted from the acquired image. Using all radiomic features to analyze an image will lead to overfitting; thus, feature selection is performed to reduce the number of features that are redundant and irrelevant. The best radiomic features can be selected by dimensionality reduction to improve model efficiency. After feature selection, a radiomics model must be generated. Most published studies use machine learning (ML) and deep learning (DL) methods to build classification and prediction models. Finally, the radiomics model can be validated in internal and external cohorts such that the model can be further optimized and the prediction performance can be maximized. The receiver operating characteristic (ROC) curve is the most commonly used method to evaluate model performance (Figure 1).

EC

Published studies have mainly investigated the predictive ability of radiomics in the staging, therapy response, and postoperative recurrence of EC[16-19].

Radiomic characteristics based on CT have good predictive potential for EC staging[20,21]. Yang *et al*[19] reported that CT radiomic characteristics were significantly correlated with the tumor (T) stage and tumor length of EC and showed good predictive performance for both; the area under the ROC curve (AUC), sensitivity, and specificitywere 0.86, 0.77 and 0.87, respectively, and 0.95, 0.92 and 0.91. Radiomic features also have good efficacy in predicting EC lymphatic metastasis[7,22-24]. Liu *et al*[20] suggested that baseline CT texture is a biomarker for the preoperative assessment of T, lymph node (N), and overall staging of esophageal squamous cell carcinoma (ESCC). Wu *et al*[25] established a model based on the radiomic characteristics of the late arterial phase of CT, which well distinguished early (I-

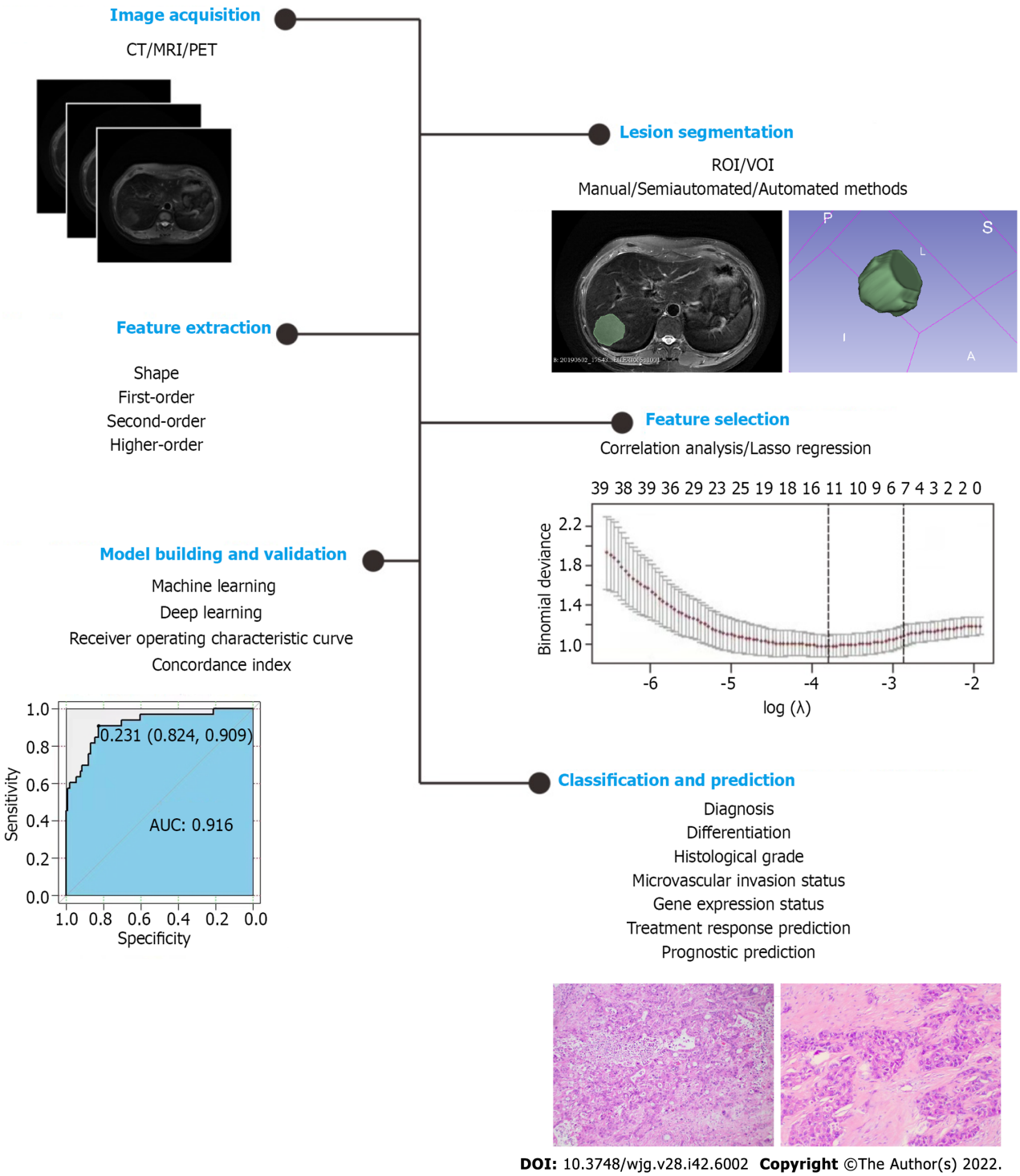

DOI: 10.3748/wjg.v28.i42.6002

Figure 1 The framework of the proposed liver lesion classification. ROI: Region of interest; VOI: Volume of interest.

II) and late (III-IV) ESCC, and the model's efficacy was better than that of tumor volume.

Locally advanced EC often requires neoadjuvant chemoradiotherapy (NACRT)[26], whose treatment outcome is associated with tumor heterogeneity[27,28]. Radiomics can extract tumor heterogeneity data and has good application potential in improving the treatment stratification of patients. Radiomic characteristics are helpful for evaluating the response of EC to NAC or NACRT, distinguishing responders from nonresponders, for which it performs better than traditional parameters[29-32]. A prospective multicenter study[33] developed and validated a three-dimensional DL model applied to preprocessed CT images to predict the response of patients with locally advanced thoracic esophageal squamous cell carcinoma (TESCC) to concurrent chemoradiotherapy. The three-dimensional DL model achieved good predictive performance, with an AUC in the training cohort of 0.897 [95% confidence interval (CI): 0.840-0.959] and an AUC in the validation cohort of 0.833 (95%CI: 0.654-1.000). It is also feasible to use radiomics to predict the pathological complete response (pCR) of EC[34,35]. Patients with

a pCR after NACRT have a higher overall survival (OS) rate[36,37], but nonresponders will not benefit from this therapy[38]. This information can provide guidance for personalized treatment of EC patients [28]. A CT-based radiomics study showed that a model that combined the intratumoral and peritumoral radiological characteristics could improve the predictive performance of the pCR of EC NACRT. In the test set, the AUC was 0.852 (95%CI: 0.753-0.951), the accuracy was 84.3%, the sensitivity was 90.3%, and the specificity was 79.5%[35]. Several studies of radiomics based on MRI or ^{18}F-fluorodeoxyglucose (^{18}F-FDG) PET also showed its efficacy in predicting the response to EC treatment[39-42]. The application of radiomics to immunotherapy has also achieved good response prediction value[43].

Radiomics has also made progress in predicting the recurrence and prognosis of EC patients[44-47]. Tang *et al*[48] predicted the early recurrence of locally advanced ESCC after trimodal therapy based on enhanced CT radiomics. The results showed that in the training cohort, the AUCs of the radiomics model, the clinical model, and the combined model were 0.754, 0.679, and 0.821, respectively, and they were 0.646, 0.658, and 0.809 in the validation cohort; the combined model was the best. Qiu *et al*[49] developed and validated a prediction model based on radiomic features extracted from contrast-enhanced CT images to estimate the recurrence-free survival (RFS) of patients who achieved pCR through NACRT and surgery. The results showed that the radiomic characteristics were significantly correlated with RFS. In the training cohort and the validation cohort, compared with the nomograms of the radiomic characteristics and of clinical risk factors, the nomogram combining the radiomic characteristics and clinical risk factors had optimal performance. Other studies have shown that combining the radiomic characteristics of primary tumors and regional lymph nodes with clinical-pathological factors can improve OS prediction[50].

Other studies showed that CT-based radiomics features also had good predictive performance for classifying patients according to histological differentiation[51-53], the expression of programmed death-ligand 1, and CD8$^+$ tumor-infiltrating lymphocytes of EC[5].

GC

In recent years, some researchers have also explored the value of radiomics to the diagnosis and treatment of GC[9,54,55]. The CT radiomics model has high application value in the identification of GC [54,56-58]. Feng *et al*[59] used a transfer learning radiomics nomogram (TLRN) with whole-slide images of GC as the source domain data to distinguish Borrmann type IV GC from primary gastric lymphoma before surgery. The TLRN that integrated transfer learning radiomics signatures (TLRS), clinical factors, and CT subjective findings was developed through multiple logistic regression (LR). The results showed that the TLRN performed better than the clinical model and the TLRS. The AUCs of the internal and two external validation cohorts were 0.958 (95%CI: 0.883-0.991), 0.867 (95%CI: 0.794-0.922), and 0.921 (95%CI: 0.860-0.960), respectively[59]. Wang *et al*[60] reported that a DL radiomics model based on CT images had a potential role in the T staging of GC. For distinguishing T2 from T3/4 tumors, the AUCs of the arterial phase-based radiomics model in the training group and the test group were 0.899 (95%CI: 0.812-0.955) and 0.825 (95%CI: 0.718-0.904), respectively. The AUC of the radiomics model based on the portal vein phase in the training and testing cohorts was 0.843 (95%CI: 0.746-0.914) and 0.818 (95%CI: 0.711-0.899), respectively[60]. An important factor in the failure of GC treatment is lymph node metastasis (LNM) and cancer spread in the peritoneal cavity[61]. In GC, the most common metastatic sites are the distant lymph nodes (56%), liver (53%), and peritoneum (51%)[62]. Accurate assessment of LNM and preoperative N staging is critical for the accurate treatment of GC patients. Most studies have shown that CT-based radiomics models have good accuracy in predicting early GC lymph node and peritoneal metastasis before surgery[63-66]. A ML model based on preoperative ^{18}F-FDG-PET/CT obtained similarly good results[67].

CT-based radiomic characteristics also perform well in predicting the response to NAC and radiotherapy in patients with advanced GC[68-71]. Jiang *et al*[72] showed that a DL CT signature could help to identify patients who might benefit from adjuvant chemotherapy for GC and improve prognostic prediction. A radiomics study based on ^{18}F-FDG-PET signatures obtained similar results[73]. In addition, radiomics can be used to predict the histological grade of GC before surgery[74] and is useful for GC classification[75,76].

CRC

The application of radiomics to CRC has mainly focused on the evaluation of stage, neoadjuvant therapy outcome, and gene mutations[77,78].

Radiomics models are helpful for CRC staging[79-81]. LNM is an independent risk factor affecting the prognosis of CRC patients. Radiomics models can effectively predict LNM in CRC patients before surgery[82-85]. Liu *et al*[84] found that multiregional-based MRI radiomics combined with clinical data could improve the efficacy of predicting LNM. He *et al*[85] developed and tested five ML models based on the radiomic features of F-18-FDG-PET/CT and PET for their preoperative prediction of LNM in the CRC region: LR, support vector machine, random forest (RF), neural network, and extreme gradient boosting. The results showed that the LR (AUC 0.866, 95%CI: 0.808-0.925) and extreme gradient boosting models (AUC 0.903, 95%CI: 0.855-0.951) performed the best, outperforming F-18-FDG-PET/CT on both the training set and the test set[85]. Other studies have also shown that radiomics has a good ability to predict metastasis to distant organs, such as the liver and lung, as well as vascular and

perineural invasion[86,87]. It is reported that the predictive power of CT-based radiomics for the preoperative staging of CRC. The results showed that the radiomic features were an independent predictor of CRC staging. CRC was successfully divided into stages I-II and III-IV in the training and validation datasets. The AUC in the training dataset was 0.792 (95%CI: 0.741-0.853), the sensitivity was 0.629, and the specificity was 0.874. The AUC in the validation dataset was 0.708 (95%CI: 0.698-0.718), the sensitivity was 0.611, and the specificity was 0.680[79].

Radiomics models have had excellent performance in noninvasively predicting the response to NAC and NACRT in patients with locally advanced CRC (including liver metastasis)[88-91]. They have also achieved good efficacy in predicting the response to CRC targeted therapy[77,92].

Mutations in the *KRAS*, *NRAS*, or *BRAF* gene indicate that CRC patients will lack a response to drugs targeting epidermal growth factor receptor. In 2016, the National Comprehensive Cancer Network guidelines recommended that all patients with suspected or confirmed metastatic CRC should be tested for *KRAS*/*NRAS*/*BRAF* mutations, but this requires pathological tissue specimens. It is gratifying that some radiogenomics studies have shown that the radiomic characteristics of CT and MRI may help to predict the genotype of CRC tumors before surgery[93-95]. Yang *et al*[96] reported that CT radiomic characteristics were associated with *KRAS*/*NRAS*/*BRAF* mutations. Another MRI radiomics study found a good correlation between quantitative features and gene mutations, while there was no correlation between qualitative features and gene mutations[97].

More recent studies have shown that radiomics can predict CRC histological grade before surgery[98,99].

LIVER CANCER

The application of radiomics to hepatocellular carcinoma (HCC) involves differential diagnosis, determination of microvascular invasion (MVI) status, histological grade, gene expression status, and treatment response, and prognostic prediction[100-104].

Because HCC has a typical enhancement mode, dynamic contrast-enhanced CT, MRI, and ultrasound have played major roles in the diagnosis and differentiation of HCC[105-107]. However, it is sometimes difficult to distinguish some small nodules from atypical lesions[108-111]. Radiomics can achieve quantitative analysis of tumor biological behavior and heterogeneity, helping identify liver nodules[112-114]. Yasaka *et al*[115] investigated the performance of a DL method to distinguish liver masses on dynamic enhanced CT. There are five types of these masses: Type A, classic HCC; type B, malignant liver tumors other than HCC; type C, indeterminate masses or mass-like lesions, plus rare benign liver masses other than hemangiomas and cysts; type D, hemangiomas; type E, cysts. The median accuracy of the mass identification on the test set was 0.84. The AUC that distinguished the types A-B from types C-E was 0.92. Hamm *et al*[116] used a DL method to classify common liver lesions with typical imaging characteristics on multiphasic MRI, including a total of 494 liver lesions from six categories, which were divided into training (n = 434) and test groups (n = 60). Their DL system had an accuracy of 92%, a sensitivity of 92%, and a specificity of 98%. For HCC classification, the true-positive rate and false-positive rate were 93.5% and 1.6%, respectively, and the AUC was 0.992[116]. Other studies have reached similar conclusions[108,110].

The 5-year recurrence rate of HCC resection can reach 70%[103]. Pathological features such as histological grade and MVI of HCC were significantly correlated with postoperative recurrence and prognosis[117-120]. Histological grade, MVI status[121-125], and gene expression[113,126,127] in HCC can be successfully predicted by radiomics models before surgery. An MRI-based radiomics study showed that the AUCs of the MVI nomogram in the validation cohort using the RF algorithm and LR analysis were 0.920 (95%CI: 0.861-0.979) and 0.879 (95%CI: 0.820-0.938), respectively[123].

Radiomics models based on contrast-enhanced CT and MRI can predict the response of middle- and late-stage HCC to local treatment and systemic treatment[10,128-130]and the early recurrence and the prognosis after HCC resection[101,102,131,132]. Zhang *et al*[133] evaluated the effectiveness of predicting OS after HCC resection based on contrast-enhanced MR imaging features. The results showed that preoperative clinical features and semantic imaging features were significantly correlated with the survival rate; the combined model had the best predictive performance[133].

Some studies using radiomics to predict the occurrence of CRC liver metastases are particularly interesting[134-137]. Rao *et al*[137] retrospectively analyzed the primary staging CT data of 29 CRC patients. The patients were divided into three groups: The non-liver-metastasis group, the simultaneous liver metastasis (LM) group, and the metachronous LM group within 18 mo. Whole-liver texture analysis was performed on the liver parenchyma that was clearly disease-free on the portal vein image. The results showed that compared with those in nonmetastatic patients, the mean entropy 1.5 (E1.5)and E2.5 values of the whole liver in patients with synchronous metastasis were significantly increased, and the uniformity 1.5 (U1.5)and U2.5 values were significantly decreased. The AUCs for the diagnosis of synchronous metastasis based on E1.5, E2.5, U1.5, and U2.5 were 0.73-0.78[137]. Beckers *et al*[138] conducted a similar retrospective multicenter study. They included a total of 165 cases of CRC, which were also divided into the nonmetastasis group, the synchronous metastasis group, and the metastasis

group (within 24 mo). Univariate analysis confirmed that U, sex, tumor site, nodal stage, and carcinoembryonic antigen (CEA) were potential predictive factors; multivariate analysis showed that U was still a factor predicting early metastasis; and none of the parameters could predict intermediate/late metastasis[138]. Other studies have shown no significant difference in CT texture parameters of liver parenchyma between CRC patients with and without liver metastasis[134,135]. The conclusions of these studies are inconsistent, so the prediction of LM of CRC based on the texture characteristics of the liver parenchyma requires further study. Recently, Liet al[139] investigated the efficacy of a radiomics model based on baseline CRC contrast-enhanced CT in predicting metachronous liver metastases in CRC patients. The AUC of the radiomics feature model was 0.78 ± 0.07, and the AUC of the clinical feature model was 0.79 ± 0.08. The model combining the two performed best, with AUCs of 0.79 ± 0.08 and 0.72 ± 0.07 in the internal and external validation cohorts, respectively. They believed that the radiomic characteristics of primary CRC lesions are often affected by fewer factors and are more stable; their radiomic characteristics have the potential to distinguish patients at risk of liver metastasis.

PANCREATIC CANCER (PC)

For PC, the application of radiomics mainly focuses on identification, treatment response prediction, and prognostic prediction[140-142]. Many studies have focused on the diagnosis and differentiation of pancreatic ductal adenocarcinoma (PDAC)[143-146]. Chu *et al*[146] investigated the utility of CT radiomics in distinguishing PDAC from normal pancreas. In their retrospective casecontrol study, 190 PDAC patients and 190 healthy potential renal donors were included. The overall accuracy of RF binary classification was 99.2%, with an AUC of 99.9%; all PDAC cases were correctly classified. Park *et al*[145] confirmed that CT-based ML of radiomics features was helpful to distinguish between autoimmune pancreatitis and PDAC, with an overall accuracy of 95.2%. The radiomics model based on PET/CT also showed good performance in distinguishing benign autoimmune pancreatitis from malignant PDAC lesions[143,144].

Other studies have shown that radiomics can better predict the treatment response and prognosis of PC[142,147]. Simpson *et al*[141] evaluated the potential of MRI-based radiomics to predict the response to PC treatment. A total of 20 patients with unresected nonmetastatic PDAC were enrolled, all of whom received NAC followed by five rounds of MR-guided stereotactic body radiotherapy. Half of the 20 patients were defined as having histopathological tumor regression or tumor response based on an enhanced CT. The AUC of the model based on the RF algorithm was 0.81 (95%CI: 0.594-1.000); the adaptive least absolute shrinkage and selection operator (LASSO) algorithm achieved AUC of 0.81 (95%CI: 0.596-1.000). Xie *et al*[148] used a CT-based radiomics nomogram to predict the survival of patients with resected PDAC. The radiomics score developed based on CT imaging features was significantly correlated with disease-free survival (DFS) and OS in patients with PDAC. The radiomics nomogram showed good discrimination in both the training cohort and the validation cohort, being superior to the clinical model and the TNM staging system for survival estimation. The model integrating the radiomics score and clinical data had the best predictive performance, but there was no correlation between the radiomics score and recurrence pattern. Similar results were seen by Healy *et al*[149].

LIMITATIONS AND FUTURE DIRECTIONS

In this editorial, we summarize the results of the application of radiomics to the field of GIC diagnosis and treatment. These results show that radiomics has great potential for decision-making about precision treatments for GIC. Moreover, these results have important reference value for studies of other systemic tumors.

However, some limitations to the clinical application of radiomics remain[150,151]. The first key challenge is the use of different imaging techniques by different institutions and/or scanners. To ensure that the academic community can obtain high-quality radiological data resources, it is necessary to establish and promote certain imaging acquisition protocols[149]. Second, the current research uses different software and different feature selection methods, focuses on different feature sets, and applies different statistical and bioinformatic methods for data analysis and interpretation, which limit the reproducibility of radiomics models[152,153]. Future research workflows need to be standardized. Third, many relevant radiomics studies employ single-center retrospective datasets. A quality-controlled multicenter prospective study plan is ideal. In addition, the evidence level rating reflects the feasibility of incorporating radiomics research into clinical practice. Recently published guidelines and checklists aiming to improve the quality of radiomics studies, including the radiomics quality score, modified Quality Assessment of Diagnostic Accuracy Studies tool, image biomarker standardization initiativeguideline, and Transparent Reporting of a multivariable prediction model for Individual Prognosis or Diagnosis checklist, have been applied to radiomics evaluations[154-157]. These studies have shown that the current scientific and reporting quality of many radiomics studies is insufficient;

feature reproducibility, open science categories, and clinical utility analyses need to be improved; and study objectives, blinding, sample sizes, and missing data must be reported[154-157]. In the future, radiomics studies should adhere to these guidelines to facilitate the translation of radiomics research into clinical practice[156].

CONCLUSION

Radiomics has great potential in precision treatment decision-making for gastrointestinal cancer. However, radiomics studies have had relatively marked heterogeneity in their workflow. In the future, it will be necessary to establish and promote an imaging data acquisition protocol, standardize the research workflow, and conduct multicenter prospective studies on quality control. In addition, the combination of radiomics with multiomics may lead to a major breakthrough in individualized medical treatment of tumors.

ACKNOWLEDGEMENTS

We thank MrTang Zhi and Miss Tao Yun-Yun for their contributions to graph creation.

FOOTNOTES

Author contributions: Mao Q, Zhou MT, Zhao ZP, Liu N, Yang L, and Zhang XM contributed to this paper; Yang L and Zhang XM designed the overall concept and outline of the manuscript; Mao Q, Zhou MT, Zhao ZP, Liu N, and Yang L contributed to the writing and editing of the manuscript and reviewed the literature.

Supported by the Project of the Medical Association of Sichuan Province, No. S20070; and Project of the City-University Science and Technology Strategic Cooperation of Nanchong City, No. 20SXQT0324.

Conflict-of-interest statement: The authors declare no conflicts of interest.

Country/Territory of origin: China

ORCID number: Qi Mao 0000-0003-1301-069X; Mao-Ting Zhou 0000-0003-2034-2086; Zhang-Ping Zhao 0000-0001-7150-161X; Ning Liu 0000-0003-3587-5440; Lin Yang 0000-0001-8746-9255; Xiao-Ming Zhang 0000-0001-5327-8506.

Corresponding Author's Membership in Professional Societies: A member of the editorial board or peer reviewer of a BPG journal, 02832130.

S-Editor: Chen YL
L-Editor: A
P-Editor: Chen YL

REFERENCES

1 **Sung H**, Ferlay J, Siegel RL, Laversanne M, Soerjomataram I, Jemal A, Bray F. Global Cancer Statistics 2020: GLOBOCAN Estimates of Incidence and Mortality Worldwide for 36 Cancers in 185 Countries. *CA Cancer J Clin* 2021; **71**: 209-249 [PMID: 33538338 DOI: 10.3322/caac.21660]
2 **Sexton RE**, Al Hallak MN, Diab M, Azmi AS. Gastric cancer: a comprehensive review of current and future treatment strategies. *Cancer Metastasis Rev* 2020; **39**: 1179-1203 [PMID: 32894370 DOI: 10.1007/s10555-020-09925-3]
3 **Lambin P**, Rios-Velazquez E, Leijenaar R, Carvalho S, van Stiphout RG, Granton P, Zegers CM, Gillies R, Boellard R, Dekker A, Aerts HJ. Radiomics: extracting more information from medical images using advanced feature analysis. *Eur J Cancer* 2012; **48**: 441-446 [PMID: 22257792 DOI: 10.1016/j.ejca.2011.11.036]
4 **Aerts HJ**, Velazquez ER, Leijenaar RT, Parmar C, Grossmann P, Carvalho S, Bussink J, Monshouwer R, Haibe-Kains B, Rietveld D, Hoebers F, Rietbergen MM, Leemans CR, Dekker A, Quackenbush J, Gillies RJ, Lambin P. Decoding tumour phenotype by noninvasive imaging using a quantitative radiomics approach. *Nat Commun* 2014; **5**: 4006 [PMID: 24892406 DOI: 10.1038/ncomms5006]

5 **Wen Q**, Yang Z, Zhu J, Qiu Q, Dai H, Feng A, Xing L. Pretreatment CT-Based Radiomics Signature as a Potential Imaging Biomarker for Predicting the Expression of PD-L1 and CD8+TILs in ESCC. *Onco Targets Ther* 2020; **13**: 12003-12013 [PMID: 33244242 DOI: 10.2147/OTT.S261068]

6 **Gong J**, Zhang W, Huang W, Liao Y, Yin Y, Shi M, Qin W, Zhao L. CT-based radiomics nomogram may predict local recurrence-free survival in esophageal cancer patients receiving definitive chemoradiation or radiotherapy: A multicenter study. *Radiother Oncol* 2022; **174**: 8-15 [PMID: 35750106 DOI: 10.1016/j.radonc.2022.06.010]

7 **Wu L**, Yang X, Cao W, Zhao K, Li W, Ye W, Chen X, Zhou Z, Liu Z, Liang C. Multiple Level CT Radiomics Features Preoperatively Predict Lymph Node Metastasis in Esophageal Cancer: A Multicentre Retrospective Study. *Front Oncol* 2019; **9**: 1548 [PMID: 32039021 DOI: 10.3389/fonc.2019.01548]

8 **Rishi A**, Zhang GG, Yuan Z, Sim AJ, Song EY, Moros EG, Tomaszewski MR, Latifi K, Pimiento JM, Fontaine JP, Mehta R, Harrison LB, Hoffe SE, Frakes JM. Pretreatment CT and ^{18}F-FDG PET-based radiomic model predicting pathological complete response and loco-regional control following neoadjuvant chemoradiation in oesophageal cancer. *J Med Imaging Radiat Oncol* 2021; **65**: 102-111 [PMID: 33258556 DOI: 10.1111/1754-9485.13128]

9 **Chen Q**, Zhang L, Liu S, You J, Chen L, Jin Z, Zhang S, Zhang B. Radiomics in precision medicine for gastric cancer: opportunities and challenges. *Eur Radiol* 2022; **32**: 5852-5868 [PMID: 35316364 DOI: 10.1007/s00330-022-08704-8]

10 **Chen BY**, Xie H, Li Y, Jiang XH, Xiong L, Tang XF, Lin XF, Li L, Cai PQ. MRI-Based Radiomics Features to Predict Treatment Response to Neoadjuvant Chemotherapy in Locally Advanced Rectal Cancer: A Single Center, Prospective Study. *Front Oncol* 2022; **12**: 801743 [PMID: 35646677 DOI: 10.3389/fonc.2022.801743]

11 **Mbanu P**, Saunders MP, Mistry H, Mercer J, Malcomson L, Yousif S, Price G, Kochhar R, Renehan AG, van Herk M, Osorio EV. Clinical and radiomics prediction of complete response in rectal cancer pre-chemoradiotherapy. *Phys Imaging Radiat Oncol* 2022; **23**: 48-53 [PMID: 35800297 DOI: 10.1016/j.phro.2022.06.010]

12 **Kekelidze M**, D'Errico L, Pansini M, Tyndall A, Hohmann J. Colorectal cancer: current imaging methods and future perspectives for the diagnosis, staging and therapeutic response evaluation. *World J Gastroenterol* 2013; **19**: 8502-8514 [PMID: 24379567 DOI: 10.3748/wjg.v19.i46.8502]

13 **Qin Y**, Zhu LH, Zhao W, Wang JJ, Wang H. Review of Radiomics- and Dosiomics-based Predicting Models for Rectal Cancer. *Front Oncol* 2022; **12**: 913683 [PMID: 36016617 DOI: 10.3389/fonc.2022.913683]

14 **Miranda Magalhaes Santos JM**, Clemente Oliveira B, Araujo-Filho JAB, Assuncao-Jr AN, de M Machado FA, Carlos Tavares Rocha C, Horvat JV, Menezes MR, Horvat N. State-of-the-art in radiomics of hepatocellular carcinoma: a review of basic principles, applications, and limitations. *Abdom Radiol (NY)* 2020; **45**: 342-353 [PMID: 31707435 DOI: 10.1007/s00261-019-02299-3]

15 **Polan DF**, Brady SL, Kaufman RA. Tissue segmentation of computed tomography images using a Random Forest algorithm: a feasibility study. *Phys Med Biol* 2016; **61**: 6553-6569 [PMID: 27530679 DOI: 10.1088/0031-9155/61/17/6553]

16 **Xie C**, Yang P, Zhang X, Xu L, Wang X, Li X, Zhang L, Xie R, Yang L, Jing Z, Zhang H, Ding L, Kuang Y, Niu T, Wu S. Sub-region based radiomics analysis for survival prediction in oesophageal tumours treated by definitive concurrent chemoradiotherapy. *EBioMedicine* 2019; **44**: 289-297 [PMID: 31129097 DOI: 10.1016/j.ebiom.2019.05.023]

17 **Shi Z**, Zhang Z, Liu Z, Zhao L, Ye Z, Dekker A, Wee L. Methodological quality of machine learning-based quantitative imaging analysis studies in esophageal cancer: a systematic review of clinical outcome prediction after concurrent chemoradiotherapy. *Eur J Nucl Med Mol Imaging* 2022; **49**: 2462-2481 [PMID: 34939174 DOI: 10.1007/s00259-021-05658-9]

18 **Peng H**, Yang Q, Xue T, Chen Q, Li M, Duan S, Cai B, Feng F. Computed tomography-based radiomics analysis to predict lymphovascular invasion in esophageal squamous cell carcinoma. *Br J Radiol* 2022; **95**: 20210918 [PMID: 34908477 DOI: 10.1259/bjr.20210918]

19 **Yang M**, Hu P, Li M, Ding R, Wang Y, Pan S, Kang M, Kong W, Du D, Wang F. Computed Tomography-Based Radiomics in Predicting T Stage and Length of Esophageal Squamous Cell Carcinoma. *Front Oncol* 2021; **11**: 722961 [PMID: 34722265 DOI: 10.3389/fonc.2021.722961]

20 **Liu S**, Zheng H, Pan X, Chen L, Shi M, Guan Y, Ge Y, He J, Zhou Z. Texture analysis of CT imaging for assessment of esophageal squamous cancer aggressiveness. *J Thorac Dis* 2017; **9**: 4724-4732 [PMID: 29268543 DOI: 10.21037/jtd.2017.06.46]

21 **Kawahara D**, Murakami Y, Tani S, Nagata Y. A prediction model for degree of differentiation for resectable locally advanced esophageal squamous cell carcinoma based on CT images using radiomics and machine-learning. *Br J Radiol* 2021; **94**: 20210525 [PMID: 34235955 DOI: 10.1259/bjr.20210525]

22 **Li X**, Liu Q, Hu B, Xu J, Huang C, Liu F. A computed tomography-based clinical-radiomics model for prediction of lymph node metastasis in esophageal carcinoma. *J Cancer Res Ther* 2021; **17**: 1665-1671 [PMID: 35381737 DOI: 10.4103/jcrt.jcrt_1755_21]

23 **Zhang C**, Shi Z, Kalendralis P, Whybra P, Parkinson C, Berbee M, Spezi E, Roberts A, Christian A, Lewis W, Crosby T, Dekker A, Wee L, Foley KG. Prediction of lymph node metastases using pre-treatment PET radiomics of the primary tumour in esophageal adenocarcinoma: an external validation study. *Br J Radiol* 2021; **94**: 20201042 [PMID: 33264032 DOI: 10.1259/bjr.20201042]

24 **Qu J**, Shen C, Qin J, Wang Z, Liu Z, Guo J, Zhang H, Gao P, Bei T, Wang Y, Liu H, Kamel IR, Tian J, Li H. The MR radiomic signature can predict preoperative lymph node metastasis in patients with esophageal cancer. *Eur Radiol* 2019; **29**: 906-914 [PMID: 30039220 DOI: 10.1007/s00330-018-5583-z]

25 **Wu L**, Wang C, Tan X, Cheng Z, Zhao K, Yan L, Liang Y, Liu Z, Liang C. Radiomics approach for preoperative identification of stages I-II and III-IV of esophageal cancer. *Chin J Cancer Res* 2018; **30**: 396-405 [PMID: 30210219 DOI: 10.21147/j.issn.1000-9604.2018.04.02]

26 **Babic B**, Fuchs HF, Bruns CJ. [Neoadjuvant chemoradiotherapy or chemotherapy for locally advanced esophageal cancer? *Chirurg* 2020; **91**: 379-383 [PMID: 32140748 DOI: 10.1007/s00104-020-01150-6]

27 **Secrier M**, Li X, de Silva N, Eldridge MD, Contino G, Bornschein J, MacRae S, Grehan N, O'Donovan M, Miremadi A, Yang TP, Bower L, Chettouh H, Crawte J, Galeano-Dalmau N, Grabowska A, Saunders J, Underwood T, Waddell N,

Barbour AP, Nutzinger B, Achilleos A, Edwards PA, Lynch AG, Tavaré S, Fitzgerald RC; Oesophageal Cancer Clinical and Molecular Stratification (OCCAMS) Consortium. Mutational signatures in esophageal adenocarcinoma define etiologically distinct subgroups with therapeutic relevance. *Nat Genet* 2016; **48**: 1131-1141 [PMID: 27595477 DOI: 10.1038/ng.3659]

28 **Yang Z**, He B, Zhuang X, Gao X, Wang D, Li M, Lin Z, Luo R. CT-based radiomic signatures for prediction of pathologic complete response in esophageal squamous cell carcinoma after neoadjuvant chemoradiotherapy. *J Radiat Res* 2019; **60**: 538-545 [PMID: 31111948 DOI: 10.1093/jrr/rrz027]

29 **Hou Z**, Li S, Ren W, Liu J, Yan J, Wan S. Radiomic analysis in T2W and SPAIR T2W MRI: predict treatment response to chemoradiotherapy in esophageal squamous cell carcinoma. *J Thorac Dis* 2018; **10**: 2256-2267 [PMID: 29850130 DOI: 10.21037/jtd.2018.03.123]

30 **Jin X**, Zheng X, Chen D, Jin J, Zhu G, Deng X, Han C, Gong C, Zhou Y, Liu C, Xie C. Prediction of response after chemoradiation for esophageal cancer using a combination of dosimetry and CT radiomics. *Eur Radiol* 2019; **29**: 6080-6088 [PMID: 31028447 DOI: 10.1007/s00330-019-06193-w]

31 **Hu Y**, Xie C, Yang H, Ho JWK, Wen J, Han L, Lam KO, Wong IYH, Law SYK, Chiu KWH, Vardhanabhuti V, Fu J. Computed tomography-based deep-learning prediction of neoadjuvant chemoradiotherapy treatment response in esophageal squamous cell carcinoma. *Radiother Oncol* 2021; **154**: 6-13 [PMID: 32941954 DOI: 10.1016/j.radonc.2020.09.014]

32 **Luo HS**, Huang SF, Xu HY, Li XY, Wu SX, Wu DH. A nomogram based on pretreatment CT radiomics features for predicting complete response to chemoradiotherapy in patients with esophageal squamous cell cancer. *Radiat Oncol* 2020; **15**: 249 [PMID: 33121507 DOI: 10.1186/s13014-020-01692-3]

33 **Li X**, Gao H, Zhu J, Huang Y, Zhu Y, Huang W, Li Z, Sun K, Liu Z, Tian J, Li B. 3D Deep Learning Model for the Pretreatment Evaluation of Treatment Response in Esophageal Carcinoma: A Prospective Study (ChiCTR2000039279). *Int J Radiat Oncol Biol Phys* 2021; **111**: 926-935 [PMID: 34229050 DOI: 10.1016/j.ijrobp.2021.06.033]

34 **Kao YS**, Hsu Y. A Meta-Analysis for Using Radiomics to Predict Complete Pathological Response in Esophageal Cancer Patients Receiving Neoadjuvant Chemoradiation. *In Vivo* 2021; **35**: 1857-1863 [PMID: 33910873 DOI: 10.21873/invivo.12448]

35 **Hu Y**, Xie C, Yang H, Ho JWK, Wen J, Han L, Chiu KWH, Fu J, Vardhanabhuti V. Assessment of Intratumoral and Peritumoral Computed Tomography Radiomics for Predicting Pathological Complete Response to Neoadjuvant Chemoradiation in Patients With Esophageal Squamous Cell Carcinoma. *JAMA Netw Open* 2020; **3**: e2015927 [PMID: 32910196 DOI: 10.1001/jamanetworkopen.2020.15927]

36 **Donahue JM**, Nichols FC, Li Z, Schomas DA, Allen MS, Cassivi SD, Jatoi A, Miller RC, Wigle DA, Shen KR, Deschamps C. Complete pathologic response after neoadjuvant chemoradiotherapy for esophageal cancer is associated with enhanced survival. *Ann Thorac Surg* 2009; **87**: 392-8; discussion 398 [PMID: 19161745 DOI: 10.1016/j.athoracsur.2008.11.001]

37 **Lin JW**, Hsu CP, Yeh HL, Chuang CY, Lin CH. The impact of pathological complete response after neoadjuvant chemoradiotherapy in locally advanced squamous cell carcinoma of esophagus. *J Chin Med Assoc* 2018; **81**: 18-24 [PMID: 29066057 DOI: 10.1016/j.jcma.2017.08.007]

38 **Dittrick GW**, Weber JM, Shridhar R, Hoffe S, Melis M, Almhanna K, Barthel J, McLoughlin J, Karl RC, Meredith KL. Pathologic nonresponders after neoadjuvant chemoradiation for esophageal cancer demonstrate no survival benefit compared with patients treated with primary esophagectomy. *Ann Surg Oncol* 2012; **19**: 1678-1684 [PMID: 22045465 DOI: 10.1245/s10434-011-2078-4]

39 **Murakami Y**, Kawahara D, Tani S, Kubo K, Katsuta T, Imano N, Takeuchi Y, Nishibuchi I, Saito A, Nagata Y. Predicting the Local Response of Esophageal Squamous Cell Carcinoma to Neoadjuvant Chemoradiotherapy by Radiomics with a Machine Learning Method Using ^{18}F-FDG PET Images. *Diagnostics (Basel)* 2021; **11** [PMID: 34200332 DOI: 10.3390/diagnostics11061049]

40 **Qu J**, Ma L, Lu Y, Wang Z, Guo J, Zhang H, Yan X, Liu H, Kamel IR, Qin J, Li H. DCE-MRI radiomics nomogram can predict response to neoadjuvant chemotherapy in esophageal cancer. *Discov Oncol* 2022; **13**: 3 [PMID: 35201487 DOI: 10.1007/s12672-022-00464-7]

41 **Li Y**, Beck M, Päßler T, Lili C, Hua W, Mai HD, Amthauer H, Biebl M, Thuss-Patience PC, Berger J, Stromberger C, Tinhofer I, Kruppa J, Budach V, Hofheinz F, Lin Q, Zschaeck S. A FDG-PET radiomics signature detects esophageal squamous cell carcinoma patients who do not benefit from chemoradiation. *Sci Rep* 2020; **10**: 17671 [PMID: 33077841 DOI: 10.1038/s41598-020-74701-w]

42 **Beukinga RJ**, Poelmann FB, Kats-Ugurlu G, Viddeleer AR, Boellaard R, De Haas RJ, Plukker JTM, Hulshoff JB. Prediction of Non-Response to Neoadjuvant Chemoradiotherapy in Esophageal Cancer Patients with ^{18}F-FDG PET Radiomics Based Machine Learning Classification. *Diagnostics (Basel)* 2022; **12** [PMID: 35626225 DOI: 10.3390/diagnostics12051070]

43 **Zhu Y**, Yao W, Xu BC, Lei YY, Guo QK, Liu LZ, Li HJ, Xu M, Yan J, Chang DD, Feng ST, Zhu ZH. Predicting response to immunotherapy plus chemotherapy in patients with esophageal squamous cell carcinoma using non-invasive Radiomic biomarkers. *BMC Cancer* 2021; **21**: 1167 [PMID: 34717582 DOI: 10.1186/s12885-021-08899-x]

44 **Luo HS**, Chen YY, Huang WZ, Wu SX, Huang SF, Xu HY, Xue RL, Du ZS, Li XY, Lin LX, Huang HC. Development and validation of a radiomics-based model to predict local progression-free survival after chemo-radiotherapy in patients with esophageal squamous cell cancer. *Radiat Oncol* 2021; **16**: 201 [PMID: 34641928 DOI: 10.1186/s13014-021-01925-z]

45 **Yan T**, Liu L, Yan Z, Peng M, Wang Q, Zhang S, Wang L, Zhuang X, Liu H, Ma Y, Wang B, Cui Y. A Radiomics Nomogram for Non-Invasive Prediction of Progression-Free Survival in Esophageal Squamous Cell Carcinoma. *Front Comput Neurosci* 2022; **16**: 885091 [PMID: 35651590 DOI: 10.3389/fncom.2022.885091]

46 **Cao B**, Mi K, Dai W, Liu T, Xie T, Li Q, Lang J, Han Y, Peng L, Wang Q. Prognostic and incremental value of computed tomography-based radiomics from tumor and nodal regions in esophageal squamous cell carcinoma. *Chin J Cancer Res* 2022; **34**: 71-82 [PMID: 35685995 DOI: 10.21147/j.issn.1000-9604.2022.02.02]

47 **Chu F**, Liu Y, Liu Q, Li W, Jia Z, Wang C, Wang Z, Lu S, Li P, Zhang Y, Liao Y, Xu M, Yao X, Wang S, Liu C, Zhang H, Yan X, Kamel IR, Sun H, Yang G, Qu J. Development and validation of MRI-based radiomics signatures models for prediction of disease-free survival and overall survival in patients with esophageal squamous cell carcinoma. *Eur Radiol* 2022; **32**: 5930-5942 [PMID: 35384460 DOI: 10.1007/s00330-022-08776-6]

48 **Tang S**, Ou J, Liu J, Wu YP, Wu CQ, Chen TW, Zhang XM, Li R, Tang MJ, Yang LQ, Tan BG, Lu FL, Hu J. Application of contrast-enhanced CT radiomics in prediction of early recurrence of locally advanced oesophageal squamous cell carcinoma after trimodal therapy. *Cancer Imaging* 2021; **21**: 38 [PMID: 34039403 DOI: 10.1186/s40644-021-00407-5]

49 **Qiu Q**, Duan J, Deng H, Han Z, Gu J, Yue NJ, Yin Y. Development and Validation of a Radiomics Nomogram Model for Predicting Postoperative Recurrence in Patients With Esophageal Squamous Cell Cancer Who Achieved pCR After Neoadjuvant Chemoradiotherapy Followed by Surgery. *Front Oncol* 2020; **10**: 1398 [PMID: 32850451 DOI: 10.3389/fonc.2020.01398]

50 **Lu N**, Zhang WJ, Dong L, Chen JY, Zhu YL, Zhang SH, Fu JH, Yin SH, Li ZC, Xie CM. Dual-region radiomics signature: Integrating primary tumor and lymph node computed tomography features improves survival prediction in esophageal squamous cell cancer. *Comput Methods Programs Biomed* 2021; **208**: 106287 [PMID: 34311416 DOI: 10.1016/j.cmpb.2021.106287]

51 **Cheng L**, Wu L, Chen S, Ye W, Liu Z, Liang C. [CT-based radiomics analysis for evaluating the differentiation degree of esophageal squamous carcinoma]. *Zhong Nan Da Xue Xue Bao Yi Xue Ban* 2019; **44**: 251-256 [PMID: 30971516 DOI: 10.11817/j.issn.1672-7347.2019.03.004]

52 **Foy JJ**, Armato SG 3rd, Al-Hallaq HA. Effects of variability in radiomics software packages on classifying patients with radiation pneumonitis. *J Med Imaging (Bellingham)* 2020; **7**: 014504 [PMID: 32118090 DOI: 10.1117/1.JMI.7.1.014504]

53 **Anthony GJ**, Cunliffe A, Castillo R, Pham N, Guerrero T, Armato SG 3rd, Al-Hallaq HA. Incorporation of pre-therapy ^{18}F-FDG uptake data with CT texture features into a radiomics model for radiation pneumonitis diagnosis. *Med Phys* 2017; **44**: 3686-3694 [PMID: 28422299 DOI: 10.1002/mp.12282]

54 **Feng B**, Huang L, Li C, Quan Y, Chen Y, Xue H, Chen Q, Sun S, Li R, Long W. A Heterogeneity Radiomic Nomogram for Preoperative Differentiation of Primary Gastric Lymphoma From Borrmann Type IV Gastric Cancer. *J Comput Assist Tomogr* 2021; **45**: 191-202 [PMID: 33273161 DOI: 10.1097/RCT.0000000000001117]

55 **Lan Q**, Guan X, Lu S, Yuan W, Jiang Z, Lin H, Long L. Radiomics in addition to computed tomography-based body composition nomogram may improve the prediction of postoperative complications in gastric cancer patients. *Ann Nutr Metab* 2022 [PMID: 36041416 DOI: 10.1159/000526787]

56 **Deng J**, Tan Y, Gu Q, Rong P, Wang W, Liu S. [Application of CT-based radiomics in differentiating primary gastric lymphoma from Borrmann type IV gastric cancer]. *Zhong Nan Da Xue Xue Bao Yi Xue Ban* 2019; **44**: 257-263 [PMID: 30971517 DOI: 10.11817/j.issn.1672-7347.2019.03.005]

57 **Ma Z**, Fang M, Huang Y, He L, Chen X, Liang C, Huang X, Cheng Z, Dong D, Xie J, Tian J, Liu Z. CT-based radiomics signature for differentiating Borrmann type IV gastric cancer from primary gastric lymphoma. *Eur J Radiol* 2017; **91**: 142-147 [PMID: 28629560 DOI: 10.1016/j.ejrad.2017.04.007]

58 **Wang R**, Liu H, Liang P, Zhao H, Li L, Gao J. Radiomics analysis of CT imaging for differentiating gastric neuroendocrine carcinomas from gastric adenocarcinomas. *Eur J Radiol* 2021; **138**: 109662 [PMID: 33774440 DOI: 10.1016/j.ejrad.2021.109662]

59 **Feng B**, Huang L, Liu Y, Chen Y, Zhou H, Yu T, Xue H, Chen Q, Zhou T, Kuang Q, Yang Z, Chen X, Peng Z, Long W. A Transfer Learning Radiomics Nomogram for Preoperative Prediction of Borrmann Type IV Gastric Cancer From Primary Gastric Lymphoma. *Front Oncol* 2021; **11**: 802205 [PMID: 35087761 DOI: 10.3389/fonc.2021.802205]

60 **Wang Y**, Liu W, Yu Y, Liu JJ, Jiang L, Xue HD, Lei J, Jin Z, Yu JC. Prediction of the Depth of Tumor Invasion in Gastric Cancer: Potential Role of CT Radiomics. *Acad Radiol* 2020; **27**: 1077-1084 [PMID: 31761666 DOI: 10.1016/j.acra.2019.10.020]

61 **Coccolini F**, Cotte E, Glehen O, Lotti M, Poiasina E, Catena F, Yonemura Y, Ansaloni L. Intraperitoneal chemotherapy in advanced gastric cancer. Meta-analysis of randomized trials. *Eur J Surg Oncol* 2014; **40**: 12-26 [PMID: 24290371 DOI: 10.1016/j.ejso.2013.10.019]

62 **Verstegen MH**, Harker M, van de Water C, van Dieren J, Hugen N, Nagtegaal ID, Rosman C, van der Post RS. Metastatic pattern in esophageal and gastric cancer: Influenced by site and histology. *World J Gastroenterol* 2020; **26**: 6037-6046 [PMID: 33132653 DOI: 10.3748/wjg.v26.i39.6037]

63 **Gao X**, Ma T, Cui J, Zhang Y, Wang L, Li H, Ye Z. A radiomics-based model for prediction of lymph node metastasis in gastric cancer. *Eur J Radiol* 2020; **129**: 109069 [PMID: 32464581 DOI: 10.1016/j.ejrad.2020.109069]

64 **Gao X**, Ma T, Cui J, Zhang Y, Wang L, Li H, Ye Z. A CT-based Radiomics Model for Prediction of Lymph Node Metastasis in Early Stage Gastric Cancer. *Acad Radiol* 2021; **28**: e155-e164 [PMID: 32507613 DOI: 10.1016/j.acra.2020.03.045]

65 **Wang X**, Li C, Fang M, Zhang L, Zhong L, Dong D, Tian J, Shan X. Integrating No.3 lymph nodes and primary tumor radiomics to predict lymph node metastasis in T1-2 gastric cancer. *BMC Med Imaging* 2021; **21**: 58 [PMID: 33757460 DOI: 10.1186/s12880-021-00587-3]

66 **Dong D**, Fang MJ, Tang L, Shan XH, Gao JB, Giganti F, Wang RP, Chen X, Wang XX, Palumbo D, Fu J, Li WC, Li J, Zhong LZ, De Cobelli F, Ji JF, Liu ZY, Tian J. Deep learning radiomic nomogram can predict the number of lymph node metastasis in locally advanced gastric cancer: an international multicenter study. *Ann Oncol* 2020; **31**: 912-920 [PMID: 32304748 DOI: 10.1016/j.annonc.2020.04.003]

67 **Liu Q**, Li J, Xin B, Sun Y, Feng D, Fulham MJ, Wang X, Song S. ^{18}F-FDG PET/CT Radiomics for Preoperative Prediction of Lymph Node Metastases and Nodal Staging in Gastric Cancer. *Front Oncol* 2021; **11**: 723345 [PMID: 34589429 DOI: 10.3389/fonc.2021.723345]

68 **Wang W**, Peng Y, Feng X, Zhao Y, Seeruttun SR, Zhang J, Cheng Z, Li Y, Liu Z, Zhou Z. Development and Validation of a Computed Tomography-Based Radiomics Signature to Predict Response to Neoadjuvant Chemotherapy for Locally Advanced Gastric Cancer. *JAMA Netw Open* 2021; **4**: e2121143 [PMID: 34410397 DOI:

10.1001/jamanetworkopen.2021.21143]
69 **Hou Z**, Yang Y, Li S, Yan J, Ren W, Liu J, Wang K, Liu B, Wan S. Radiomic analysis using contrast-enhanced CT: predict treatment response to pulsed low dose rate radiotherapy in gastric carcinoma with abdominal cavity metastasis. *Quant Imaging Med Surg* 2018; **8**: 410-420 [PMID: 29928606 DOI: 10.21037/qims.2018.05.01]
70 **Chen Y**, Xu W, Li YL, Liu W, Sah BK, Wang L, Xu Z, Wels M, Zheng Y, Yan M, Zhang H, Ma Q, Zhu Z, Li C. CT-Based Radiomics Showing Generalization to Predict Tumor Regression Grade for Advanced Gastric Cancer Treated With Neoadjuvant Chemotherapy. *Front Oncol* 2022; **12**: 758863 [PMID: 35280802 DOI: 10.3389/fonc.2022.758863]
71 **Chen Y**, Yuan F, Wang L, Li E, Xu Z, Wels M, Yao W, Zhang H. Evaluation of dual-energy CT derived radiomics signatures in predicting outcomes in patients with advanced gastric cancer after neoadjuvant chemotherapy. *Eur J Surg Oncol* 2022; **48**: 339-347 [PMID: 34304951 DOI: 10.1016/j.ejso.2021.07.014]
72 **Jiang Y**, Jin C, Yu H, Wu J, Chen C, Yuan Q, Huang W, Hu Y, Xu Y, Zhou Z, Fisher GA Jr, Li G, Li R. Development and Validation of a Deep Learning CT Signature to Predict Survival and Chemotherapy Benefit in Gastric Cancer: A Multicenter, Retrospective Study. *Ann Surg* 2021; **274**: e1153-e1161 [PMID: 31913871 DOI: 10.1097/SLA.0000000000003778]
73 **Jiang Y**, Yuan Q, Lv W, Xi S, Huang W, Sun Z, Chen H, Zhao L, Liu W, Hu Y, Lu L, Ma J, Li T, Yu J, Wang Q, Li G. Radiomic signature of ^{18}F fluorodeoxyglucose PET/CT for prediction of gastric cancer survival and chemotherapeutic benefits. *Theranostics* 2018; **8**: 5915-5928 [PMID: 30613271 DOI: 10.7150/thno.28018]
74 **Huang J**, Yao H, Li Y, Dong M, Han C, He L, Huang X, Xia T, Yi Z, Wang H, Zhang Y, He J, Liang C, Liu Z. Development and validation of a CT-based radiomics nomogram for preoperative prediction of tumor histologic grade in gastric adenocarcinoma. *Chin J Cancer Res* 2021; **33**: 69-78 [PMID: 33707930 DOI: 10.21147/j.issn.1000-9604.2021.01.08]
75 **Wang XX**, Ding Y, Wang SW, Dong D, Li HL, Chen J, Hu H, Lu C, Tian J, Shan XH. Intratumoral and peritumoral radiomics analysis for preoperative Lauren classification in gastric cancer. *Cancer Imaging* 2020; **20**: 83 [PMID: 33228815 DOI: 10.1186/s40644-020-00358-3]
76 **Sun Z**, Jin L, Zhang S, Duan S, Xing W, Hu S. Preoperative prediction for lauren type of gastric cancer: A radiomics nomogram analysis based on CT images and clinical features. *J Xray Sci Technol* 2021; **29**: 675-686 [PMID: 34024809 DOI: 10.3233/XST-210888]
77 **Zhao Y**, Yang J, Luo M, Yang Y, Guo X, Zhang T, Hao J, Yao Y, Ma X. Contrast-Enhanced CT-based Textural Parameters as Potential Prognostic Factors of Survival for Colorectal Cancer Patients Receiving Targeted Therapy. *Mol Imaging Biol* 2021; **23**: 427-435 [PMID: 33108800 DOI: 10.1007/s11307-020-01552-2]
78 **Vicini S**, Bortolotto C, Rengo M, Ballerini D, Bellini D, Carbone I, Preda L, Laghi A, Coppola F, Faggioni L. A narrative review on current imaging applications of artificial intelligence and radiomics in oncology: focus on the three most common cancers. *Radiol Med* 2022; **127**: 819-836 [PMID: 35771379 DOI: 10.1007/s11547-022-01512-6]
79 **Liang C**, Huang Y, He L, Chen X, Ma Z, Dong D, Tian J, Liang C, Liu Z. The development and validation of a CT-based radiomics signature for the preoperative discrimination of stage I-II and stage III-IV colorectal cancer. *Oncotarget* 2016; **7**: 31401-31412 [PMID: 27120787 DOI: 10.18632/oncotarget.8919]
80 **Lin X**, Zhao S, Jiang H, Jia F, Wang G, He B, Ma X, Li J, Shi Z. A radiomics-based nomogram for preoperative T staging prediction of rectal cancer. *Abdom Radiol (NY)* 2021; **46**: 4525-4535 [PMID: 34081158 DOI: 10.1007/s00261-021-03137-1]
81 **Dou Y**, Liu Y, Kong X, Yang S. T staging with functional and radiomics parameters of computed tomography in colorectal cancer patients. *Medicine (Baltimore)* 2022; **101**: e29244 [PMID: 35623068 DOI: 10.1097/MD.0000000000029244]
82 **Li J**, Zhou Y, Wang X, Zhou M, Chen X, Luan K. An MRI-based multi-objective radiomics model predicts lymph node status in patients with rectal cancer. *Abdom Radiol (NY)* 2021; **46**: 1816-1824 [PMID: 33241428 DOI: 10.1007/s00261-020-02863-2]
83 **Li C**, Yin J. Radiomics Based on T2-Weighted Imaging and Apparent Diffusion Coefficient Images for Preoperative Evaluation of Lymph Node Metastasis in Rectal Cancer Patients. *Front Oncol* 2021; **11**: 671354 [PMID: 34041033 DOI: 10.3389/fonc.2021.671354]
84 **Liu X**, Yang Q, Zhang C, Sun J, He K, Xie Y, Zhang Y, Fu Y, Zhang H. Multiregional-Based Magnetic Resonance Imaging Radiomics Combined With Clinical Data Improves Efficacy in Predicting Lymph Node Metastasis of Rectal Cancer. *Front Oncol* 2020; **10**: 585767 [PMID: 33680919 DOI: 10.3389/fonc.2020.585767]
85 **He J**, Wang Q, Zhang Y, Wu H, Zhou Y, Zhao S. Preoperative prediction of regional lymph node metastasis of colorectal cancer based on ^{18}F-FDG PET/CT and machine learning. *Ann Nucl Med* 2021; **35**: 617-627 [PMID: 33738763 DOI: 10.1007/s12149-021-01605-8]
86 **Huang Y**, He L, Dong D, Yang C, Liang C, Chen X, Ma Z, Huang X, Yao S, Tian J, Liu Z. Individualized prediction of perineural invasion in colorectal cancer: development and validation of a radiomics prediction model. *Chin J Cancer Res* 2018; **30**: 40-50 [PMID: 29545718 DOI: 10.21147/j.issn.1000-9604.2018.01.05]
87 **Zhang K**, Ren Y, Xu S, Lu W, Xie S, Qu J, Wang X, Shen B, Pang P, Cai X, Sun J. A clinical-radiomics model incorporating T2-weighted and diffusion-weighted magnetic resonance images predicts the existence of lymphovascular invasion / perineural invasion in patients with colorectal cancer. *Med Phys* 2021; **48**: 4872-4882 [PMID: 34042185 DOI: 10.1002/mp.15001]
88 **Siriwardena AK**, Mason JM, Mullamitha S, Hancock HC, Jegatheeswaran S. Management of colorectal cancer presenting with synchronous liver metastases. *Nat Rev Clin Oncol* 2014; **11**: 446-459 [PMID: 24889770 DOI: 10.1038/nrclinonc.2014.90]
89 **Ayez N**, Burger JW, van der Pool AE, Eggermont AM, Grunhagen DJ, de Wilt JH, Verhoef C. Long-term results of the "liver first" approach in patients with locally advanced rectal cancer and synchronous liver metastases. *Dis Colon Rectum* 2013; **56**: 281-287 [PMID: 23392140 DOI: 10.1097/DCR.0b013e318279b743]
90 **Liu Z**, Zhang XY, Shi YJ, Wang L, Zhu HT, Tang Z, Wang S, Li XT, Tian J, Sun YS. Radiomics Analysis for Evaluation of Pathological Complete Response to Neoadjuvant Chemoradiotherapy in Locally Advanced Rectal Cancer. *Clin Cancer*

Res 2017; **23**: 7253-7262 [PMID: 28939744 DOI: 10.1158/1078-0432.CCR-17-1038]
91 **Wang J**, Chen J, Zhou R, Gao Y, Li J. Machine learning-based multiparametric MRI radiomics for predicting poor responders after neoadjuvant chemoradiotherapy in rectal Cancer patients. *BMC Cancer* 2022; **22**: 420 [PMID: 35439946 DOI: 10.1186/s12885-022-09518-z]
92 **Giannini V**, Rosati S, Defeudis A, Balestra G, Vassallo L, Cappello G, Mazzetti S, De Mattia C, Rizzetto F, Torresin A, Sartore-Bianchi A, Siena S, Vanzulli A, Leone F, Zagonel V, Marsoni S, Regge D. Radiomics predicts response of individual HER2-amplified colorectal cancer liver metastases in patients treated with HER2-targeted therapy. *Int J Cancer* 2020; **147**: 3215-3223 [PMID: 32875550 DOI: 10.1002/ijc.33271]
93 **Zhang Z**, Shen L, Wang Y, Wang J, Zhang H, Xia F, Wan J, Zhang Z. MRI Radiomics Signature as a Potential Biomarker for Predicting *KRAS* Status in Locally Advanced Rectal Cancer Patients. *Front Oncol* 2021; **11**: 614052 [PMID: 34026605 DOI: 10.3389/fonc.2021.614052]
94 **Zhang G**, Chen L, Liu A, Pan X, Shu J, Han Y, Huan Y, Zhang J. Comparable Performance of Deep Learning-Based to Manual-Based Tumor Segmentation in KRAS/NRAS/BRAF Mutation Prediction With MR-Based Radiomics in Rectal Cancer. *Front Oncol* 2021; **11**: 696706 [PMID: 34395262 DOI: 10.3389/fonc.2021.696706]
95 **Xue T**, Peng H, Chen Q, Li M, Duan S, Feng F. Preoperative prediction of KRAS mutation status in colorectal cancer using a CT-based radiomics nomogram. *Br J Radiol* 2022; **95**: 20211014 [PMID: 35312376 DOI: 10.1259/bjr.20211014]
96 **Yang L**, Dong D, Fang M, Zhu Y, Zang Y, Liu Z, Zhang H, Ying J, Zhao X, Tian J. Can CT-based radiomics signature predict KRAS/NRAS/BRAF mutations in colorectal cancer? *Eur Radiol* 2018; **28**: 2058-2067 [PMID: 29335867 DOI: 10.1007/s00330-017-5146-8]
97 **Horvat N**, Veeraraghavan H, Pelossof RA, Fernandes MC, Arora A, Khan M, Marco M, Cheng CT, Gonen M, Golia Pernicka JS, Gollub MJ, Garcia-Aguillar J, Petkovska I. Radiogenomics of rectal adenocarcinoma in the era of precision medicine: A pilot study of associations between qualitative and quantitative MRI imaging features and genetic mutations. *Eur J Radiol* 2019; **113**: 174-181 [PMID: 30927944 DOI: 10.1016/j.ejrad.2019.02.022]
98 **Golia Pernicka JS**, Gagniere J, Chakraborty J, Yamashita R, Nardo L, Creasy JM, Petkovska I, Do RRK, Bates DDB, Paroder V, Gonen M, Weiser MR, Simpson AL, Gollub MJ. Radiomics-based prediction of microsatellite instability in colorectal cancer at initial computed tomography evaluation. *Abdom Radiol (NY)* 2019; **44**: 3755-3763 [PMID: 31250180 DOI: 10.1007/s00261-019-02117-w]
99 **Li Z**, Chen F, Zhang S, Ma X, Xia Y, Shen F, Lu Y, Shao C. The feasibility of MRI-based radiomics model in presurgical evaluation of tumor budding in locally advanced rectal cancer. *Abdom Radiol (NY)* 2022; **47**: 56-65 [PMID: 34673995 DOI: 10.1007/s00261-021-03311-5]
100 **Gong XQ**, Tao YY, Wu YK, Liu N, Yu X, Wang R, Zheng J, Huang XH, Li JD, Yang G, Wei XQ, Yang L, Zhang XM. Progress of MRI Radiomics in Hepatocellular Carcinoma. *Front Oncol* 2021; **11**: 698373 [PMID: 34616673 DOI: 10.3389/fonc.2021.698373]
101 **He Y**, Hu B, Zhu C, Xu W, Ge Y, Hao X, Dong B, Chen X, Dong Q, Zhou X. A Novel Multimodal Radiomics Model for Predicting Prognosis of Resected Hepatocellular Carcinoma. *Front Oncol* 2022; **12**: 745258 [PMID: 35321432 DOI: 10.3389/fonc.2022.745258]
102 **Liu Q**, Li J, Liu F, Yang W, Ding J, Chen W, Wei Y, Li B, Zheng L. A radiomics nomogram for the prediction of overall survival in patients with hepatocellular carcinoma after hepatectomy. *Cancer Imaging* 2020; **20**: 82 [PMID: 33198809 DOI: 10.1186/s40644-020-00360-9]
103 **Zhang W**, Zhang B, Chen XP. Adjuvant treatment strategy after curative resection for hepatocellular carcinoma. *Front Med* 2021; **15**: 155-169 [PMID: 33754281 DOI: 10.1007/s11684-021-0848-3]
104 **Lee S**, Kim SH, Lee JE, Sinn DH, Park CK. Preoperative gadoxetic acid-enhanced MRI for predicting microvascular invasion in patients with single hepatocellular carcinoma. *J Hepatol* 2017; **67**: 526-534 [PMID: 28483680 DOI: 10.1016/j.jhep.2017.04.024]
105 **Zhou W**, Jian W, Cen X, Zhang L, Guo H, Liu Z, Liang C, Wang G. Prediction of Microvascular Invasion of Hepatocellular Carcinoma Based on Contrast-Enhanced MR and 3D Convolutional Neural Networks. *Front Oncol* 2021; **11**: 588010 [PMID: 33854959 DOI: 10.3389/fonc.2021.588010]
106 **Feng ST**, Jia Y, Liao B, Huang B, Zhou Q, Li X, Wei K, Chen L, Li B, Wang W, Chen S, He X, Wang H, Peng S, Chen ZB, Tang M, Chen Z, Hou Y, Peng Z, Kuang M. Preoperative prediction of microvascular invasion in hepatocellular cancer: a radiomics model using Gd-EOB-DTPA-enhanced MRI. *Eur Radiol* 2019; **29**: 4648-4659 [PMID: 30689032 DOI: 10.1007/s00330-018-5935-8]
107 **Ariff B**, Lloyd CR, Khan S, Shariff M, Thillainayagam AV, Bansi DS, Khan SA, Taylor-Robinson SD, Lim AK. Imaging of liver cancer. *World J Gastroenterol* 2009; **15**: 1289-1300 [PMID: 19294758 DOI: 10.3748/wjg.15.1289]
108 **Mokrane FZ**, Lu L, Vavasseur A, Otal P, Peron JM, Luk L, Yang H, Ammari S, Saenger Y, Rousseau H, Zhao B, Schwartz LH, Dercle L. Radiomics machine-learning signature for diagnosis of hepatocellular carcinoma in cirrhotic patients with indeterminate liver nodules. *Eur Radiol* 2020; **30**: 558-570 [PMID: 31444598 DOI: 10.1007/s00330-019-06347-w]
109 **Abdelrahman AS**, Madkour SS, Ekladious MEY. Interrater reliability and agreement of the liver imaging reporting and data system (LI-RADS) v2018 for the evaluation of hepatic lesions. *Pol J Radiol* 2022; **87**: e316-e324 [PMID: 35892071 DOI: 10.5114/pjr.2022.117590]
110 **Zhong X**, Guan T, Tang D, Li J, Lu B, Cui S, Tang H. Differentiation of small (≤ 3 cm) hepatocellular carcinomas from benign nodules in cirrhotic liver: the added additive value of MRI-based radiomics analysis to LI-RADS version 2018 algorithm. *BMC Gastroenterol* 2021; **21**: 155 [PMID: 33827440 DOI: 10.1186/s12876-021-01710-y]
111 **Zhong X**, Tang H, Guan T, Lu B, Zhang C, Tang D, Li J, Cui S. Added Value of Quantitative Apparent Diffusion Coefficients for Identifying Small Hepatocellular Carcinoma from Benign Nodule Categorized as LI-RADS 3 and 4 in Cirrhosis. *J Clin Transl Hepatol* 2022; **10**: 34-41 [PMID: 35233371 DOI: 10.14218/JCTH.2021.00053]
112 **Hectors SJ**, Wagner M, Bane O, Besa C, Lewis S, Remark R, Chen N, Fiel MI, Zhu H, Gnjatic S, Merad M, Hoshida Y, Taouli B. Quantification of hepatocellular carcinoma heterogeneity with multiparametric magnetic resonance imaging. *Sci Rep* 2017; **7**: 2452 [PMID: 28550313 DOI: 10.1038/s41598-017-02706-z]

113 **Hectors SJ**, Lewis S, Besa C, King MJ, Said D, Putra J, Ward S, Higashi T, Thung S, Yao S, Laface I, Schwartz M, Gnjatic S, Merad M, Hoshida Y, Taouli B. MRI radiomics features predict immuno-oncological characteristics of hepatocellular carcinoma. *Eur Radiol* 2020; **30**: 3759-3769 [PMID: 32086577 DOI: 10.1007/s00330-020-06675-2]

114 **Kurucay M**, Kloth C, Kaufmann S, Nikolaou K, Bösmüller H, Horger M, Thaiss WM. Multiparametric imaging for detection and characterization of hepatocellular carcinoma using gadoxetic acid-enhanced MRI and perfusion-CT: which parameters work best? *Cancer Imaging* 2017; **17**: 18 [PMID: 28659180 DOI: 10.1186/s40644-017-0121-9]

115 **Yasaka K**, Akai H, Abe O, Kiryu S. Deep Learning with Convolutional Neural Network for Differentiation of Liver Masses at Dynamic Contrast-enhanced CT: A Preliminary Study. *Radiology* 2018; **286**: 887-896 [PMID: 29059036 DOI: 10.1148/radiol.2017170706]

116 **Hamm CA**, Wang CJ, Savic LJ, Ferrante M, Schobert I, Schlachter T, Lin M, Duncan JS, Weinreb JC, Chapiro J, Letzen B. Deep learning for liver tumor diagnosis part I: development of a convolutional neural network classifier for multi-phasic MRI. *Eur Radiol* 2019; **29**: 3338-3347 [PMID: 31016442 DOI: 10.1007/s00330-019-06205-9]

117 **Hui TCH**, Chuah TK, Low HM, Tan CH. Predicting early recurrence of hepatocellular carcinoma with texture analysis of preoperative MRI: a radiomics study. *Clin Radiol* 2018; **73**: 1056.e11-1056.e16 [PMID: 30213434 DOI: 10.1016/j.crad.2018.07.109]

118 **Zhang Z**, Jiang H, Chen J, Wei Y, Cao L, Ye Z, Li X, Ma L, Song B. Hepatocellular carcinoma: radiomics nomogram on gadoxetic acid-enhanced MR imaging for early postoperative recurrence prediction. *Cancer Imaging* 2019; **19**: 22 [PMID: 31088553 DOI: 10.1186/s40644-019-0209-5]

119 **Shi G**, Han X, Wang Q, Ding Y, Liu H, Zhang Y, Dai Y. Evaluation of Multiple Prognostic Factors of Hepatocellular Carcinoma with Intra-Voxel Incoherent Motions Imaging by Extracting the Histogram Metrics. *Cancer Manag Res* 2020; **12**: 6019-6031 [PMID: 32765101 DOI: 10.2147/CMAR.S262973]

120 **Zhou Y**, Sun SW, Liu QP, Xu X, Zhang Y, Zhang YD. TED: Two-stage expert-guided interpretable diagnosis framework for microvascular invasion in hepatocellular carcinoma. *Med Image Anal* 2022; **82**: 102575 [PMID: 36063747 DOI: 10.1016/j.media.2022.102575]

121 **Ma X**, Wei J, Gu D, Zhu Y, Feng B, Liang M, Wang S, Zhao X, Tian J. Preoperative radiomics nomogram for microvascular invasion prediction in hepatocellular carcinoma using contrast-enhanced CT. *Eur Radiol* 2019; **29**: 3595-3605 [PMID: 30770969 DOI: 10.1007/s00330-018-5985-y]

122 **Xu X**, Zhang HL, Liu QP, Sun SW, Zhang J, Zhu FP, Yang G, Yan X, Zhang YD, Liu XS. Radiomic analysis of contrast-enhanced CT predicts microvascular invasion and outcome in hepatocellular carcinoma. *J Hepatol* 2019; **70**: 1133-1144 [PMID: 30876945 DOI: 10.1016/j.jhep.2019.02.023]

123 **Chong HH**, Yang L, Sheng RF, Yu YL, Wu DJ, Rao SX, Yang C, Zeng MS. Multi-scale and multi-parametric radiomics of gadoxetate disodium-enhanced MRI predicts microvascular invasion and outcome in patients with solitary hepatocellular carcinoma ≤ 5 cm. *Eur Radiol* 2021; **31**: 4824-4838 [PMID: 33447861 DOI: 10.1007/s00330-020-07601-2]

124 **Xu T**, Ren L, Liao M, Zhao B, Wei R, Zhou Z, He Y, Zhang H, Chen D, Chen H, Liao W. Preoperative Radiomics Analysis of Contrast-Enhanced CT for Microvascular Invasion and Prognosis Stratification in Hepatocellular Carcinoma. *J Hepatocell Carcinoma* 2022; **9**: 189-201 [PMID: 35340666 DOI: 10.2147/JHC.S356573]

125 **Brancato V**, Garbino N, Salvatore M, Cavaliere C. MRI-Based Radiomic Features Help Identify Lesions and Predict Histopathological Grade of Hepatocellular Carcinoma. *Diagnostics (Basel)* 2022; **12** [PMID: 35626241 DOI: 10.3390/diagnostics12051085]

126 **Segal E**, Sirlin CB, Ooi C, Adler AS, Gollub J, Chen X, Chan BK, Matcuk GR, Barry CT, Chang HY, Kuo MD. Decoding global gene expression programs in liver cancer by noninvasive imaging. *Nat Biotechnol* 2007; **25**: 675-680 [PMID: 17515910 DOI: 10.1038/nbt1306]

127 **Gu D**, Xie Y, Wei J, Li W, Ye Z, Zhu Z, Tian J, Li X. MRI-Based Radiomics Signature: A Potential Biomarker for Identifying Glypican 3-Positive Hepatocellular Carcinoma. *J Magn Reson Imaging* 2020; **52**: 1679-1687 [PMID: 32491239 DOI: 10.1002/jmri.27199]

128 **Wang F**, Tan BF, Poh SS, Siow TR, Lim FLWT, Yip CSP, Wang MLC, Nei W, Tan HQ. Predicting outcomes for locally advanced rectal cancer treated with neoadjuvant chemoradiation with CT-based radiomics. *Sci Rep* 2022; **12**: 6167 [PMID: 35418656 DOI: 10.1038/s41598-022-10175-2]

129 **Shahzadi I**, Zwanenburg A, Lattermann A, Linge A, Baldus C, Peeken JC, Combs SE, Diefenhardt M, Rödel C, Kirste S, Grosu AL, Baumann M, Krause M, Troost EGC, Löck S. Analysis of MRI and CT-based radiomics features for personalized treatment in locally advanced rectal cancer and external validation of published radiomics models. *Sci Rep* 2022; **12**: 10192 [PMID: 35715462 DOI: 10.1038/s41598-022-13967-8]

130 **Bonomo P**, Socarras Fernandez J, Thorwarth D, Casati M, Livi L, Zips D, Gani C. Simulation CT-based radiomics for prediction of response after neoadjuvant chemo-radiotherapy in patients with locally advanced rectal cancer. *Radiat Oncol* 2022; **17**: 84 [PMID: 35484597 DOI: 10.1186/s13014-022-02053-y]

131 **Zhang L**, Hu J, Hou J, Jiang X, Guo L, Tian L. Radiomics-based model using gadoxetic acid disodium-enhanced MR images: associations with recurrence-free survival of patients with hepatocellular carcinoma treated by surgical resection. *Abdom Radiol (NY)* 2021; **46**: 3845-3854 [PMID: 33733337 DOI: 10.1007/s00261-021-03034-7]

132 **Zhu HB**, Zheng ZY, Zhao H, Zhang J, Zhu H, Li YH, Dong ZY, Xiao LS, Kuang JJ, Zhang XL, Liu L. Radiomics-based nomogram using CT imaging for noninvasive preoperative prediction of early recurrence in patients with hepatocellular carcinoma. *Diagn Interv Radiol* 2020; **26**: 411-419 [PMID: 32490826 DOI: 10.5152/dir.2020.19623]

133 **Zhang Z**, Chen J, Jiang H, Wei Y, Zhang X, Cao L, Duan T, Ye Z, Yao S, Pan X, Song B. Gadoxetic acid-enhanced MRI radiomics signature: prediction of clinical outcome in hepatocellular carcinoma after surgical resection. *Ann Transl Med* 2020; **8**: 870 [PMID: 32793714 DOI: 10.21037/atm-20-3041]

134 **Lee SJ**, Zea R, Kim DH, Lubner MG, Deming DA, Pickhardt PJ. CT texture features of liver parenchyma for predicting development of metastatic disease and overall survival in patients with colorectal cancer. *Eur Radiol* 2018; **28**: 1520-1528 [PMID: 29164382 DOI: 10.1007/s00330-017-5111-6]

135 **Beckers RCJ**, Beets-Tan RGH, Schnerr RS, Maas M, da Costa Andrade LA, Beets GL, Dejong CH, Houwers JB, Lambregts DMJ. Whole-volume vs. segmental CT texture analysis of the liver to assess metachronous colorectal liver

metastases. *Abdom Radiol (NY)* 2017; **42**: 2639-2645 [PMID: 28555265 DOI: 10.1007/s00261-017-1190-8]

136 **Ganeshan B**, Miles KA, Young RC, Chatwin CR. Texture analysis in non-contrast enhanced CT: impact of malignancy on texture in apparently disease-free areas of the liver. *Eur J Radiol* 2009; **70**: 101-110 [PMID: 18242909 DOI: 10.1016/j.ejrad.2007.12.005]

137 **Rao SX**, Lambregts DM, Schnerr RS, van Ommen W, van Nijnatten TJ, Martens MH, Heijnen LA, Backes WH, Verhoef C, Zeng MS, Beets GL, Beets-Tan RG. Whole-liver CT texture analysis in colorectal cancer: Does the presence of liver metastases affect the texture of the remaining liver? *United European Gastroenterol J* 2014; **2**: 530-538 [PMID: 25452849 DOI: 10.1177/2050640614552463]

138 **Beckers RCJ**, Lambregts DMJ, Schnerr RS, Maas M, Rao SX, Kessels AGH, Thywissen T, Beets GL, Trebeschi S, Houwers JB, Dejong CH, Verhoef C, Beets-Tan RGH. Whole liver CT texture analysis to predict the development of colorectal liver metastases-A multicentre study. *Eur J Radiol* 2017; **92**: 64-71 [PMID: 28624022 DOI: 10.1016/j.ejrad.2017.04.019]

139 **Li Y**, Gong J, Shen X, Li M, Zhang H, Feng F, Tong T. Assessment of Primary Colorectal Cancer CT Radiomics to Predict Metachronous Liver Metastasis. *Front Oncol* 2022; **12**: 861892 [PMID: 35296011 DOI: 10.3389/fonc.2022.861892]

140 **Bian Y**, Jiang H, Ma C, Cao K, Fang X, Li J, Wang L, Zheng J, Lu J. Performance of CT-based radiomics in diagnosis of superior mesenteric vein resection margin in patients with pancreatic head cancer. *Abdom Radiol (NY)* 2020; **45**: 759-773 [PMID: 31932878 DOI: 10.1007/s00261-019-02401-9]

141 **Simpson G**, Spieler B, Dogan N, Portelance L, Mellon EA, Kwon D, Ford JC, Yang F. Predictive value of 0.35 T magnetic resonance imaging radiomic features in stereotactic ablative body radiotherapy of pancreatic cancer: A pilot study. *Med Phys* 2020; **47**: 3682-3690 [PMID: 32329904 DOI: 10.1002/mp.14200]

142 **Parr E**, Du Q, Zhang C, Lin C, Kamal A, McAlister J, Liang X, Bavitz K, Rux G, Hollingsworth M, Baine M, Zheng D. Radiomics-Based Outcome Prediction for Pancreatic Cancer Following Stereotactic Body Radiotherapy. *Cancers (Basel)* 2020; **12** [PMID: 32344538 DOI: 10.3390/cancers12041051]

143 **Zhang Y**, Cheng C, Liu Z, Wang L, Pan G, Sun G, Chang Y, Zuo C, Yang X. Radiomics analysis for the differentiation of autoimmune pancreatitis and pancreatic ductal adenocarcinoma in ^{18}F-FDG PET/CT. *Med Phys* 2019; **46**: 4520-4530 [PMID: 31348535 DOI: 10.1002/mp.13733]

144 **Liu Z**, Li M, Zuo C, Yang Z, Yang X, Ren S, Peng Y, Sun G, Shen J, Cheng C. Radiomics model of dual-time 2-[^{18}F]FDG PET/CT imaging to distinguish between pancreatic ductal adenocarcinoma and autoimmune pancreatitis. *Eur Radiol* 2021; **31**: 6983-6991 [PMID: 33677645 DOI: 10.1007/s00330-021-07778-0]

145 **Park S**, Chu LC, Hruban RH, Vogelstein B, Kinzler KW, Yuille AL, Fouladi DF, Shayesteh S, Ghandili S, Wolfgang CL, Burkhart R, He J, Fishman EK, Kawamoto S. Differentiating autoimmune pancreatitis from pancreatic ductal adenocarcinoma with CT radiomics features. *Diagn Interv Imaging* 2020; **101**: 555-564 [PMID: 32278586 DOI: 10.1016/j.diii.2020.03.002]

146 **Chu LC**, Park S, Kawamoto S, Fouladi DF, Shayesteh S, Zinreich ES, Graves JS, Horton KM, Hruban RH, Yuille AL, Kinzler KW, Vogelstein B, Fishman EK. Utility of CT Radiomics Features in Differentiation of Pancreatic Ductal Adenocarcinoma From Normal Pancreatic Tissue. *AJR Am J Roentgenol* 2019; **213**: 349-357 [PMID: 31012758 DOI: 10.2214/AJR.18.20901]

147 **Tomaszewski MR**, Latifi K, Boyer E, Palm RF, El Naqa I, Moros EG, Hoffe SE, Rosenberg SA, Frakes JM, Gillies RJ. Delta radiomics analysis of Magnetic Resonance guided radiotherapy imaging data can enable treatment response prediction in pancreatic cancer. *Radiat Oncol* 2021; **16**: 237 [PMID: 34911546 DOI: 10.1186/s13014-021-01957-5]

148 **Xie T**, Wang X, Li M, Tong T, Yu X, Zhou Z. Pancreatic ductal adenocarcinoma: a radiomics nomogram outperforms clinical model and TNM staging for survival estimation after curative resection. *Eur Radiol* 2020; **30**: 2513-2524 [PMID: 32006171 DOI: 10.1007/s00330-019-06600-2]

149 **Healy GM**, Salinas-Miranda E, Jain R, Dong X, Deniffel D, Borgida A, Hosni A, Ryan DT, Njeze N, McGuire A, Conlon KC, Dodd JD, Ryan ER, Grant RC, Gallinger S, Haider MA. Pre-operative radiomics model for prognostication in resectable pancreatic adenocarcinoma with external validation. *Eur Radiol* 2022; **32**: 2492-2505 [PMID: 34757450 DOI: 10.1007/s00330-021-08314-w]

150 **van Timmeren JE**, Cester D, Tanadini-Lang S, Alkadhi H, Baessler B. Radiomics in medical imaging-"how-to" guide and critical reflection. *Insights Imaging* 2020; **11**: 91 [PMID: 32785796 DOI: 10.1186/s13244-020-00887-2]

151 **Verma V**, Simone CB 2nd, Krishnan S, Lin SH, Yang J, Hahn SM. The Rise of Radiomics and Implications for Oncologic Management. *J Natl Cancer Inst* 2017; **109** [PMID: 28423406 DOI: 10.1093/jnci/djx055]

152 **Lambin P**, Leijenaar RTH, Deist TM, Peerlings J, de Jong EEC, van Timmeren J, Sanduleanu S, Larue RTHM, Even AJG, Jochems A, van Wijk Y, Woodruff H, van Soest J, Lustberg T, Roelofs E, van Elmpt W, Dekker A, Mottaghy FM, Wildberger JE, Walsh S. Radiomics: the bridge between medical imaging and personalized medicine. *Nat Rev Clin Oncol* 2017; **14**: 749-762 [PMID: 28975929 DOI: 10.1038/nrclinonc.2017.141]

153 **Zwanenburg A**, Vallières M, Abdalah MA, Aerts HJWL, Andrearczyk V, Apte A, Ashrafinia S, Bakas S, Beukinga RJ, Boellaard R, Bogowicz M, Boldrini L, Buvat I, Cook GJR, Davatzikos C, Depeursinge A, Desseroit MC, Dinapoli N, Dinh CV, Echegaray S, El Naqa I, Fedorov AY, Gatta R, Gillies RJ, Goh V, Götz M, Guckenberger M, Ha SM, Hatt M, Isensee F, Lambin P, Leger S, Leijenaar RTH, Lenkowicz J, Lippert F, Losnegård A, Maier-Hein KH, Morin O, Müller H, Napel S, Nioche C, Orlhac F, Pati S, Pfaehler EAG, Rahmim A, Rao AUK, Scherer J, Siddique MM, Sijtsema NM, Socarras Fernandez J, Spezi E, Steenbakkers RJHM, Tanadini-Lang S, Thorwarth D, Troost EGC, Upadhaya T, Valentini V, van Dijk LV, van Griethuysen J, van Velden FHP, Whybra P, Richter C, Löck S. The Image Biomarker Standardization Initiative: Standardized Quantitative Radiomics for High-Throughput Image-based Phenotyping. *Radiology* 2020; **295**: 328-338 [PMID: 32154773 DOI: 10.1148/radiol.2020191145]

154 **Zhong J**, Hu Y, Xing Y, Ge X, Ding D, Zhang H, Yao W. A systematic review of radiomics in pancreatitis: applying the evidence level rating tool for promoting clinical transferability. *Insights Imaging* 2022; **13**: 139 [PMID: 35986798 DOI: 10.1186/s13244-022-01279-4]

155 **Zhong J**, Hu Y, Ge X, Xing Y, Ding D, Zhang G, Zhang H, Yang Q, Yao W. A systematic review of radiomics in

chondrosarcoma: assessment of study quality and clinical value needs handy tools. *Eur Radiol* 2022 [PMID: 36018355 DOI: 10.1007/s00330-022-09060-3]

156 **Park CJ**, Park YW, Ahn SS, Kim D, Kim EH, Kang SG, Chang JH, Kim SH, Lee SK. Quality of Radiomics Research on Brain Metastasis: A Roadmap to Promote Clinical Translation. *Korean J Radiol* 2022; **23**: 77-88 [PMID: 34983096 DOI: 10.3348/kjr.2021.0421]

157 **Park JE**, Kim D, Kim HS, Park SY, Kim JY, Cho SJ, Shin JH, Kim JH. Quality of science and reporting of radiomics in oncologic studies: room for improvement according to radiomics quality score and TRIPOD statement. *Eur Radiol* 2020; **30**: 523-536 [PMID: 31350588 DOI: 10.1007/s00330-019-06360-z]

World Journal of Gastroenterology

Submit a Manuscript: https://www.f6publishing.com

World J Gastroenterol 2022 November 14; 28(42): 6017-6033

DOI: 10.3748/wjg.v28.i42.6017

ISSN 1007-9327 (print) ISSN 2219-2840 (online)

REVIEW

COVID-19 associated liver injury: A general review with special consideration of pregnancy and obstetric outcomes

Katherine M. Cooper, Alessandro Colletta, Alison M. Asirwatham, Tiffany A. Moore Simas, Deepika Devuni

Specialty type: Gastroenterology and hepatology

Provenance and peer review: Invited article; Externally peer reviewed.

Peer-review model: Single blind

Peer-review report's scientific quality classification

Grade A (Excellent): 0
Grade B (Very good): B, B
Grade C (Good): C
Grade D (Fair): 0
Grade E (Poor): 0

P-Reviewer: Naem AA, Germany; Rotondo JC, Italy; Zhang XQ, China

Received: September 12, 2022
Peer-review started: September 12, 2022
First decision: October 19, 2022
Revised: October 24, 2022
Accepted: October 27, 2022
Article in press: October 27, 2022
Published online: November 14, 2022

Katherine M. Cooper, Alessandro Colletta, Deepika Devuni, Department of Medicine, University of Massachusetts Chan Medical School, Worcester, MA 01605, United States

Alison M. Asirwatham, Tiffany A. Moore Simas, Department of Obstetrics and Gynecology, University of Massachusetts Chan Medical School, Worcester, MA 01605, United States

Tiffany A. Moore Simas, Departments of Pediatrics, Psychiatry, and Population & Quantitative Health Sciences, University of Massachusetts Chan Medical School, Worcester, MA 01605, United States

Deepika Devuni, Division of Gastroenterology and Hepatology, University of Massachusetts Chan Medical School, Worcester, MA 1605, United States

Corresponding author: Katherine M. Cooper, MD, Doctor, Department of Medicine, University of Massachusetts Chan Medical School, 55 N Lake Ave, Worcester, MA 01605, United States. katherine.cooper@umassmed.edu

Abstract

Liver injury is an increasingly recognized extra-pulmonary manifestation of severe acute respiratory syndrome coronavirus 2 (SARS-CoV-2) infection. Coronavirus disease 2019 (COVID-19) associated liver injury (COVALI) is a clinical syndrome encompassing all patients with biochemical liver injury identified in the setting of SARS-CoV-2 infection. Despite profound clinical implications, its pathophysiology is poorly understood. Unfortunately, most information on COVALI is derived from the general population and may not be applicable to individuals under-represented in research, including pregnant individuals. This manuscript reviews: Clinical features of COVALI, leading theories of COVALI, and existing literature on COVALI during pregnancy, a topic not widely explored in the literature. Ultimately, we synthesized data from the general and perinatal populations that demonstrates COVALI to be a hepatocellular transaminitis that is likely induced by systemic inflammation and that is strongly associated with disease severity and poorer clinical outcome, and offered perspective on approaching transaminitis in the potentially COVID-19 positive patient in the obstetric setting.

Key Words: COVID-19 liver injury; Pregnancy; Perinatal liver disease; Systemic inflammation; Special populations

Core Tip: Liver injury is an increasingly recognized extra-pulmonary manifestation of coronavirus disease 2019 (COVID-19). COVID-19 associated liver injury (COVALI) is a clinical syndrome encompassing all patients with COVID-19 infection and biochemical liver injury. Unfortunately, most information on COVALI is derived from the general population and may not be applicable to individuals under-represented in research, including pregnant individuals. In this review we summarize clinical features of COVALI and the leading theories of pathophysiology and present existing literature on COVALI during pregnancy, a topic not widely explored in the literature.

Citation: Cooper KM, Colletta A, Asirwatham AM, Moore Simas TA, Devuni D. COVID-19 associated liver injury: A general review with special consideration of pregnancy and obstetric outcomes. *World J Gastroenterol* 2022; 28(42): 6017-6033
URL: https://www.wjgnet.com/1007-9327/full/v28/i42/6017.htm
DOI: https://dx.doi.org/10.3748/wjg.v28.i42.6017

INTRODUCTION

Severe acute respiratory syndrome coronavirus 2 (SARS-CoV-2) disease pandemic (COVID-19) is responsible for and upwards of 6.3 million fatalities worldwide[1]. The SARS-CoV-2 virus is a member of the *Coronaviridae* family, a diverse family of single-stranded positive RNA viruses[2]. Coronaviruses are frequently implicated in mild upper respiratory infections and cause 15%-30% of cases of the "common cold"[3,4]. However, *Coronaviridae* viruses have also demonstrated an ability to infect the lower respiratory tract and cause severe lung disease associated with substantial mortality[5,6].

Mortality associated with COVID-19 is usually secondary to lung pathology that causes severe respiratory distress syndrome[7-9]. However, patients infected with SARS-CoV-2 often suffer other devastating end-organ injuries[10], suggesting the virus causes systemic infection and inflammation. These observations have prompted interest in the extra-pulmonary manifestations of COVID-19[11], including those in the heart[12,13], intestines[14,15], kidney[16], reproductive system[17,18], and the liver, where the effect of SARS-CoV-2 is poorly understood[19,20].

COVID-19 associated liver injury (COVALI) is a clinical entity encompassing any abnormal liver function test present in individuals positive for SARS-CoV-2[20]. Currently there are no specific or unique diagnostic criteria for COVALI relative to other causes of transaminitis[21] which complicates the process of synthesizing evidence from clinical studies. This is most salient when applying available data to those underrepresented in the literature, such as pregnant and birthing persons.

In the first section of this review, we will summarize clinical features of COVALI and the leading theories on the mechanism of liver damage in the general population. In the second section, we present existing literature on liver injury in SARS-CoV-2 positive pregnant persons, a topic not widely explored in the literature despite significant clinical relevance. Ultimately, we aim to synthesize data on COVALI in the general and perinatal populations and offer perspective on approaching this problem in the obstetric setting.

GENERAL POPULATION

Background

At the present time, COVALI is an umbrella term that applies to all patients with SARS-CoV-2 infection and transaminitis. Meta-analyses estimate that one in four patients with COVID-19 develop acute liver injury[22-24], but this figure is variable across studies and ranges from 14%-74%[25-27]. There seem to be no demographic factors to account for this variability, which may ultimately be due to differences in the study timeline or definition of liver injury[28]. Interestingly, only one of the three cited meta-analyses on COVALI included a study involving pregnant patients (n = 9)[29]. In the following sections we will review clinical and pathophysiologic considerations for COVALI in the general population.

Clinical Considerations

COVID-19 associated liver injury is a hepatocellular or mixed pattern liver injury with aspartate aminotransferase (AST) predominant transaminitis[28,30-33]. Most studies report mild liver injury with liver enzymes that peak at values less than five times the upper limit of normal[34-38]. Conversely, some reports suggest up to 25% of patients' aminotransaminases exceed this threshold[39,40] and there

is mounting evidence that liver enzymes can increase to the thousands (U/L) in patients with severe COVID-19[26,38,41-45]. The timeline of developing liver injury is not fully elucidated and has varied between studies[32,33].

Non-transaminase laboratory evidence of liver damage has also been identified, but is reported less consistently in the literature. Specifically, total bilirubin and alkaline phosphatase have been reported to be elevated in 1%-53%[46-48] and 0.3%-80.0%[48,49] of patients, respectively. This variability may be due to study timeline relative to the temporal course of laboratory changes in patients with COVALI. For example, it has been shown that alkaline phosphatase elevations begin and peak later in the disease course than aminotransaminases and may not be captured by studies that don't follow laboratory data for extended periods[50,51].

The interest in COVALI is rooted in its association with disease severity and negative patient outcomes. First, patients with elevated liver enzymes at presentation or at hospital admission are more likely to develop severe COVID-19 lung disease[5,52-54]. Additionally, a large study by Guan *et al*[55] reported laboratory data from patients at over 500 hospitals and found patients with severe COVID-19 were more likely to have transaminitis compared to patients with non-severe COVID-19. Going further, Bloom *et al*[31] studied trends in aminotransaminase levels from time of admission to peak in patients hospitalized for COVID-19 and found that in addition to higher mean AST and alanine aminotransferase (ALT), there was a greater change from baseline to peak transaminases in patients with severe compared to non-severe COVID-19. A small single center study found that elevated AST was observed more often in patients who required intensive level care compared to those who did not require intensive care[56]. Further, in a cohort of 1611 hospitalized patients across 11 Latin American countries, abnormal liver enzymes conferred a 2.6-fold risk for severe COVID-19 pneumonia and a 1.5-fold risk of death[37].

Within the umbrella of COVALI, AST has been shown to have specific prognostic value[29,37,57]. For example, the numeric value for serum AST has been incorporated in clinical calculators created to predict progression from mild or moderate to severe COVID-19 disease[57]. Moreover, elevated AST has been found to be independently associated with increased risk of death, apart from other markers of hepatic dysfunction[29,34,50,58,59]. In a study including 206 patients across 26 institutions in Brazil, AST level greater than twice the upper limit of normal significantly increased the risk of in-hospital mortality when adjusted for age and biologic sex[29]. However, is important to note that when elevated, bilirubin may be a stronger predictor of death than AST in some cohorts[34].

Given the association with poor patient outcomes, identifying potential risk factors for COVALI is imperative. We found one meta-analysis that sought to define predictors for the development of COVALI. In this study Harapan *et al*[60] pooled data from 16 studies (n = 6253) to assess whether any of the following were associated with development of severe liver injury in patients infected with SARS-CoV-2: Age, biologic sex, body mass index (BMI), diabetes mellitus, coronary artery disease, hypertension, underling liver disease, white blood cell count, lymphocyte count, and neutrophil count. They observed significant association between male sex, higher BMI, presence underlying liver disease, elevated white blood cell, and elevated lymphocyte counts with development of acute liver injury. After controlling for bias introduced by the meta-analysis, they concluded male sex and lymphocyte count were found to be independent risk factors for COVALI[60]. Not evaluated in this meta-analysis, inflammatory markers have also been shown to be a risk factor associated with liver injury[61-64]. For example, multiple studies have inflammatory markers directly correlate with liver enzymes[64] and that liver injury can be predicted using inflammatory markers such as ferritin and C-reactive protein[61,62].

Professional societies recommend clinically relevant work up for other causes of liver injury in patients who develop COVALI[21,65-68]. The American and Asian Pacific Association(s) for the Study of Liver Diseases suggest ruling out other causes of viral and toxin-mediated hepatitis in all COVID-19 patients with liver injury[21,66]. More nuanced suggestions include considering cytokine-syndrome, myositis, or cardiac injury in patients with disproportionally elevated AST, and primary sclerosing cholangitis in critically ill patients with cholestatic liver injury[21,65,66]. They advise trending liver enzymes of patients hospitalized with COVID-19, those with known chronic liver disease diagnosed with COVID-19 and of those receiving anti-retroviral medications for treatment of COVID-19 pneumonia[66]. Patients with chronic hepatitis B may be at particularly high risk both due to risk of severe infection and viral reactivation when receiving immunosuppressive therapy[66,69]. However, they do not recommend changing management and offer no specific intervention for liver injury in most cases of COVALI. They endorse targeting the viral illness in the acute setting is sufficient for liver injury and encourage work up for chronic liver disease when illness is resolved.

Pathophysiology

The underlying mechanism(s) of liver injury in COVID-19 are not fully understood. While there is increasing literature on this topic, the absence of explicit diagnostic criteria has resulted in heterogeneity in clinical studies and has impeded recognition of specific mechanisms of injury. There is consensus that COVALI is likely multifactorial and due to a combination of exacerbation of underlying liver disease, direct cytotoxicity, hypoxic liver injury, drug induced injury and systemic inflammation with immune dysregulation[28,70].

Early theories focused on exacerbation of underlying liver disease and toxicity from pharmacologic agents used to treat severe COVID-19 infection as a sources of liver injury. It is true that patients with cirrhosis are at risk for developing severe pneumonia and hepatic decompensation during SARS-CoV-2 infection[21]. Likewise, some antiviral medications used to treat COVID-19 have hepatotoxic properties and have been associated with abnormal liver function during the pandemic (*e.g.*, lopinavir/ritonavir)[27,40,61,71]. In a combination of these, SARS-CoV2 infection treated with corticosteroids or tocilizumab has been showed facilitate reactivation and accelerate liver injury in patients with chronic hepatitis B[72]. However, these two factors are unable to explain most of this phenomena as: (1) Over 90% of patients with COVALI have no evidence of underlying liver disease; and (2) transaminitis is often present at baseline prior to administration of medications[73]. While it is possible that liver injury during SARS-CoV-2 infection may be exacerbated by these factors, COVALI is likely a distinct clinical entity.

Diverse studies have demonstrated direct viral infection of the liver can occur during COVID-19 infection. In a study including 156 autopsy samples, postmortem hepatic tissue evaluation revealed typical coronavirus particles in hepatocyte cytoplasm with associated mitochondrial swelling and endoplasmic reticulum dilatation in patients who died with COVID-19[74]. Other reports have shown SARS-CoV-2 nuclear material in liver tissue, including RNA in hepatocytes of live patients who underwent liver biopsy during SARS-CoV-2 infection[75]. Some of the most convincing data comes from a recent paper by Wanner *et al*[76] who demonstrated SARS-CoV-2 can be detected in up to three-fourths of post-mortem liver biopsies using reverse transcriptase-polymerase chain reaction. Ultimately, there is irrefutable histologic evidence that SARS-CoV-2 directly infects hepatocytes, providing strong evidence that SARS-CoV-2-mediated cytopathy plays a role in COVALI. It is thought that angiotensin converting enzyme 2 and/or its receptor (ACE-2) may mediate cytopathy by enabling viral access to the liver[76,77]. However, the understanding of SARS-CoV-2 hepatotropism of is still evolving.

Epidemiology-based correlates support direct ACE-2 mediated entry into hepatocytes based on data that shows groups at increased risk of COVALI also have increased hepatic ACE-2 expression. For example, ACE-2 Levels are higher in males than females[78] and ACE-2 is upregulated in decompensated cirrhosis[79]. Interestingly, it has been shown that ACE-2 is dominantly expressed in cholangiocytes relative to hepatocytes and that infection of cholangiocytes may occur more often than infection of hepatocytes[80]. While this may seem to contradict direct cytotoxicity, it is possible that cholangiocyte infection can still result in direct viral access to the liver. In-vitro infection with SARS-CoV-2 has been associated with decreased expression of the cholangiocellular tight junctions that usually protect parenchymal liver cells from toxins in the biliary tree[81]. It has been further speculated that reduced barrier function of cholangiocytes during active COVID-19 infection may lead to hepatic injury through leakage of toxic bile into the adjacent liver parenchyma[81]. Lastly, it is known that ACE-2 can mediate viral entry into endothelial cells[82]. Viral infection of the portal systems and vascular cells in the liver may contribute to the endothelitis, microvascular changes, and intravascular thrombosis visualized in post-mortem examination of hepatic tissue in patients who died from COVID-19[83].

Reduced blood oxygen, which can negatively affect the liver, occurs in up to 50% of patients with COVID-19 infection[84]. However, only a small percentage of patients have transaminitis to the degree expected in ischemic hepatitis[34-38]. While ischemia from low blood oxygen seems to have a limited direct role in COVALI pathophysiology, the relationship between hypoxia and inflammatory pathways is significant. Specifically, hypoxia can trigger and amplify immune dysregulation *via* inflammatory pathways mediated by hypoxia inducible factor and tumor necrosis factor[85]. This may explain the link between severity of lung disease with liver injury and provide support for and transition to the inflammatory hypotheses of COVALI[86].

There is substantial data suggesting systemic inflammation and associated immune dysregulation, endotheliopathy and thrombosis are central to the pathophysiology of COVALI[87,88]. It is well established that severe COVID-19 infection induces systemic inflammation and that concentrations of several clinically evaluated inflammatory markers are increased in patients with COVID-19, such as D-dimer, C-reactive protein, procalcitonin, ferritin, and interleukin-6 (IL-6)[89-92]. Inflammatory markers are also higher in COVID-19 positive patients with biochemical liver derangements compared to COVID-19 positive patients without such derangements across, suggesting a link between liver injury and inflammation[61,62,92-94]. For example, a large retrospective analysis (n = 800) showed patients with COVID-19 complicated by COVALI had higher levels of C-reactive protein, procalcitonin, D-dimer, and serum ferritin compared to patients without COVALI[61]. In a unique study, Diaz-Louzao *et al*[86] used joint regression modeling to evaluate the temporal relationship between increases in markers of liver injury and inflammation. They found that elevation of inflammatory markers precedes elevation of liver enzymes. Ultimately they created a statistical model that implicates inflammation in causation of liver injury. The specific inflammatory markers increased during COVALI are known to be involved in *in vivo* endotheliopathy and hypercoagulability[95,96], as has been visualized in hepatic tissue of patients with liver injury secondary to COVID-19. Further, histologic findings of macrovesicular steatosis, mild acute hepatitis, portal inflammation and portal/sinusoidal thrombosis in hepatic tissue of patients who have direct viral infection of the liver support that even with direct cytopathy, inflammation may have a preceding role[83,97-100].

Interleukin-6 is an inflammatory cytokine associated with endotheliopathy and a hallmark indicator of severe COVID-19. It has been shown that IL-6 can activate platelets and precipitate endothelitis in multiple organs during systemic COVID-19 infection, particularly those with a predilection for intravascular clot formation (*e.g.*, the liver)[95]. Due to its association with biochemical liver injury[85,101-103] and known function[85,101,102], IL-6 has received interest as a likely active contributor to development of liver injury in COVID-19[103]. Recent work by McConnell *et al*[102] found a potential mechanism for this in that activating a soluble form of the IL-6 receptor triggers downstream pro-inflammatory and pro-coagulation pathways in the liver[102,104]. Further, that IL-6 signaling induces a hypercoagulable state in liver sinusoidal cells[85,104], which may contribute to the known endothelitis and thrombosis in hepatic tissue of patients with COVALI. Similarly, increased staining of a well-known platelet marker (CD-61) has been identified within dilated sinusoids in COVID-19 patients with elevated liver enzymes, suggesting activated platelets and endotheliopathy are critical in liver injury during COVID-19[85]. These findings are consistent with studies showing portal or sinusoidal vascular thrombosis is present in hepatic tissue of up to 50% of patients with COVID-19[83]. In context of literature on inflammatory markers in COVALI, Il-6 shows true mechanistic potential and bolsters the theory that inflammation, endotheliopathy and thrombosis are at the crux of this clinical syndrome.

OBSTETRIC POPULATION

Background

Liver injury is a rare and potentially serious complication of pregnancy that is estimated to affect 3%-5% of birthing persons[105]. The differential diagnosis for hepatic dysfunction in this population includes specific pregnancy related (perinatal) liver diseases[106], such as pre-eclampsia/eclampsia, hemolysis elevated liver enzymes and low platelet (HELLP) syndrome, acute fatty liver of pregnancy and intrahepatic cholestasis of pregnancy (obstetric cholestasis), and non-pregnancy related liver diseases, such as auto-immune hepatitis, viral hepatitis, non-alcoholic steatohepatitis, and now COVALI[107-109]. Perinatal liver diseases are associated with significant mortality and often require prompt delivery of the fetus for safety of the mother (summarized in Table 1). Because liver injury can strongly influence decisions regarding delivery[107], COVALI during pregnancy is of serious clinical significance.

Clinical considerations

General clinical course: Clinical characteristics of COVID-19 during pregnancy given current knowledge are well represented in the literature, but there is limited data specific to the course of liver injury. In the obstetric setting, COVALI is an AST-predominant transaminitis that affects 13%-42% of COVID-19 positive pregnant patients[108,110-112]. While these statistics are comparable to the general population, a meta-analysis that included pregnant patients reported key differences. They found (1) higher prevalence of COVALI in pregnant patients compared to non-pregnant patients; and (2) more severely elevated liver enzymes in pregnant patients with COVALI compared to non-pregnant patients with COVALI[113]. This was confirmed in a study that directly compared laboratory values of COVID-19 positive pregnant patients with non-pregnant counterparts and found COVALI was more common in pregnancy[110]. The authors of this study cautioned that many of their observations were likely related to physiological changes of pregnancy, but they concluded the rate of COVID-19 positive pregnant individuals with acute liver injury was out of proportion to expected physiologic changes. This may indicate that COVID-19 confers an increased risk of liver injury specific to pregnancy.

Clinical Cases: Obstetric providers are tasked with differentiating liver disease that necessitates urgent delivery for the health and safety of the pregnant person *vs* that which can be managed expectantly and will be stable or resolve without delivery. Multiple reports illustrate this dilemma through cases of pregnant patients with acute liver injury who are COVID-19 positive and have concurrent features of high-risk perinatal liver diseases[114-120]. We identified seven cases and classified them according to the pattern in which liver enzymes improved throughout the clinical course: A, improved without delivery; B, improved with delivery; C, other (no improvement within 72 h of delivery, no timeline of COVID-19 symptoms) (Table 2). We will discuss cases that improved without delivery and highlight features that favored COVALI relative to perinatal liver diseases.

In a case described by Azimi *et al*[115], a 27-year-old Gravida (G) 2 Para (P) 1 woman presented at 30-wk' gestation with a headache and was found to have abnormal liver enzymes, low platelets, increased inflammatory markers (LDH, ferritin D-dimer), and chest radiograph showing diffuse ground glass opacities, concerning for autoimmune disease *vs* HELLP *vs* systemic COVID-19. Pending extensive laboratory evaluation that was negative for autoantibodies and signs of hemolysis, the patient was noted to be improving with only supportive care. She was discharged at 33-wk' gestation and underwent normal delivery at 39-wk' gestation. The next case was that of a 35-year-old G2 P1 with prior obstetric cholestasis presenting at 28-wk' gestation with progressive fever and cough who was found to have high ALT and elevated serum bile acids[114]. The patient denied pruritis and had normal labs at her 20-wk appointment which reduced the likelihood of obstetric cholestasis; she subsequently tested

Table 1 Clinical characteristics and management of COVID-19 and perinatal liver diseases

	COVID-19	PEC/severe PEC	HELLP	ICHP	AFLP
Epidemiology	-	5.0%-7.5%	1%	0.3%-5.6%	0.005%-0.010%
Symptoms	Respiratory +/- GI symptoms	Variable: Headache, swelling, vision changes (or none)	Variable: Headache, nausea, vomiting, RUQ pain (or none)	Pruritis; starting at palms + soles (can be diffuse)	Nausea, vomiting, abdominal pain
Pathophysiology of liver disease	SARS-CoV-2 infection and systemic inflammation	Inflammation and imbalanced endothelial activity	Thrombotic micro-angiopathy	Hormonal cholangiopathy	Mitochondrial dysfunction + fatty acid accumulation in hepatocytes
Increased transaminases	13%-42%, 2-5 × ULN	Approximately 50%, > 2 × ULN	Typical, > 2 × ULN	Typical, > 2 × ULN	Always, < 10 × ULN
Jaundice	Rare (unclear%)	Rare	Rare (< 5%)	Uncommon (< 25%)	Mostly (> 70%)
Other findings	Radiographic lung disease	HTN, ↑ sFLT-1/PIGF	↓ PLC; ↓ haptoglobin; ↑ LDH ↑ D-dimer	↑ ALP; ↑ bile acids	Coagulopathy; hypoglycemia
Diagnosis	Viral antigen PCR or Nucleic acid amplification test (NAAT)	HTN ≥ 140/90 + organ dysfunction (proteinuria not required)	Tennessee or Mississippi classification	Bile acids (BA); > 10 umol/L	Swansea criteria; biopsy if unclear
Management	Anti-virals +/- Steroids Mono-clonal antibodies	HTN control; delivery if > 37 wk GA or > 34 wk if severe	Delivery after 34 wk GA	Ursodiol; delivery at 36 wk GA if BA > 100 or 36-39 wk if BA < 100	Prompt delivery
Complications	↑ Risk of post-partum hemorrhage; ↑ multi-systemic organ failure	↑ Complications; mortality: 1%-5%; ↑ Neonatal respiratory distress + mortality	↑ Complications Mortality: 1%-3%	↑ Neonatal complications	↑ Maternal + neonatal complications; morality: 20% (mother); 6%-77% (neonate)

Comparison of the clinical presentation and management of Coronavirus disease 2019 (COVID-19) complicated by COVID-19 associated liver injury (COVALI) in pregnant compared to liver diseases specific to pregnancy[105-107,134-138]. Many of the diseases present along a spectrum however, they each have features that can help narrow the differential diagnosis. Importantly, management of perinatal liver diseases includes early delivery in most cases based on American College of Obstetrics and Gynecology recommendations, whereas management of COVALI does not involve decisions about pregnancy delivery. SARS-CoV-2: Severe acute respiratory syndrome coronavirus 2; PEC: Pre-ec clampsia; HELLP: Hemolysis, elevated liver enzymes, low platelets; Ahellp: atypical HELLP; AFLP: Acute fatty liver of pregnancy; ICHP: Intrahepatic cholestasis of pregnancy/obstetric cholestasis; LDH: Lactate dehydrogenase; PLC: Platelet count.

positive for COVID-19 which was then thought to be the source of her liver injury. The final case is that of a 39-year-old G5P1 presenting at 26 wk' gestation with progressive dry cough and dyspnea. She was found to have new hypertension (BP 152/132), severe transaminitis (AST 1154 U/L, ALT 864 U/L), and PCR proven COVID-19 infection, concerning for pre-eclampsia with severe features *vs* systemic COVID-19[116]. Based on high suspicion for pre-eclampsia, the patient received betamethasone and dexamethasone to assist fetal lung maturation. Surprisingly, the patient's blood pressure was noted to be improving, inconsistent with pre-eclampsia which requires delivery to return to normotension. To further evaluate this, serum maternal placental growth factor was tested and normal. Normal maternal placental growth factor effectively ruled out pre-eclampsia and favored a diagnosis of COVID-19 with COVALI. This patient went on to deliver a healthy full-term fetus. In each case hypertension and liver injury improved with conservative management for COVID-19 and did not require delivery as is the case with perinatal liver diseases.

Cases in the latter two sections demonstrate complicated cases that are difficult to parse out based on clinical course. For example, in the case by Arslan *et al*[118], the patient's proteinuria was concerning for pre-eclampsia and liver enzymes trended down as expected after cesarean delivery, though both maternal and neonatal outcomes were poor which complicates interpretation of the case. Similarly, in the case by Choudhary *et al*[111], hypoglycemia and elevated bilirubin were highly suspicious for AFLP, but liver enzymes remained elevated for multiple days after delivery.

Outcomes: COVID-19 associated liver injury correlates with worse clinical outcomes and increased mortality in the obstetric setting. A retrospective cohort study of 122 COVID-19 positive pregnant patients in Istanbul found acute liver injury conferred a 3.5-fold risk of becoming critically ill during hospitalization[112]. Maternal mortality is reportedly more common in pregnant patients who delivered while COVID-19 positive with acute liver injury than COVID-19 positive without liver injury[111].

The largest published study evaluating COVALI in pregnancy is a 249-patient prospective cohort study performed at large tertiary care hospital in eastern India[111]. Unlike in previous studies, patients with hypertensive disorders, diabetic disorders, or concern for intrahepatic cholestasis were not excluded. Overall, 107 (42.1%) had evidence of hepatic dysfunction, but liver injury was more common

Table 2 Summary of case reports

Ref.	Patient	Case information	Laboratory data		Clinical course
Improved without delivery					
Anness and Siddiqui [114], 2020	35 y/o G2P1, GA 28^{5}w, PMH: IHCP	CC: Progressive dyspnea and cough; vitals: HR 133, RR 42, O2 96%; chest CT: Patchy peri-hilar inflammatory changes; differential: ICHP *vs* ICHP + COVID-19 *vs* COVID-19	AST		Normal bile acids @ GA 20
			ALT	571	↑ Bile acids and NO itch
			Bilirubin	0.76	Conservative management
			PLC	135	LFTs resolved with COVID-10
			CRP	60	Discharged home
			LDH	194	Healthy delivery at GA 39^{1}
			Ferritin		
Azimi *et al*[115], 2021	27 y/o G2P1, GA 30 wk	CC: Headache and lower limb pain; vitals: BP 100/70, HR 90-100; chest CT: Peripheral GGO's + consolidation; differential: HELLP *vs* systemic lupus *vs* COVID-19	AST	126	No delivery
			ALT	89	LFTs resolved with COVID-19
			Bilirubin	2.3	Discharged at GA 33
			PLC	220	Healthy delivery at GA 39
			CRP	114	
			LDH	1036	
			Ferritin	1360	
Naeh *et al*[116], 2022	39 y/o G5P1, GA 26^{4} wk	CC: Dry cough and dyspnea; vitals: BP 152/132, HR 141, RR 20, SpO2 96%; chest CT: Patchy multi-focal GGO's; differential: PEC with severe features *vs* COVID-19	AST	1154	Evaluated for PEC with PIGF
			ALT	864	PIGF 158 (high)→No delivery
			Bilirubin		LFTs resolving with COVID-10
			PLC	WNL	Discharged HD13; AST 331
			CRP		Healthy delivery at GA 39^{2}
			LDH	1018	
			Ferritin		
Improved with delivery					
Ronnje *et al*[117], 2020	26 y/o, G2P1, GA 32^{1} wk	CC: Cough, fever. Dyspnea, abdominal pain; vitals: BP 116/71, HR 113, RR 22, SpO2 95; chest CT bilateral diffuse GGO; differential: aHELLP *vs* COVID-19	AST	1687	5 d earlier normal labs
			ALT	348	Delivery on HD2 @ GA 32^{6}
			Bilirubin	1.23	LFTs trend down after delivery
			PLC	122	
			CRP	136	
			LDH	2039	
			Ferritin	875	
Arslan *et al*[118], 2022	30 y/o G3P2, GA 32 wk	CC: 6 d of chills, cough, dyspnea; vitals: RR 26, SpO2 84%; chest CT bilateral GGO's + peripheral thickening; differential: HELLP *vs* PEC *vs* AFLP *vs* SLE *vs* COVID-19	AST	146	HD 2: BP 185/120, + *proteinuria*, intubated, IV nitroprusside
			ALT	102	HD 3: Cardiac injury, ↓ PLC, ↑ fetal distress→ Cesarean section
			Bilirubin	2.54	HD4: LFTs improved
			PLC	59	Patient + child died
			CRP	215	
			LDH	697	
			Ferritin		
Delivery without improvement in 24-72 h of delivery (or other)					
Madaan *et al*[119], 2022	26 y/o G1P0, GA 39w	CC: RUQ pain and headache; vitals: BP 160/100, HR 98, SpO2 95%; chest	AST	589	Suspicion of HELLP→ Cesarean section

		CT: Bilateral diffuse GGO's; differential: Not given	ALT	300	Improved over hospitalization and LFTs trended down (no timeline given)
			Bilirubin	9.4	
			PLC	90	
			CRP	78.5	
			LDH	3100	
			Ferritin	734	
Choudhary *et al*[120], 2021	27 y/o G1P0, GA 35 wk, di-di twins	CC: Cough, fever, abdominal pain; vitals: BP 142/94, HR 88, RR 20. SpO2 98%; chest X-ray: Bilateral basal opacities; differential: aHELLP *vs* PEC *vs* AFLP *vs* COVID 19	AST	728.5	Suspicion of aHELLP→Cesarean-section
			ALT	473.2	POD 0: Hypo-glycemia, altered mentation, ↑ bilirubin→AFLP
			Bilirubin	4.9	Transfer to ICU + IV labetalol
			PLC	162	POD 8 discharged, normal LFT's
			CRP	22	
			LDH	96.9	
			Ferritin	120	

Gestational age is noted as week[d]. Vitals reported as: BP: Blood pressure (mmHg); HR: Heart rate (beats per minute); RR: Respiratory rate (breaths per minute); Spo2: Oxygen saturation (%). Laboratory values are reported with the following standardized units: AST: Aspartate aminotransaminase (U/L); ALT: Alanine aminotransaminase (U/L); bilirubin (mg/dL); PLC: Platelet count (× 10^3/ mm); CRP: C-reactive protein (mg/dL); LDH: Lactate dehydrogenase (u/L); ferritin (ng/dL). PEC: Pre-ec clampsia; HELLP: Hemolysis, elevated liver enzymes, low platelets; Ahellp: Atypical HELLP; AFLP: Acute fatty liver of pregnancy; ICHP: Intrahepatic cholestasis of pregnancy/obstetric cholestasis; CT: Computed tomography; GGO: Ground glass opacities; GA: Gestational age; WNL: Within normal limits; LFTs: Liver function tests; HD: Hospital day; C-section: Cesarean section; POD: Post-operative day; ICU: Intensive care unit.

in patients with perinatal hypertensive, diabetic, or cholestatic disorders (47/87, 54%) compared to those without (60/162, 37%). Although no statistical metric of significance was provided by the study, it appears that COVID-19 may increase risk of or exacerbate underlying obstetric conditions associated with liver injury. The primary aim of the study was to evaluate the relationship between liver injury in COVID-19 and obstetric outcomes. While no associations between liver injury and mode of delivery or neonatal outcomes were identified, those with liver injury tended to deliver pre-term and/or require cesarean delivery more often, both of which increase morbidity. Their key finding was that obstetric complications were significantly higher in COVID-19 positive pregnant patients with liver injury, despite no differences in maternal or gestational age[111]. Specifically, pregnant persons with COVALI were less likely to have a normal vaginal delivery than those without liver injury (18.7% *vs* 30.3%). Further, postpartum hemorrhage, sepsis, and death were more common in those who delivered while COVID-19 positive with acute liver injury[111].

Pathophysiology

The pathophysiology COVID-19 is not well studied outside the general population and thus the pathophysiology of COVALI in pregnancy is not well understood. Studies comparing COVID-19 positive pregnant individuals with acute liver injury and COVID-19 positive pregnant individuals with normal liver enzymes are crucial to build understanding of disease mechanisms in this cohort. However, there are only a handful of published studies on this to date[111,112,121]. We first use these studies to establish that relationships relevant to pathophysiology in the general population also exist in the obstetric population.

Specifically: (1) What is the relationship between severe COVID-19 disease and COVALI in pregnant patients? Patients with severe COVID-19 are more likely to develop COVALI. A prospective cohort study found that 87.5% of pregnant patients with severe COVID-19 pneumonia during hospitalization developed abnormal liver enzymes after having normal liver enzymes at baseline[122]. A later study demonstrated pregnant patients with liver injury had more severe disease and two thirds of this cohort ultimately died due to COVID-19 lung disease[111]; (2) what is the relationship between COVALI and markers of inflammation in pregnant patients? COVALI during pregnancy has been associated with elevated markers of inflammation. COVID-19 positive pregnant patients with liver injury have higher serum ferritin than expected in normal pregnancy, where a state of physiologic anemia is to be expected [112]. Furthermore, a study by Deng *et al*[121] evaluating liver chemistries in 37 COVID-19 positive pregnant patients found those with liver injury had higher inflammatory markers, such as procalcitonin and IL-6; and (3) what is the relationship between COVALI and systemic inflammatory manifestations

of COVID-19? Research by Choudhary *et al*[111] showed that obstetric complications were found to be more common in patients with COVALI. Most of these complications were related to inflammation, endotheliopathy, and coagulopathy. For example, they found pregnant persons with liver injury had higher prothrombin time and were more likely to experience postpartum hemorrhage requiring blood transfusion. Further, systemic inflammation was more common in those who delivered while COVID-19 positive with acute liver injury, as evidence by increased risk of sepsis with multi-organ failure[111].

Overall, these studies suggest the relationships between liver injury and disease severity, patient outcomes, and inflammation identified in the general population persist in the obstetric population. While pathophysiology is likely stable across cohorts, considering the increased risk of COVALI during pregnancy could help further elucidate pathophysiology.

One potential link to the increased risk is the upregulation of ACE-2 to increased plasma levels above non-pregnant individuals, secondary to increase in estrogen production[123,124]. During pregnancy ACE-2 is highly expressed in the placenta and helps regulate blood pressure *via* systemic vascular resistance. This suggests there is increased activity of ACE-2 in the endothelium of pregnant patients [125] leading to the placenta as a potential target for COVID-19 infection. The interruption of the physiologic function of ACE-2 in pregnancy has been postulated to be a major contributing factor to the development of complications[126]. Lower levels of ACE-2 have been detected in the placentas from COVID-19 positive patients, suggesting that COVID-19 infection may alter ACE-2 expression and its biologic function in both the placenta and more widely in maternal circulation[124], potentially causing endothelial dysregulation as seen in COVALI.

Based on clinical manifestations, it is also reasonable to consider that pathophysiology of COVALI resembles or amplifies that of obstetric hepatobiliary pathology. This is exhibited in the case reports narrating the difficulty of differentiating COVALI from obstetric disorders that cause transaminitis in the clinical setting. Overall, the greatest overlap occurs between severe pre-eclampsia and the extra-pulmonary manifestations of COVID-19, and pre-eclampsia has been diagnosed more often in pregnant persons with COVID-19 compared to pregnant persons without COVID-19[127,128]. A potential link to the increased risk is alpha-1-antitrypsin, an enzyme that can inhibit SARS-CoV-2 infection and protects endothelial cells from oxidative stress during pregnancy, which is reduced in seen in pregnant patients with pre-eclampsia[129,130].

Work by Mendoza *et al*[122] sought to determine the prevalence of "pre-eclampsia findings" in 42 COVID-19 positive pregnant women. Eight women had severe pneumonia secondary to COVID-19 of which seven (87.5%) had elevated liver enzymes consistent with COVALI and five (62.5%) had hypertension meeting criteria for pre-eclampsia. However, sonographic evidence of placental hypoperfusion was only found in one patient who ultimately required delivery to prompt resolution of hypertension and liver injury. The remaining patients did not require delivery and instead, liver injury and hypertension improved in parallel with symptoms of pneumonia due to COVID-19. They measured ratio of soluble fms-like tyrosine kinase-1 (sFlt-1) ad serum placental growth factor (PIGF), which has been shown to be predictive of pre-eclampsia[131], and found sFlt-1/PIGF normal ratio in patients who did not require delivery compared to an elevated sFlt-1/PIGF ratio in the patient with evidence of placental hypoperfusion who required delivery. These findings suggest severe COVID-19 complicated by COVALI can mimic hypertensive disease of pregnancy and may represent shared disease mechanisms (Figure 1).

Literature that was published during the writing of this review directly compared the pathophysiology of pre-eclampsia and COVID-19. In this study, Palomo *et al*[132] compared endothelial inflammation and angiogenesis in pregnant patients with pre-eclampsia *vs* COVID-19 pneumonia *vs* normotensive controls. They measured circulating inflammatory markers in patient blood and found different biomarker profiles of coagulopathy, endothelial inflammation, and angiogenesis. Both COVID-19 and pre-eclampsia had increased vascular cell adhesion molecules expression relative to controls and increased markers of innate immunity. Fortunately, there were multiple factors helpful in differentiating pre-eclampsia and COVID-19: (1) COVID-19 had higher von Willebrand factor and soluble tumor necrosis factor-receptor but lower PIGF; and (2) Pre-eclampsia had higher soluble tumor necrosis factor-receptor and sFlt-1but lower von Willebrand factor. They observed altered sFlt-1 to PlGF ratio was predictive of pre-eclampsia, consistent with findings of Mendoza *et al*[122] In the latter part of their study they observed how sera from each patient cohort induced change when applied to human dermal microvascular cells. Despite different angiogenic and endothelial profiles, sera from both cohorts activated a common downstream pathway associated with endothelial inflammation, potentially indicating a shared end-pathway. While liver injury was not specifically evaluated in this study, these findings can be interpreted as evidence supporting endothelial dysfunction and inflammation as drivers of systemic manifestations of COVID-19 that are also present in pre-eclampsia, such as liver injury. Shared histologic findings in COVALI and pre-eclampsia including microvascular changes and signs of platelet activation, further support this theory[106,133].

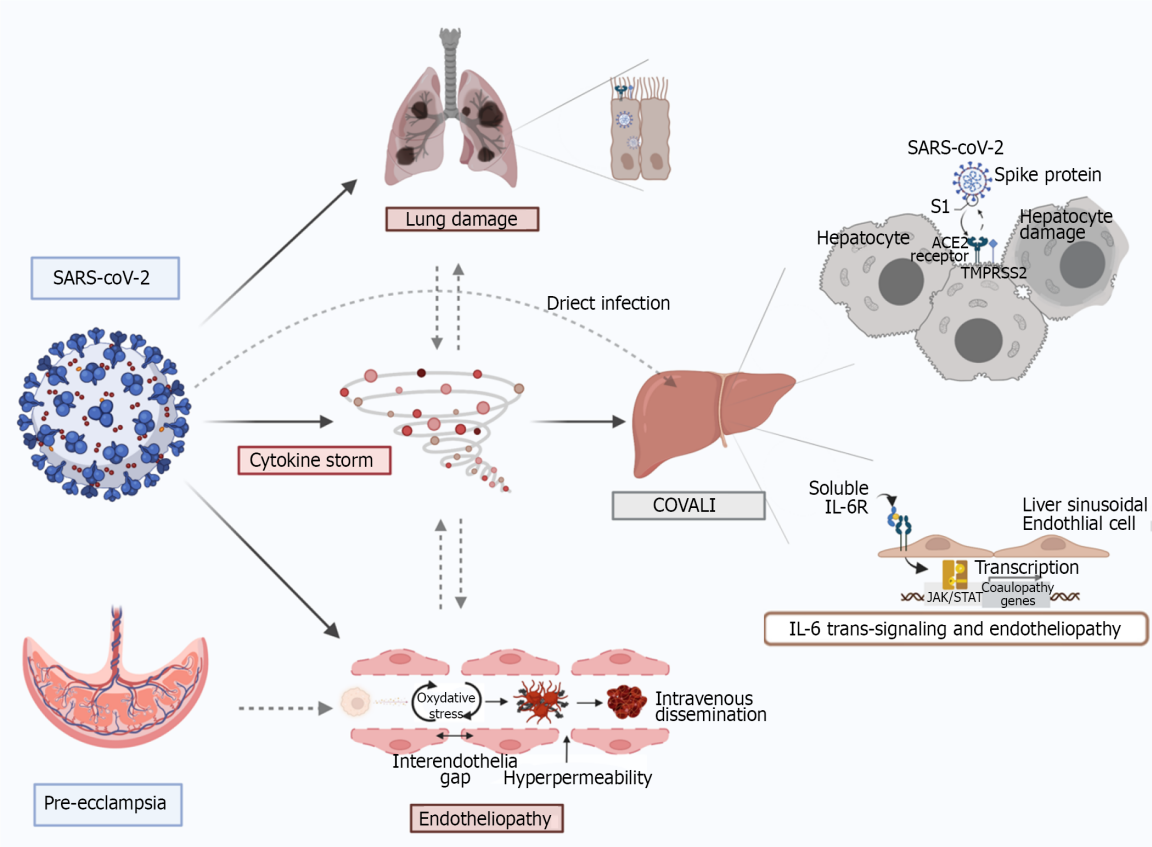

DOI: 10.3748/wjg.v28.i42.6017

Figure 1 Mechanisms of COVID-19-associated liver injury: Inter-organ crosstalk. Severe acute respiratory syndrome coronavirus 2 (SARS-CoV-2) enters host cells *via* interaction of its spike protein with the receptor angiotensin converting enzyme 2 in the presence of TMPRSS2 in many tissues. Proposed mechanisms for SARS-CoV-2-mediaded liver injury include: (1) Direct viral cytopathic effect; (2) IL-6 trans-signaling in liver sinusoidal endothelial cells which leads to endotheliopathy; (3) cytokine storm-induced damage; and (4) hypoxemic injury. There is also a lung-gut crosstalk which promotes an increased inflammatory state as well as dysbiosis which increases intestinal permeability, thus facilitating viral entry. Furthermore, direct viral injury to the vascular endothelium leads to increased cytokine release, enhanced reactive oxygen species production and thrombo-embolic events involving both micro and macro circulation. In a similar fashion, pre-eclampsia spectrum syndromes cause inflammation and endotheliopathy that pre-disposes to liver injury and can be synergistic coronavirus disease 2019 (COVID-19) and COVID-19 associated liver injury. Original figure was created with BioRender.com.

CONCLUSION

In this paper we reviewed COVID-19 associated liver injury with a special focus on pregnancy. We demonstrated COVALI to be an inflammatory mediated AST-predominant transaminitis associated with COVID-19 disease severity and poorer patient outcomes. Emerging research in the general and obstetric populations supports inflammation and endothelial dysfunction as central to pathophysiology in systemic COVID-19 and COVALI. Figure 1 summarizes proposed mechanisms of COVALI and illustrates how some physiologic changes in pregnancy can pre-dispose or exacerbate processes of liver injury during COVID-19. There is significant opportunity to improve understanding of COVALI during pregnancy. At present COVALI appears to be independently associated with worse post-partum outcomes, though this has not been fully parsed on in the literature. Further research should be done to elucidate the relationship between post-partum outcomes and COVALI, relevant to short and long-term outcomes. There is also data supporting the use of specific of circulating biomarkers to differentiate systemic COVID-19 from other causes of transaminitis in pregnancy, but further research is required to define criteria that can guide management.

FOOTNOTES

Author contributions: Cooper KM conceptualized this article, completed research collection, and lead the writing and editing of the manuscript; Colletta A assisted in conceptualizing the article, wrote portions of the manuscript, edited the initial, and revised manuscripts; Asirwatham AM assisted in conceptualizing portions of the article and provided expert feedback in the area of Obstetrics and Gynecology; Moore Simas TA reviewed content, edited the initial and revised manuscript, and provided expert feedback in the area of Obstetrics and Gynecology; Devuni D reviewed content, edited the initial and revised manuscript, and provided expert feedback in the area of Hepatology.

Conflict-of-interest statement: Devuni D is an Associate Professor of Medicine at UMass Chan Medical School, she has received grant funding from Sequana Medical for a clinical trial unrelated to the present work; all other authors have no conflicts of interest to report.

Country/Territory of origin: United States

ORCID number: Katherine M. Cooper 0000-0002-6030-4773; Tiffany A. Moore Simas 0000-0002-8356-6418.

S-Editor: Chen YL
L-Editor: A
P-Editor: Chen YL

REFERENCES

1 **World Health Organization**. WHO Coronavirus (COVID-19) Dashboard. July 9, 2022. [cited 23 October 2022]. Available from: https://covid19.who.int
2 **V'kovski P**, Kratzel A, Steiner S, Stalder H, Thiel V. Coronavirus biology and replication: implications for SARS-CoV-2. *Nat Rev Microbiol* 2021; **19**: 155-170 [PMID: 33116300 DOI: 10.1038/s41579-020-00468-6]
3 **Mesel-Lemoine M**, Millet J, Vidalain PO, Law H, Vabret A, Lorin V, Escriou N, Albert ML, Nal B, Tangy F. A human coronavirus responsible for the common cold massively kills dendritic cells but not monocytes. *J Virol* 2012; **86**: 7577-7587 [PMID: 22553325 DOI: 10.1128/JVI.00269-12]
4 **Abbasi J**. COVID-19 and the Common Cold-Preexisting Coronavirus Antibodies May Hinder SARS-CoV-2 Immunity. *JAMA* 2022; **327**: 609-610 [PMID: 35080593 DOI: 10.1001/jama.2022.0326]
5 **Zhang C**, Shi L, Wang FS. Liver injury in COVID-19: management and challenges. *Lancet Gastroenterol Hepatol* 2020; **5**: 428-430 [PMID: 32145190 DOI: 10.1016/S2468-1253(20)30057-1]
6 **Coronaviridae Study Group of the International Committee on Taxonomy of Viruses**. The species Severe acute respiratory syndrome-related coronavirus: classifying 2019-nCoV and naming it SARS-CoV-2. *Nat Microbiol* 2020; **5**: 536-544 [PMID: 32123347 DOI: 10.1038/s41564-020-0695-z]
7 **Wang FS**, Zhang C. What to do next to control the 2019-nCoV epidemic? *Lancet* 2020; **395**: 391-393 [PMID: 32035533 DOI: 10.1016/S0140-6736(20)30300-7]
8 **Slater TA**, Straw S, Drozd M, Kamalathasan S, Cowley A, Witte KK. Dying 'due to' or 'with' COVID-19: a cause of death analysis in hospitalised patients. *Clin Med (Lond)* 2020; **20**: e189-e190 [PMID: 32753516 DOI: 10.7861/clinmed.2020-0440]
9 **Ketcham SW**, Bolig TC, Molling DJ, Sjoding MW, Flanders SA, Prescott HC. Causes and Circumstances of Death among Patients Hospitalized with COVID-19: A Retrospective Cohort Study. *Ann Am Thorac Soc* 2021; **18**: 1076-1079 [PMID: 33315531 DOI: 10.1513/AnnalsATS.202011-1381RL]
10 **Gupta A**, Madhavan MV, Sehgal K, Nair N, Mahajan S, Sehrawat TS, Bikdeli B, Ahluwalia N, Ausiello JC, Wan EY, Freedberg DE, Kirtane AJ, Parikh SA, Maurer MS, Nordvig AS, Accili D, Bathon JM, Mohan S, Bauer KA, Leon MB, Krumholz HM, Uriel N, Mehra MR, Elkind MSV, Stone GW, Schwartz A, Ho DD, Bilezikian JP, Landry DW. Extrapulmonary manifestations of COVID-19. *Nat Med* 2020; **26**: 1017-1032 [PMID: 32651579 DOI: 10.1038/s41591-020-0968-3]
11 **Louis TJ**, Qasem A, Abdelli LS, Naser SA. Extra-Pulmonary Complications in SARS-CoV-2 Infection: A Comprehensive Multi Organ-System Review. *Microorganisms* 2022; **10** [PMID: 35056603 DOI: 10.3390/microorganisms10010153]
12 **Zaccone G**, Tomasoni D, Italia L, Lombardi CM, Metra M. Myocardial Involvement in COVID-19: an Interaction Between Comorbidities and Heart Failure with Preserved Ejection Fraction. A Further Indication of the Role of Inflammation. *Curr Heart Fail Rep* 2021; **18**: 99-106 [PMID: 33890193 DOI: 10.1007/s11897-021-00509-y]
13 **Haddadin FI**, Mahdawi TE, Hattar L, Beydoun H, Fram F, Homoud M. A case of complete heart block in a COVID-19 infected patient. *J Cardiol Cases* 2021; **23**: 27-30 [PMID: 32904735 DOI: 10.1016/j.jccase.2020.08.006]
14 **Tao W**, Wang X, Zhang G, Guo M, Ma H, Zhao D, Sun Y, He J, Liu L, Zhang K, Wang Y, Weng J, Ma X, Jin T, Zhu S. Re-detectable positive SARS-CoV-2 RNA tests in patients who recovered from COVID-19 with intestinal infection. *Protein Cell* 2021; **12**: 230-235 [PMID: 32978728 DOI: 10.1007/s13238-020-00778-8]
15 **Lehmann M**, Allers K, Heldt C, Meinhardt J, Schmidt F, Rodriguez-Sillke Y, Kunkel D, Schumann M, Böttcher C, Stahl-Hennig C, Elezkurtaj S, Bojarski C, Radbruch H, Corman VM, Schneider T, Loddenkemper C, Moos V, Weidinger C, Kühl AA, Siegmund B. Human small intestinal infection by SARS-CoV-2 is characterized by a mucosal infiltration with activated $CD8^+$ T cells. *Mucosal Immunol* 2021; **14**: 1381-1392 [PMID: 34420043 DOI: 10.1038/s41385-021-00437-z]
16 **Puelles VG**, Lütgehetmann M, Lindenmeyer MT, Sperhake JP, Wong MN, Allweiss L, Chilla S, Heinemann A, Wanner N, Liu S, Braun F, Lu S, Pfefferle S, Schröder AS, Edler C, Gross O, Glatzel M, Wichmann D, Wiech T, Kluge S, Pueschel K, Aepfelbacher M, Huber TB. Multiorgan and Renal Tropism of SARS-CoV-2. *N Engl J Med* 2020; **383**: 590-

592 [PMID: 32402155 DOI: 10.1056/NEJMc2011400]
17 **Wang N**, Qin L, Ma L, Yan H. Effect of severe acute respiratory syndrome coronavirus-2 (SARS-CoV-2) on reproductive system. *Stem Cell Res* 2021; **52**: 102189 [PMID: 33582547 DOI: 10.1016/j.scr.2021.102189]
18 **Liu C**, Mu C, Zhang Q, Yang X, Yan H, Jiao H. Effects of Infection with SARS-CoV-2 on the Male and Female Reproductive Systems: A Review. *Med Sci Monit* 2021; **27**: e930168 [PMID: 34193809 DOI: 10.12659/MSM.930168]
19 **Marjot T**, Webb GJ, Barritt AS 4th, Moon AM, Stamataki Z, Wong VW, Barnes E. COVID-19 and liver disease: mechanistic and clinical perspectives. *Nat Rev Gastroenterol Hepatol* 2021; **18**: 348-364 [PMID: 33692570 DOI: 10.1038/s41575-021-00426-4]
20 **Mohammed SA**, Eid KM, Anyiam FE, Wadaaallah H, Muhamed MAM, Morsi MH, Dahman NBH. Liver injury with COVID-19: laboratory and histopathological outcome-systematic review and meta-analysis. *Egypt Liver J* 2022; **12**: 9 [PMID: 35096428 DOI: 10.1186/s43066-022-00171-6]
21 **APASL Covid-19 Task Force**, Lau G, Sharma M. Clinical practice guidance for hepatology and liver transplant providers during the COVID-19 pandemic: APASL expert panel consensus recommendations. *Hepatol Int* 2020; **14**: 415-428 [PMID: 32447721 DOI: 10.1007/s12072-020-10054-w]
22 **Wijarnpreecha K**, Ungprasert P, Panjawatanan P, Harnois DM, Zaver HB, Ahmed A, Kim D. COVID-19 and liver injury: a meta-analysis. *Eur J Gastroenterol Hepatol* 2021; **33**: 990-995 [PMID: 32639420 DOI: 10.1097/MEG.0000000000001817]
23 Alimentary Pharmacology and Therapeutics in 2018 - big changes but much the same. *Aliment Pharmacol Ther* 2018; **47**: 4 [PMID: 29226419 DOI: 10.1111/apt.14344]
24 **Labenz C**, Toenges G, Wörns MA, Sprinzl MF, Galle PR, Schattenberg JM. Liver injury in patients with severe acute respiratory syndrome coronavirus-2 infection: a systematic review and meta-analysis. *Eur J Gastroenterol Hepatol* 2021; **33**: 1194-1200 [PMID: 32796355 DOI: 10.1097/MEG.0000000000001827]
25 **Cai Q**, Huang D, Ou P, Yu H, Zhu Z, Xia Z, Su Y, Ma Z, Zhang Y, Li Z, He Q, Liu L, Fu Y, Chen J. COVID-19 in a designated infectious diseases hospital outside Hubei Province, China. *Allergy* 2020; **75**: 1742-1752 [PMID: 32239761 DOI: 10.1111/all.14309]
26 **Cai Q**, Huang D, Yu H, Zhu Z, Xia Z, Su Y, Li Z, Zhou G, Gou J, Qu J, Sun Y, Liu Y, He Q, Chen J, Liu L, Xu L. COVID-19: Abnormal liver function tests. *J Hepatol* 2020; **73**: 566-574 [PMID: 32298767 DOI: 10.1016/j.jhep.2020.04.006]
27 **Fan Z**, Chen L, Li J, Cheng X, Yang J, Tian C, Zhang Y, Huang S, Liu Z, Cheng J. Clinical Features of COVID-19-Related Liver Functional Abnormality. *Clin Gastroenterol Hepatol* 2020; **18**: 1561-1566 [PMID: 32283325 DOI: 10.1016/j.cgh.2020.04.002]
28 **Yu D**, Du Q, Yan S, Guo XG, He Y, Zhu G, Zhao K, Ouyang S. Liver injury in COVID-19: clinical features and treatment management. *Virol J* 2021; **18**: 121 [PMID: 34108015 DOI: 10.1186/s12985-021-01593-1]
29 **Pozzobon FM**, Perazzo H, Bozza FA, Rodrigues RS, de Mello Perez R, Chindamo MC. Liver injury predicts overall mortality in severe COVID-19: a prospective multicenter study in Brazil. *Hepatol Int* 2021; **15**: 493-501 [PMID: 33534084 DOI: 10.1007/s12072-021-10141-6]
30 **Pazgan-Simon M**, Serafińska S, Kukla M, Kucharska M, Zuwała-Jagiełło J, Buczyńska I, Zielińska K, Simon K. Liver Injury in Patients with COVID-19 without Underlying Liver Disease. *J Clin Med* 2022; **11** [PMID: 35054003 DOI: 10.3390/jcm11020308]
31 **Bloom PP**, Meyerowitz EA, Reinus Z, Daidone M, Gustafson J, Kim AY, Schaefer E, Chung RT. Liver Biochemistries in Hospitalized Patients With COVID-19. *Hepatology* 2021; **73**: 890-900 [PMID: 32415860 DOI: 10.1002/hep.31326]
32 **Gomi K**, Ito T, Yamaguchi F, Kamio Y, Sato Y, Mori H, Endo K, Abe T, Sakakura S, Kobayashi K, Shimada K, Noda J, Hibiki T, Ohta S, Sagara H, Tanaka A, Jinno M, Yamawaki M, Nishimoto F, Inoue K, Nagahama M. Clinical features and mechanism of liver injury in patients with mild or moderate coronavirus disease 2019. *JGH Open* 2021; **5**: 888-895 [PMID: 34386596 DOI: 10.1002/jgh3.12599]
33 **Chew M**, Tang Z, Radcliffe C, Caruana D, Doilicho N, Ciarleglio MM. Significant liver injury during hospitalization for COVID-19 is not associated with liver insufficiency or death. *Clin Gastroenterol Hepatol* 2021; **19**: 2182-91. e7
34 **Zhang SS**, Dong L, Wang GM, Tian Y, Ye XF, Zhao Y, Liu ZY, Zhai JY, Zhao ZL, Wang JH, Zhang HM, Li XL, Wu CX, Yang CT, Yang LJ, Du HX, Wang H, Ge QG, Xiu DR, Shen N. Progressive liver injury and increased mortality risk in COVID-19 patients: A retrospective cohort study in China. *World J Gastroenterol* 2021; **27**: 835-853 [PMID: 33727773 DOI: 10.3748/wjg.v27.i9.835]
35 **Wong YJ**, Tan M, Zheng Q, Li JW, Kumar R, Fock KM, Teo EK, Ang TL. A systematic review and meta-analysis of the COVID-19 associated liver injury. *Ann Hepatol* 2020; **19**: 627-634 [PMID: 32882393 DOI: 10.1016/j.aohep.2020.08.064]
36 **Zhang Q**, Li J, Zhang Y, Gao J, Wang P, Ai M, Ding W, Tan X. Differences in clinical characteristics and liver injury between suspected and confirmed COVID-19 patients in Jingzhou, Hubei Province of China. *Medicine (Baltimore)* 2021; **100**: e25913 [PMID: 34106656 DOI: 10.1097/MD.0000000000025913]
37 **Mendizabal M**, Piñero F, Ridruejo E, Anders M, Silveyra MD, Torre A, Montes P, Urzúa A, Pages J, Toro LG, Díaz J, Gonzalez Ballerga E, Miranda-Zazueta G, Peralta M, Gutiérrez I, Michelato D, Venturelli MG, Varón A, Vera-Pozo E, Tagle M, García M, Tassara A, Brutti J, Ruiz García S, Bustios C, Escajadillo N, Macias Y, Higuera-de la Tijera F, Gómez AJ, Dominguez A, Castillo-Barradas M, Contreras F, Scarpin A, Schinoni MI, Toledo C, Girala M, Mainardi V, Sanchez A, Bessone F, Rubinstein F, Silva MO. Prospective Latin American cohort evaluating outcomes of patients with COVID-19 and abnormal liver tests on admission. *Ann Hepatol* 2021; **21**: 100298 [PMID: 33359234 DOI: 10.1016/j.aohep.2020.100298]
38 **Chen N**, Zhou M, Dong X, Qu J, Gong F, Han Y, Qiu Y, Wang J, Liu Y, Wei Y, Xia J, Yu T, Zhang X, Zhang L. Epidemiological and clinical characteristics of 99 cases of 2019 novel coronavirus pneumonia in Wuhan, China: a descriptive study. *Lancet* 2020; **395**: 507-513 [PMID: 32007143 DOI: 10.1016/S0140-6736(20)30211-7]
39 **Serviddio G**, Villani R, Stallone G, Scioscia G, Foschino-Barbaro MP, Lacedonia D. Tocilizumab and liver injury in patients with COVID-19. *Therap Adv Gastroenterol* 2020; **13**: 1756284820959183 [PMID: 33101458 DOI: 10.1177/1756284820959183]

40 **Hundt MA**, Deng Y, Ciarleglio MM, Nathanson MH, Lim JK. Abnormal Liver Tests in COVID-19: A Retrospective Observational Cohort Study of 1,827 Patients in a Major U.S. Hospital Network. *Hepatology* 2020; **72**: 1169-1176 [PMID: 32725890 DOI: 10.1002/hep.31487]

41 **Orandi BJ**, Li G, Dhall D, Bajpai P, Manne U, Arora N. Acute liver failure in a healthy young female with COVID-19. *JPGN Reports* 2021; **2**: e108 [DOI: 10.1097/pg9.0000000000000108]

42 **Wander P**, Epstein M, Bernstein D. COVID-19 Presenting as Acute Hepatitis. *Am J Gastroenterol* 2020; **115**: 941-942 [PMID: 32301760 DOI: 10.14309/ajg.0000000000000660]

43 **Dehghani S**, Teimouri A. Severe Acute Hepatitis in a COVID-19 patient: A Case Report. *Clin Case Rep* 2021; **9**: e04869 [PMID: 34667602 DOI: 10.1002/ccr3.4869]

44 **Gurala D**, Al Moussawi H, Philipose J, Abergel JR. Acute Liver Failure in a COVID-19 Patient Without any Preexisting Liver Disease. *Cureus* 2020; **12**: e10045 [PMID: 32983735 DOI: 10.7759/cureus.10045]

45 **Elmunzer BJ**, Spitzer RL, Foster LD, Merchant AA, Howard EF, Patel VA, West MK, Qayed E, Nustas R, Zakaria A, Piper MS, Taylor JR, Jaza L, Forbes N, Chau M, Lara LF, Papachristou GI, Volk ML, Hilson LG, Zhou S, Kushnir VM, Lenyo AM, McLeod CG, Amin S, Kuftinec GN, Yadav D, Fox C, Kolb JM, Pawa S, Pawa R, Canakis A, Huang C, Jamil LH, Aneese AM, Glamour BK, Smith ZL, Hanley KA, Wood J, Patel HK, Shah JN, Agarunov E, Sethi A, Fogel EL, McNulty G, Haseeb A, Trieu JA, Dixon RE, Yang JY, Mendelsohn RB, Calo D, Aroniadis OC, LaComb JF, Scheiman JM, Sauer BG, Dang DT, Piraka CR, Shah ED, Pohl H, Tierney WM, Mitchell S, Condon A, Lenhart A, Dua KS, Kanagala VS, Kamal A, Singh VK, Pinto-Sanchez MI, Hutchinson JM, Kwon RS, Korsnes SJ, Singh H, Solati Z, Willingham FF, Yachimski PS, Conwell DL, Mosier E, Azab M, Patel A, Buxbaum J, Wani S, Chak A, Hosmer AE, Keswani RN, DiMaio CJ, Bronze MS, Muthusamy R, Canto MI, Gjeorgjievski VM, Imam Z, Odish F, Edhi AI, Orosey M, Tiwari A, Patwardhan S, Brown NG, Patel AA, Ordiah CO, Sloan IP, Cruz L, Koza CL, Okafor U, Hollander T, Furey N, Reykhart O, Zbib NH, Damianos JA, Esteban J, Hajidiacos N, Saul M, Mays M, Anderson G, Wood K, Mathews L, Diakova G, Caisse M, Wakefield L, Nitchie H, Waljee AK, Tang W, Zhang Y, Zhu J, Deshpande AR, Rockey DC, Alford TB, Durkalski V; North American Alliance for the Study of Digestive Manifestations of COVID-19. Digestive Manifestations in Patients Hospitalized With Coronavirus Disease 2019. *Clin Gastroenterol Hepatol* 2021; **19**: 1355-1365.e4 [PMID: 33010411 DOI: 10.1016/j.cgh.2020.09.041]

46 **Kumar A**, Kumar P, Dungdung A, Kumar Gupta A, Anurag A, Kumar A. Pattern of liver function and clinical profile in COVID-19: A cross-sectional study of 91 patients. *Diabetes Metab Syndr* 2020; **14**: 1951-1954 [PMID: 33039937 DOI: 10.1016/j.dsx.2020.10.001]

47 **Hwaiz R**, Merza M, Hamad B, HamaSalih S, Mohammed M, Hama H. Evaluation of hepatic enzymes activities in COVID-19 patients. *Int Immunopharmacol* 2021; **97**: 107701 [PMID: 33930704 DOI: 10.1016/j.intimp.2021.107701]

48 **Bzeizi K**, Abdulla M, Mohammed N, Alqamish J, Jamshidi N, Broering D. Effect of COVID-19 on liver abnormalities: a systematic review and meta-analysis. *Sci Rep* 2021; **11**: 10599 [PMID: 34012016 DOI: 10.1038/s41598-021-89513-9]

49 **Sivandzadeh GR**, Askari H, Safarpour AR, Ejtehadi F, Raeis-Abdollahi E, Vaez Lari A, Abazari MF, Tarkesh F, Bagheri Lankarani K. COVID-19 infection and liver injury: Clinical features, biomarkers, potential mechanisms, treatment, and management challenges. *World J Clin Cases* 2021; **9**: 6178-6200 [PMID: 34434987 DOI: 10.12998/wjcc.v9.i22.6178]

50 **Lei F**, Liu YM, Zhou F, Qin JJ, Zhang P, Zhu L, Zhang XJ, Cai J, Lin L, Ouyang S, Wang X, Yang C, Cheng X, Liu W, Li H, Xie J, Wu B, Luo H, Xiao F, Chen J, Tao L, Cheng G, She ZG, Zhou J, Wang H, Lin J, Luo P, Fu S, Ye P, Xiao B, Mao W, Liu L, Yan Y, Chen G, Huang X, Zhang BH, Yuan Y. Longitudinal Association Between Markers of Liver Injury and Mortality in COVID-19 in China. *Hepatology* 2020; **72**: 389-398 [PMID: 32359177 DOI: 10.1002/hep.31301]

51 **Xu W**, Huang C, Fei L, Li Q, Chen L. Dynamic Changes in Liver Function Tests and Their Correlation with Illness Severity and Mortality in Patients with COVID-19: A Retrospective Cohort Study. *Clin Interv Aging* 2021; **16**: 675-685 [PMID: 33911856 DOI: 10.2147/CIA.S303629]

52 **Kunutsor SK**, Laukkanen JA. Markers of liver injury and clinical outcomes in COVID-19 patients: A systematic review and meta-analysis. *J Infect* 2021; **82**: 159-198 [PMID: 32474033 DOI: 10.1016/j.jinf.2020.05.045]

53 **Chen Y**, Zhou X, Yan H, Huang H, Li S, Jiang Z, Zhao J, Meng Z. CANPT Score: A Tool to Predict Severe COVID-19 on Admission. *Front Med (Lausanne)* 2021; **8**: 608107 [PMID: 33681245 DOI: 10.3389/fmed.2021.608107]

54 **Piano S**, Dalbeni A, Vettore E, Benfaremo D, Mattioli M, Gambino CG, Framba V, Cerruti L, Mantovani A, Martini A, Luchetti MM, Serra R, Cattelan A, Vettor R, Angeli P; COVID-LIVER study group. Abnormal liver function tests predict transfer to intensive care unit and death in COVID-19. *Liver Int* 2020; **40**: 2394-2406 [PMID: 32526083 DOI: 10.1111/liv.14565]

55 **Guan WJ**, Ni ZY, Hu Y, Liang WH, Ou CQ, He JX. Clinical characteristics of 2019 novel coronavirus infection in China. *MedRxiv* 2020 [DOI: 10.1101/2020.02.06.20020974]

56 **Huang C**, Wang Y, Li X, Ren L, Zhao J, Hu Y, Zhang L, Fan G, Xu J, Gu X, Cheng Z, Yu T, Xia J, Wei Y, Wu W, Xie X, Yin W, Li H, Liu M, Xiao Y, Gao H, Guo L, Xie J, Wang G, Jiang R, Gao Z, Jin Q, Wang J, Cao B. Clinical features of patients infected with 2019 novel coronavirus in Wuhan, China. *Lancet* 2020; **395**: 497-506 [PMID: 31986264 DOI: 10.1016/S0140-6736(20)30183-5]

57 **Wang M**, Wu D, Liu CH, Li Y, Hu J, Wang W, Jiang W, Zhang Q, Huang Z, Bai L, Tang H. Predicting progression to severe COVID-19 using the PAINT score. *BMC Infect Dis* 2022; **22**: 498 [PMID: 35619076 DOI: 10.1186/s12879-022-07466-4]

58 **Madian A**, Eliwa A, Abdalla H, Aly HAA. Hepatocellular injury and the mortality risk among patients with COVID-19: A retrospective cohort study. *World J Hepatol* 2021; **13**: 939-948 [PMID: 34552700 DOI: 10.4254/wjh.v13.i8.939]

59 **Ding ZY**, Li GX, Chen L, Shu C, Song J, Wang W, Wang YW, Chen Q, Jin GN, Liu TT, Liang JN, Zhu P, Zhu W, Li Y, Zhang BH, Feng H, Zhang WG, Yin ZY, Yu WK, Yang Y, Zhang HQ, Tang ZP, Wang H, Hu JB, Liu JH, Yin P, Chen XP, Zhang B; Tongji Multidisciplinary Team for Treating COVID-19 (TTTC). Association of liver abnormalities with in-hospital mortality in patients with COVID-19. *J Hepatol* 2021; **74**: 1295-1302 [PMID: 33347952 DOI: 10.1016/j.jhep.2020.12.012]

60 **Harapan H**, Fajar JK, Supriono S, Soegiarto G, Wulandari L, Seratin F, Prayudi NG, Dewi DP, Monica Elsina MT, Atamou L, Wiranata S, Aprianto DP, Friska E, Sari Firdaus DF, Alaidin M, Wardhani FA, Husnah M, Hidayati NW,

Hendriyanti Y, Wardani K, Evatta A, Manugan RA, Pradipto W, Rahmawati A, Tamara F, Mahendra AI, Nainu F, Santoso B, Irawan Primasatya CA, Tjionganata N, Budiman HA. The prevalence, predictors and outcomes of acute liver injury among patients with COVID-19: A systematic review and meta-analysis. *Rev Med Virol* 2022; **32**: e2304 [PMID: 34643006 DOI: 10.1002/rmv.2304]

61 **Chu H**, Bai T, Chen L, Hu L, Xiao L, Yao L, Zhu R, Niu X, Li Z, Zhang L, Han C, Song S, He Q, Zhao Y, Zhu Q, Chen H, Schnabl B, Yang L, Hou X. Multicenter Analysis of Liver Injury Patterns and Mortality in COVID-19. *Front Med (Lausanne)* 2020; **7**: 584342 [PMID: 33195339 DOI: 10.3389/fmed.2020.584342]

62 **Cao P**, Wu Y, Wu S, Wu T, Zhang Q, Zhang R, Wang Z, Zhang Y. Elevated serum ferritin level effectively discriminates severity illness and liver injury of coronavirus disease 2019 pneumonia. *Biomarkers* 2021; **26**: 207-212 [PMID: 33284041 DOI: 10.1080/1354750X.2020.1861098]

63 **Goel H**, Harmouch F, Garg K, Saraiya P, Daly T, Kumar A, Hippen JT. The liver in COVID-19: prevalence, patterns, predictors, and impact on outcomes of liver test abnormalities. *Eur J Gastroenterol Hepatol* 2021; **33**: e274-e281 [PMID: 33369962 DOI: 10.1097/MEG.0000000000002021]

64 **Mishra K**, Naffouj S, Gorgis S, Ibrahim H, Gill S, Fadel R, Chatfield A, Tang A, Salgia R. Liver Injury as a Surrogate for Inflammation and Predictor of Outcomes in COVID-19. *Hepatol Commun* 2021; **5**: 24-32 [PMID: 33437898 DOI: 10.1002/hep4.1586]

65 **Hartl L**, Haslinger K, Angerer M, Semmler G, Schneeweiss-Gleixner M, Jachs M, Simbrunner B, Bauer DJM, Eigenbauer E, Strassl R, Breuer M, Kimberger O, Laxar D, Lampichler K, Halilbasic E, Stättermayer AF, Ba-Ssalamah A, Mandorfer M, Scheiner B, Reiberger T, Trauner M. Progressive cholestasis and associated sclerosing cholangitis are frequent complications of COVID-19 in patients with chronic liver disease. *Hepatology* 2022 [PMID: 35596929 DOI: 10.1002/hep.32582]

66 **Fix OK**, Hameed B, Fontana RJ, Kwok RM, McGuire BM, Mulligan DC, Pratt DS, Russo MW, Schilsky ML, Verna EC, Loomba R, Cohen DE, Bezerra JA, Reddy KR, Chung RT. Clinical Best Practice Advice for Hepatology and Liver Transplant Providers During the COVID-19 Pandemic: AASLD Expert Panel Consensus Statement. *Hepatology* 2020; **72**: 287-304 [PMID: 32298473 DOI: 10.1002/hep.31281]

67 **Moore JB**, June CH. Cytokine release syndrome in severe COVID-19. *Science* 2020; **368**: 473-474 [PMID: 32303591 DOI: 10.1126/science.abb8925]

68 **Boettler T**, Marjot T, Newsome PN, Mondelli MU, Maticic M, Cordero E, Jalan R, Moreau R, Cornberg M, Berg T. Impact of COVID-19 on the care of patients with liver disease: EASL-ESCMID position paper after 6 months of the pandemic. *JHEP Rep* 2020; **2**: 100169 [PMID: 32835190 DOI: 10.1016/j.jhepr.2020.100169]

69 **Alqahtani SA**, Buti M. COVID-19 and hepatitis B infection. *Antivir Ther* 2020; **25**: 389-397 [PMID: 33616549 DOI: 10.3851/IMP3382]

70 **Gracia-Ramos AE**, Jaquez-Quintana JO, Contreras-Omaña R, Auron M. Liver dysfunction and SARS-CoV-2 infection. *World J Gastroenterol* 2021; **27**: 3951-3970 [PMID: 34326607 DOI: 10.3748/wjg.v27.i26.3951]

71 **Yip TC**, Lui GC, Wong VW, Chow VC, Ho TH, Li TC, Tse YK, Hui DS, Chan HL, Wong GL. Liver injury is independently associated with adverse clinical outcomes in patients with COVID-19. *Gut* 2021; **70**: 733-742 [PMID: 32641471 DOI: 10.1136/gutjnl-2020-321726]

72 **Sagnelli C**, Montella L, Grimaldi P, Pisaturo M, Alessio L, De Pascalis S, Sagnelli E, Coppola N. COVID-19 as Another Trigger for HBV Reactivation: Clinical Case and Review of Literature. *Pathogens* 2022; **11** [PMID: 35890060 DOI: 10.3390/pathogens11070816]

73 **Mantovani A**, Beatrice G, Dalbeni A. Coronavirus disease 2019 and prevalence of chronic liver disease: A meta-analysis. *Liver Int* 2020; **40**: 1316-1320 [PMID: 32329563 DOI: 10.1111/liv.14465]

74 **Wang Y**, Liu S, Liu H, Li W, Lin F, Jiang L, Li X, Xu P, Zhang L, Zhao L, Cao Y, Kang J, Yang J, Li L, Liu X, Li Y, Nie R, Mu J, Lu F, Zhao S, Lu J, Zhao J. SARS-CoV-2 infection of the liver directly contributes to hepatic impairment in patients with COVID-19. *J Hepatol* 2020; **73**: 807-816 [PMID: 32437830 DOI: 10.1016/j.jhep.2020.05.002]

75 **Fiel MI**, El Jamal SM, Paniz-Mondolfi A, Gordon RE, Reidy J, Bandovic J, Advani R, Kilaru S, Pourmand K, Ward S, Thung SN, Schiano T. Findings of Hepatic Severe Acute Respiratory Syndrome Coronavirus-2 Infection. *Cell Mol Gastroenterol Hepatol* 2021; **11**: 763-770 [PMID: 32992052 DOI: 10.1016/j.jcmgh.2020.09.015]

76 **Wanner N**, Andrieux G, Badia-I-Mompel P, Edler C, Pfefferle S, Lindenmeyer MT, Schmidt-Lauber C, Czogalla J, Wong MN, Okabayashi Y, Braun F, Lütgehetmann M, Meister E, Lu S, Noriega MLM, Günther T, Grundhoff A, Fischer N, Bräuninger H, Lindner D, Westermann D, Haas F, Roedl K, Kluge S, Addo MM, Huber S, Lohse AW, Reiser J, Ondruschka B, Sperhake JP, Saez-Rodriguez J, Boerries M, Hayek SS, Aepfelbacher M, Scaturro P, Puelles VG, Huber TB. Molecular consequences of SARS-CoV-2 liver tropism. *Nat Metab* 2022; **4**: 310-319 [PMID: 35347318 DOI: 10.1038/s42255-022-00552-6]

77 **Hoffmann M**, Kleine-Weber H, Schroeder S, Krüger N, Herrler T, Erichsen S, Schiergens TS, Herrler G, Wu NH, Nitsche A, Müller MA, Drosten C, Pöhlmann S. SARS-CoV-2 Cell Entry Depends on ACE2 and TMPRSS2 and Is Blocked by a Clinically Proven Protease Inhibitor. *Cell* 2020; **181**: 271-280.e8 [PMID: 32142651 DOI: 10.1016/j.cell.2020.02.052]

78 **Patel SK**, Velkoska E, Burrell LM. Emerging markers in cardiovascular disease: where does angiotensin-converting enzyme 2 fit in? *Clin Exp Pharmacol Physiol* 2013; **40**: 551-559 [PMID: 23432153 DOI: 10.1111/1440-1681.12069]

79 **Gao F**, Zheng KI, Fan YC, Targher G, Byrne CD, Zheng MH. ACE2: A Linkage for the Interplay Between COVID-19 and Decompensated Cirrhosis. *Am J Gastroenterol* 2020; **115**: 1544 [PMID: 32694292 DOI: 10.14309/ajg.0000000000000780]

80 **Chai X**, Hu L, Zhang Y, Han W, Lu Z, Ke A. Specific ACE2 expression in cholangiocytes may cause liver damage after 2019-nCoV infection. *Biorxiv* 2020 [DOI: 10.1101/2020.02.03.931766]

81 **Zhao B**, Ni C, Gao R, Wang Y, Yang L, Wei J, Lv T, Liang J, Zhang Q, Xu W, Xie Y, Wang X, Yuan Z, Zhang R, Lin X. Recapitulation of SARS-CoV-2 infection and cholangiocyte damage with human liver ductal organoids. *Protein Cell* 2020; **11**: 771-775 [PMID: 32303993 DOI: 10.1007/s13238-020-00718-6]

82 **Xu L**, Liu J, Lu M, Yang D, Zheng X. Liver injury during highly pathogenic human coronavirus infections. *Liver Int*

2020; **40**: 998-1004 [PMID: 32170806 DOI: 10.1111/liv.14435]
83 **Sonzogni A**, Previtali G, Seghezzi M, Grazia Alessio M, Gianatti A, Licini L, Morotti D, Zerbi P, Carsana L, Rossi R, Lauri E, Pellegrinelli A, Nebuloni M. Liver histopathology in severe COVID 19 respiratory failure is suggestive of vascular alterations. *Liver Int* 2020; **40**: 2110-2116 [PMID: 32654359 DOI: 10.1111/liv.14601]
84 **Rai DK**, Thakur S. Study to identify predictor of hypoxia in COVID-19 infection: A single-center, retrospective study. *J Family Med Prim Care* 2021; **10**: 1852-1855 [PMID: 34195115 DOI: 10.4103/jfmpc.jfmpc_2252_20]
85 **McConnell MJ**, Kawaguchi N, Kondo R, Sonzogni A, Licini L, Valle C, Bonaffini PA, Sironi S, Alessio MG, Previtali G, Seghezzi M, Zhang X, Lee AI, Pine AB, Chun HJ, Fernandez-Hernando C, Qing H, Wang A, Price C, Sun Z, Utsumi T, Hwa J, Strazzabosco M, Iwakiri Y. Liver injury in COVID-19 and IL-6 trans-signaling-induced endotheliopathy. *J Hepatol* 2021; **75**: 647-658 [PMID: 33991637 DOI: 10.1016/j.jhep.2021.04.050]
86 **Diaz-Louzao C**, Barrera-Lopez L, Lopez-Rodriguez M, Casar C, Vazquez-Agra N, Pernas-Pardavila H, Marques-Afonso A, Vidal-Vazquez M, Montoya JG, Andrade AH, Fernandez-Castro I, Varela P, Gonzalez-Quintela A, Otero E, Gude F, Cadarso-Suarez C, Tome S. Longitudinal relationship of liver injury with inflammation biomarkers in COVID-19 hospitalized patients using a joint modeling approach. *Sci Rep* 2022; **12**: 5547 [PMID: 35365705 DOI: 10.1038/s41598-022-09290-x]
87 **Saviano A**, Wrensch F, Ghany MG, Baumert TF. Liver Disease and Coronavirus Disease 2019: From Pathogenesis to Clinical Care. *Hepatology* 2021; **74**: 1088-1100 [PMID: 33332624 DOI: 10.1002/hep.31684]
88 **Liao D**, Zhou F, Luo L, Xu M, Wang H, Xia J, Gao Y, Cai L, Wang Z, Yin P, Wang Y, Tang L, Deng J, Mei H, Hu Y. Haematological characteristics and risk factors in the classification and prognosis evaluation of COVID-19: a retrospective cohort study. *Lancet Haematol* 2020; **7**: e671-e678 [PMID: 32659214 DOI: 10.1016/S2352-3026(20)30217-9]
89 **Kermali M**, Khalsa RK, Pillai K, Ismail Z, Harky A. The role of biomarkers in diagnosis of COVID-19 - A systematic review. *Life Sci* 2020; **254**: 117788 [PMID: 32475810 DOI: 10.1016/j.lfs.2020.117788]
90 **Ali N**. Elevated level of C-reactive protein may be an early marker to predict risk for severity of COVID-19. *J Med Virol* 2020; **92**: 2409-2411 [PMID: 32516845 DOI: 10.1002/jmv.26097]
91 **Ghahramani S**, Tabrizi R, Lankarani KB, Kashani SMA, Rezaei S, Zeidi N, Akbari M, Heydari ST, Akbari H, Nowrouzi-Sohrabi P, Ahmadizar F. Laboratory features of severe vs. non-severe COVID-19 patients in Asian populations: a systematic review and meta-analysis. *Eur J Med Res* 2020; **25**: 30 [PMID: 32746929 DOI: 10.1186/s40001-020-00432-3]
92 **Del Valle DM**, Kim-Schulze S, Huang HH, Beckmann ND, Nirenberg S, Wang B, Lavin Y, Swartz TH, Madduri D, Stock A, Marron TU, Xie H, Patel M, Tuballes K, Van Oekelen O, Rahman A, Kovatch P, Aberg JA, Schadt E, Jagannath S, Mazumdar M, Charney AW, Firpo-Betancourt A, Mendu DR, Jhang J, Reich D, Sigel K, Cordon-Cardo C, Feldmann M, Parekh S, Merad M, Gnjatic S. An inflammatory cytokine signature predicts COVID-19 severity and survival. *Nat Med* 2020; **26**: 1636-1643 [PMID: 32839624 DOI: 10.1038/s41591-020-1051-9]
93 **Feng G**, Zheng KI, Yan QQ, Rios RS, Targher G, Byrne CD, Poucke SV, Liu WY, Zheng MH. COVID-19 and Liver Dysfunction: Current Insights and Emergent Therapeutic Strategies. *J Clin Transl Hepatol* 2020; **8**: 18-24 [PMID: 32274342 DOI: 10.14218/JCTH.2020.00018]
94 **Amiri-Dashatan N**, Koushki M, Ghorbani F, Naderi N. Increased inflammatory markers correlate with liver damage and predict severe COVID-19: a systematic review and meta-analysis. *Gastroenterol Hepatol Bed Bench* 2020; **13**: 282-291 [PMID: 33244370]
95 **Iba T**, Connors JM, Levy JH. The coagulopathy, endotheliopathy, and vasculitis of COVID-19. *Inflamm Res* 2020; **69**: 1181-1189 [PMID: 32918567 DOI: 10.1007/s00011-020-01401-6]
96 **Bonaventura A**, Vecchié A, Dagna L, Martinod K, Dixon DL, Van Tassell BW, Dentali F, Montecucco F, Massberg S, Levi M, Abbate A. Endothelial dysfunction and immunothrombosis as key pathogenic mechanisms in COVID-19. *Nat Rev Immunol* 2021; **21**: 319-329 [PMID: 33824483 DOI: 10.1038/s41577-021-00536-9]
97 **Rapkiewicz AV**, Mai X, Carsons SE, Pittaluga S, Kleiner DE, Berger JS, Thomas S, Adler NM, Charytan DM, Gasmi B, Hochman JS, Reynolds HR. Megakaryocytes and platelet-fibrin thrombi characterize multi-organ thrombosis at autopsy in COVID-19: A case series. *EClinicalMedicine* 2020; **24**: 100434 [PMID: 32766543 DOI: 10.1016/j.eclinm.2020.100434]
98 **Xu Z**, Shi L, Wang Y, Zhang J, Huang L, Zhang C, Liu S, Zhao P, Liu H, Zhu L, Tai Y, Bai C, Gao T, Song J, Xia P, Dong J, Zhao J, Wang FS. Pathological findings of COVID-19 associated with acute respiratory distress syndrome. *Lancet Respir Med* 2020; **8**: 420-422 [PMID: 32085846 DOI: 10.1016/S2213-2600(20)30076-X]
99 **Lagana SM**, Kudose S, Iuga AC, Lee MJ, Fazlollahi L, Remotti HE, Del Portillo A, De Michele S, de Gonzalez AK, Saqi A, Khairallah P, Chong AM, Park H, Uhlemann AC, Lefkowitch JH, Verna EC. Hepatic pathology in patients dying of COVID-19: a series of 40 cases including clinical, histologic, and virologic data. *Mod Pathol* 2020; **33**: 2147-2155 [PMID: 32792598 DOI: 10.1038/s41379-020-00649-x]
100 **Zhao CL**, Rapkiewicz A, Maghsoodi-Deerwester M, Gupta M, Cao W, Palaia T, Zhou J, Ram B, Vo D, Rafiee B, Hossein-Zadeh Z, Dabiri B, Hanna I. Pathological findings in the postmortem liver of patients with coronavirus disease 2019 (COVID-19). *Hum Pathol* 2021; **109**: 59-68 [PMID: 33307078 DOI: 10.1016/j.humpath.2020.11.015]
101 **Da BL**, Kushner T, El Halabi M, Paka P, Khalid M, Uberoi A, Lee BT, Perumalswami PV, Rutledge SM, Schiano TD, Friedman SL, Saberi B. Liver Injury in Patients Hospitalized with Coronavirus Disease 2019 Correlates with Hyperinflammatory Response and Elevated Interleukin-6. *Hepatol Commun* 2021; **5**: 177-188 [PMID: 33230491 DOI: 10.1002/hep4.1631]
102 **McConnell MJ**, Kondo R, Kawaguchi N, Iwakiri Y. Covid-19 and Liver Injury: Role of Inflammatory Endotheliopathy, Platelet Dysfunction, and Thrombosis. *Hepatol Commun* 2022; **6**: 255-269 [PMID: 34658172 DOI: 10.1002/hep4.1843]
103 **Effenberger M**, Grander C, Grabherr F, Griesmacher A, Ploner T, Hartig F, Bellmann-Weiler R, Joannidis M, Zoller H, Weiss G, Adolph TE, Tilg H. Systemic inflammation as fuel for acute liver injury in COVID-19. *Dig Liver Dis* 2021; **53**: 158-165 [PMID: 32873520 DOI: 10.1016/j.dld.2020.08.004]
104 **Goshua G**, Pine AB, Meizlish ML, Chang CH, Zhang H, Bahel P, Baluha A, Bar N, Bona RD, Burns AJ, Dela Cruz CS, Dumont A, Halene S, Hwa J, Koff J, Menninger H, Neparidze N, Price C, Siner JM, Tormey C, Rinder HM, Chun HJ, Lee AI. Endotheliopathy in COVID-19-associated coagulopathy: evidence from a single-centre, cross-sectional study. *Lancet*

Haematol 2020; **7**: e575-e582 [PMID: 32619411 DOI: 10.1016/S2352-3026(20)30216-7]
105 **Tran TT**, Ahn J, Reau NS. ACG clinical guideline: liver disease and pregnancy. *Am J Gastroenterol* 2016; **111**: 176-94
106 **Brady CW**. Liver Disease in Pregnancy: What's New. *Hepatol Commun* 2020; **4**: 145-156 [PMID: 32025601 DOI: 10.1002/hep4.1470]
107 **Westbrook RH**, Dusheiko G, Williamson C. Pregnancy and liver disease. *J Hepatol* 2016; **64**: 933-945 [PMID: 26658682 DOI: 10.1016/j.jhep.2015.11.030]
108 **Raju S**, Ziemann S, Mayigegowda KK, Nevah MI, Reddy PM, Machicao VI. Su323 The patterns of liver injury in covid-19 positive pregnant females: A Case series. *Gastroenterology* 2021; **160**: S-849
109 **Klyachman L**, Advani R, Sun E. S2425 Pregnancy and Transaminitis in the COVID-19 Era. *Am J Gastroenterol* 2020; **115**: S1286
110 **Li Q**, Chen L, Jiang H, Zheng D, Wang Y, Mei J. Clinical characteristics of pregnant women infected with Coronavirus Disease 2019 in China: a nationwide case-control study. *MedRxiv* 2021 [DOI: 10.1101/2021.10.21.21265313]
111 **Choudhary A**, Singh V, Bharadwaj M. Maternal and Neonatal Outcomes in Pregnant Women With SARS-CoV-2 Infection Complicated by Hepatic Dysfunction. *Cureus* 2022; **14**: e25347 [PMID: 35761912 DOI: 10.7759/cureus.25347]
112 **Can E**, Oğlak SC, Ölmez F. Abnormal liver function tests in pregnant patients with COVID-19 - a retrospective cohort study in a tertiary center. *Ginekol Pol* 2022 [PMID: 35072238 DOI: 10.5603/GP.a2021.0182]
113 **Chen H**, Guo J, Wang C, Luo F, Yu X, Zhang W, Li J, Zhao D, Xu D, Gong Q, Liao J, Yang H, Hou W, Zhang Y. Clinical characteristics and intrauterine vertical transmission potential of COVID-19 infection in nine pregnant women: a retrospective review of medical records. *Lancet* 2020; **395**: 809-815 [PMID: 32151335 DOI: 10.1016/S0140-6736(20)30360-3]
114 **Anness A**, Siddiqui F. COVID-19 complicated by hepatic dysfunction in a 28-week pregnant woman. *BMJ Case Rep* 2020; **13** [PMID: 32878840 DOI: 10.1136/bcr-2020-237007]
115 **Azimi H**, Saghafi N, Tara F, Mirzaeian S, Hatamian Z, Afshar Delkhah F. COVID-19 Mimicking Hemolysis, Elevated Liver Enzymes and Low Platelets (HELLP) Syndrome: A Case Report. *J Midwifery Womens Health* 2021; **9**: 3050-4 [DOI: 10.5348/100060z06sr2019cr]
116 **Naeh A**, Berezowsky A, Yudin MH, Dhalla IA, Berger H. Preeclampsia-Like Syndrome in a Pregnant Patient With Coronavirus Disease 2019 (COVID-19). *J Obstet Gynaecol Can* 2022; **44**: 193-195 [PMID: 34648956 DOI: 10.1016/j.jogc.2021.09.015]
117 **Ronnje L**, Länsberg JK, Vikhareva O, Hansson SR, Herbst A, Zaigham M. Complicated COVID-19 in pregnancy: a case report with severe liver and coagulation dysfunction promptly improved by delivery. *BMC Pregnancy Childbirth* 2020; **20**: 511 [PMID: 32887569 DOI: 10.1186/s12884-020-03172-8]
118 **Arslan E**. COVID-19: A Cause of HELLP Syndrome? *Int J Womens Health* 2022; **14**: 617-623 [PMID: 35506047 DOI: 10.2147/IJWH.S362877]
119 **Madaan S**, Talwar D, Kumar S, Jaiswal A, Acharya N, Acharya S. HELLP Syndrome and COVID-19; association or accident: A case series. *J Family Med Prim Care* 2022; **11**: 802-806 [PMID: 35360752 DOI: 10.4103/jfmpc.jfmpc_1136_21]
120 **Choudhary A**, Singh V, Bharadwaj M, Barik A. Pregnancy With SARS-CoV-2 Infection Complicated by Preeclampsia and Acute Fatty Liver of Pregnancy. *Cureus* 2021; **13**: e15645 [PMID: 34306855 DOI: 10.7759/cureus.15645]
121 **Deng G**, Zeng F, Zhang L, Chen H, Chen X, Yin M. Characteristics of pregnant patients with COVID-19 and liver injury. *J Hepatol* 2020; **73**: 989-991 [PMID: 32569609 DOI: 10.1016/j.jhep.2020.06.022]
122 **Mendoza M**, Garcia-Ruiz I, Maiz N, Rodo C, Garcia-Manau P, Serrano B, Lopez-Martinez RM, Balcells J, Fernandez-Hidalgo N, Carreras E, Suy A. Pre-eclampsia-like syndrome induced by severe COVID-19: a prospective observational study. *BJOG* 2020; **127**: 1374-1380 [PMID: 32479682 DOI: 10.1111/1471-0528.16339]
123 **Levy A**, Yagil Y, Bursztyn M, Barkalifa R, Scharf S, Yagil C. ACE2 expression and activity are enhanced during pregnancy. *Am J Physiol Regul Integr Comp Physiol* 2008; **295**: R1953-R1961 [PMID: 18945956 DOI: 10.1152/ajpregu.90592.2008]
124 **Azinheira Nobrega Cruz N**, Stoll D, Casarini DE, Bertagnolli M. Role of ACE2 in pregnancy and potential implications for COVID-19 susceptibility. *Clin Sci (Lond)* 2021; **135**: 1805-1824 [PMID: 34338772 DOI: 10.1042/CS20210284]
125 **Dhaundiyal A**, Kumari P, Jawalekar SS, Chauhan G, Kalra S, Navik U. Is highly expressed ACE 2 in pregnant women "a curse" in times of COVID-19 pandemic? *Life Sci* 2021; **264**: 118676 [PMID: 33129880 DOI: 10.1016/j.lfs.2020.118676]
126 **Sanghavi M**, Rutherford JD. Cardiovascular physiology of pregnancy. *Circulation* 2014; **130**: 1003-1008 [PMID: 25223771 DOI: 10.1161/CIRCULATIONAHA.114.009029]
127 **Papageorghiou AT**, Deruelle P, Gunier RB, Rauch S, García-May PK, Mhatre M, Usman MA, Abd-Elsalam S, Etuk S, Simmons LE, Napolitano R, Deantoni S, Liu B, Prefumo F, Savasi V, do Vale MS, Baafi E, Zainab G, Nieto R, Maiz N, Aminu MB, Cardona-Perez JA, Craik R, Winsey A, Tavchioska G, Bako B, Oros D, Rego A, Benski AC, Hassan-Hanga F, Savorani M, Giuliani F, Sentilhes L, Risso M, Takahashi K, Vecchiarelli C, Ikenoue S, Thiruvengadam R, Soto Conti CP, Ferrazzi E, Cetin I, Nachinab VB, Ernawati E, Duro EA, Kholin A, Firlit ML, Easter SR, Sichitiu J, Bowale A, Casale R, Cerbo RM, Cavoretto PI, Eskenazi B, Thornton JG, Bhutta ZA, Kennedy SH, Villar J. Preeclampsia and COVID-19: results from the INTERCOVID prospective longitudinal study. *Am J Obstet Gynecol* 2021; **225**: 289.e1-289.e17 [PMID: 34187688 DOI: 10.1016/j.ajog.2021.05.014]
128 **Conde-Agudelo A**, Romero R. SARS-CoV-2 infection during pregnancy and risk of preeclampsia: a systematic review and meta-analysis. *Am J Obstet Gynecol* 2022; **226**: 68-89.e3 [PMID: 34302772 DOI: 10.1016/j.ajog.2021.07.009]
129 **Feng Y**, Xu J, Zhou Q, Wang R, Liu N, Wu Y, Yuan H, Che H. Alpha-1 Antitrypsin Prevents the Development of Preeclampsia Through Suppression of Oxidative Stress. *Front Physiol* 2016; **7**: 176 [PMID: 27303303 DOI: 10.3389/fphys.2016.00176]
130 **Azouz NP**, Klingler AM, Callahan V, Akhrymuk IV, Elez K, Raich L, Henry BM, Benoit JL, Benoit SW, Noé F, Kehn-Hall K, Rothenberg ME. Alpha 1 Antitrypsin is an Inhibitor of the SARS-CoV-2-Priming Protease TMPRSS2. *bioRxiv* 2020 [PMID: 33052338 DOI: 10.1101/2020.05.04.077826]
131 **Moore Simas TA**, Crawford SL, Solitro MJ, Frost SC, Meyer BA, Maynard SE. Angiogenic factors for the prediction of

preeclampsia in high-risk women. *Am J Obstet Gynecol* 2007; **197**: 244.e1-244.e8 [PMID: 17826405 DOI: 10.1016/j.ajog.2007.06.030]

132 **Palomo M**, Youssef L, Ramos A, Torramade-Moix S, Moreno-Castaño AB, Martinez-Sanchez J, Bonastre L, Pino M, Gomez-Ramirez P, Martin L, Garcia Mateos E, Sanchez P, Fernandez S, Crovetto F, Escolar G, Carreras E, Castro P, Gratacos E, Crispi F, Diaz-Ricart M. Differences and similarities in endothelial and angiogenic profiles of preeclampsia and COVID-19 in pregnancy. *Am J Obstet Gynecol* 2022; **227**: 277.e1-277.e16 [PMID: 35351411 DOI: 10.1016/j.ajog.2022.03.048]

133 Gestational Hypertension and Preeclampsia: ACOG Practice Bulletin Summary, Number 222. *Obstet Gynecol* 2020; **135**: 1492-1495 [PMID: 32443077 DOI: 10.1097/AOG.0000000000003892]

134 **Morrison MA**, Chung Y, Heneghan MA. Managing hepatic complications of pregnancy: practical strategies for clinicians. *BMJ Open Gastroenterol* 2022; **9** [PMID: 35292523 DOI: 10.1136/bmjgast-2021-000624]

135 **Goel A**, Jamwal KD, Ramachandran A, Balasubramanian KA, Eapen CE. Pregnancy-related liver disorders. *J Clin Exp Hepatol* 2014; **4**: 151-162 [PMID: 25755551 DOI: 10.1016/j.jceh.2013.03.220]

136 **Terrault NA**, Williamson C. Pregnancy-Associated Liver Diseases. *Gastroenterology* 2022; **163**: 97-117.e1 [PMID: 35276220 DOI: 10.1053/j.gastro.2022.01.060]

137 **Hammoud GM**, Ibdah JA. Preeclampsia-induced Liver Dysfunction, HELLP syndrome, and acute fatty liver of pregnancy. *Clin Liver Dis (Hoboken)* 2014; **4**: 69-73 [PMID: 30992924 DOI: 10.1002/cld.409]

138 **Kongwattanakul K**, Saksiriwuttho P, Chaiyarach S, Thepsuthammarat K. Incidence, characteristics, maternal complications, and perinatal outcomes associated with preeclampsia with severe features and HELLP syndrome. *Int J Womens Health* 2018; **10**: 371-377 [PMID: 30046254 DOI: 10.2147/IJWH.S168569]

World Journal of Gastroenterology

Submit a Manuscript: https://www.f6publishing.com

World J Gastroenterol 2022 November 14; 28(42): 6034-6044

DOI: 10.3748/wjg.v28.i42.6034

ISSN 1007-9327 (print) ISSN 2219-2840 (online)

MINIREVIEWS

Angiogenesis and immune checkpoint dual blockade: Opportunities and challenges for hepatocellular carcinoma therapy

Si-Qi Li, Yang Yang, Lin-Sen Ye

Specialty type: Gastroenterology and hepatology

Provenance and peer review: Invited article; Externally peer reviewed.

Peer-review model: Single blind

Peer-review report's scientific quality classification

Grade A (Excellent): 0
Grade B (Very good): B, B
Grade C (Good): C
Grade D (Fair): 0
Grade E (Poor): 0

P-Reviewer: Kwee S, United States; Liang Y, China; Sehrawat A, India

Received: August 27, 2022
Peer-review started: August 27, 2022
First decision: September 30, 2022
Revised: October 6, 2022
Accepted: November 2, 2022
Article in press: November 2, 2022
Published online: November 14, 2022

Si-Qi Li, Yang Yang, Lin-Sen Ye, Department of Hepatic Surgery and Liver Transplantation Center, The Third Affiliated Hospital of Sun Yat-sen University, Guangzhou 510630, Guangdong Province, China

Corresponding author: Lin-Sen Ye, Doctor, MD, PhD, Doctor, Postdoc, Surgeon, Department of Hepatic Surgery and Liver Transplantation Center, The Third Affiliated Hospital of Sun Yat-sen University, No. 600 Tianhe Road, Guangzhou 510630, Guangdong Province, China.
ye_linsen@163.com

Abstract

The disease burden related to hepatocellular carcinoma (HCC) is increasing. Most HCC patients are diagnosed at the advanced stage and multikinase inhibitors have been the only treatment choice for them. Recently, the approval of immune checkpoint inhibitors (ICIs) has provided a new therapeutic strategy for HCC. It is noteworthy that the positive outcomes of the phase III clinical trial IMBrave150 [atezolizumab (anti-programmed cell death ligand 1 antibody) combined with bevacizumab (anti-vascular endothelial growth factor monoclonal antibody)], showed that overall survival and progression-free survival were significantly better with sorafenib. This combination therapy has become the new standard therapy for advanced HCC and has also attracted more attention in the treatment of HCC with anti-angiogenesis-immune combination therapy. Currently, the synergistic antitumor efficacy of this combination has been shown in many preclinical and clinical studies. In this review, we discuss the mechanism and clinical application of anti-angiogenics and immunotherapy in HCC, outline the relevant mechanism and rationality of the combined application of anti-angiogenics and ICIs, and point out the existing challenges of the combination therapy.

Key Words: Anti-angiogenesis; Immunotherapy; Combination therapy; Vascular endothelial growth factor; Immune checkpoint blockade; Hepatocellular carcinoma

Core Tip: Anti-angiogenesis combined with immunotherapy in hepatocellular carcinoma (HCC) has attracted extensive attention. Although the mechanism of these combinations is largely understood, the biomarkers for predicting treatment response are still lacking. Thus, we outline the relevant mechanism and rationality of the combined application of anti-angiogenics and immune checkpoint inhibitors, and further explore the biomarkers that are associated with treatment response, which are critical in studies of HCC.

Citation: Li SQ, Yang Y, Ye LS. Angiogenesis and immune checkpoint dual blockade: Opportunities and challenges for hepatocellular carcinoma therapy. *World J Gastroenterol* 2022; 28(42): 6034-6044
URL: https://www.wjgnet.com/1007-9327/full/v28/i42/6034.htm
DOI: https://dx.doi.org/10.3748/wjg.v28.i42.6034

INTRODUCTION

According to the statistics from the National Cancer Center of China, the incidence and mortality of hepatocellular carcinoma (HCC) are increasing annually[1]. The World Health Organization (WHO) estimates that, from 2015 to 2030, approximately 10 million people in China will die due to liver cirrhosis and HCC. Although early-stage disease can be cured by surgical removed, transplantation, or interventional therapy, most patients have unresectable disease at the time of diagnosis[2], and current treatments are insufficient to prevent the high metastasis and recurrence rates after HCC treatment.

Currently, immunotherapy is receiving a great deal of attention in the treatment of tumors. Among the immunotherapy options, immune checkpoint blockade (ICB)-based immunotherapy which reactivates dysfunctional or exhausted T cells has shown excellent efficacy in a variety of solid cancers and hematological tumors[3-7]. However, 50%-80% of cancer patients still do not benefit from immunotherapy, and many of them suffer serious adverse events (AEs) during treatment[8]. In fact, there is still no clear mechanism to explain the tolerance of many cancers to immune checkpoint inhibitors (ICIs). HCC is a solid tumor with complex pathophysiological barriers. It is difficult for external lymphocytes to penetrate and infiltrate into tumor tissue. In addition, the rapidly growing tumor cells release immunosuppressive factors, which result in HCC forming an immunosuppressive immune microenvironment, which greatly limits the efficacy of immunotherapy[9]. In addition, the rapidly growing tumor cells release several factors, which result in HCC forming an immunosuppressive immune microenvironment, that greatly limits the efficacy of immunotherapy[10,11]. Therefore, normalizing tumor vasculature and improving the tumor hypoxic microenvironment is expected to reverse the immunosuppressive microenvironment of HCC and promote HCC immunotherapy.

The TME is mainly composed of the vasculature, resident or infiltrating immune cells and various stromal cells. Previous studies have shown that abnormal tumor vasculature promotes the formation of an immunosuppressive TME[11]. Therefore, therapies that promote normalization of the vasculature are of great significance for enhancing immunotherapy of HCC. This review outlines measures to normalize the vasculature of HCC and the common immunotherapy regimens for HCC, and further describes and discusses how to normalize the tumor vasculature to improve the efficacy of immunotherapy in HCC (especially ICB). Additionally, we discuss the challenges associated with emerging combinations of vascular normalization therapy and immunotherapy for HCC.

ABNORMAL ANGIOGENESIS AND VASCULAR NORMALIZATION MEASURES FOR HCC

Abnormal angiogenesis and vascular endothelial growth factor/vascular endothelial growth factor receptor

The excessive growth and abnormal proliferation of tumor cells depend on rapid tumor angiogenesis. Tumor angiogenesis not only provides tumor cells with oxygen, nutrients and removes waste, but also serves as a channel for metastasis of tumor cells and immune cell infiltration[12,13]. However, compared with vessels in normal tissues, tumor neo-vessels have obvious aberrations in both structure and function[11]. Leakage is one of the most notable features of tumor vessels. On the one hand, this property can lead to tumor hypoxia and decreased intra-tumoral pH by impairing perfusion, and on the other hand, leakage will increase interstitial pressure in the TME[10]. Tumor cells overcome these harsh conditions through multiple mechanisms to gain a survival advantage[11]. Abnormal vessels limit the circulation of drugs and immune cells into the tumor, thereby limiting anti-tumor activity[11]. The hypoxia and pH reduction in the tumor caused by abnormal vessels will further lead to abnormal neovascularization, forming a vicious circle.

In the field of cancer research, most studies on angiogenesis has focused on the increased expression of angiogenesis factors [such as vascular endothelial growth factor (VEGF), platelet-derived growth factor (PDGF), fibroblast growth factor (FGF), angiopoietin, hepatocyte growth factor, endoglin (CD105, *etc*)] and decreased expression of anti-angiogenesis factors, such as angiostatin, endostatin, and thrombospondin 1, which is mainly caused by upregulation of the hypoxia-inducible factor protein. Among these, VEGF/VEGF receptor (VEGFR) axis are widely known to play a major role in vascular abnormalities and are crucial for the occurrence and progression of HCC[14-16]. The VEGF family consists of VEGFA, VEGFB, VEGFC, VEGFD and placental growth factor (PlGF) 1-4, which are involved in tumor angiogenesis (VEGFA, PlGF), maintenance of new blood vessels (VEGFB), lymph-angiogenesis and angiogenesis (VEGFC/D), vascular permeability (VEGFA/C), chemotaxis (VEGFB), migration (VEGFA, PlGF), differentiation (VEGFD) and survival (VEGFA/B/C, PlGF)[17,18]. VEGFR mainly includes VEGFR1, VEGFR2, and VEGFR3[15]. Of these, VEGFR2 is the critical receptor of this family, which is expressed on almost all endothelial cells and is activated by binding to VEGFA, VEGFC or VEGFD, and VEGFA is its major ligand[19]. This binding results in the phosphorylation cascade that triggers downstream cellular pathways, ultimately leading to endothelial cell proliferation and migration, and the formation and branching of new tumor blood vessels[19]. These neo-vessels often manifest as abnormal leaky vasculature, resulting in high interstitial pressure and severe hypoxia or necrosis in tissue regions, further promoting the malignant potential of tumor cells[20]. Previous studies have shown that circulating VEGF levels are increased in HCC, and increased VEGFA has been shown to be associated with angiogenesis in HCC[21,22]. In addition, related studies also observed a positive association between increased local and circulating VEGF and high tumor micro-vessel density with rapid disease progression and decreased survival. These findings support the application of therapies that target the VEGF/VEGFR pathway in HCC[21,22].

Vascular normalization measures in HCC and targeting of the VEGF/VEGFR axis

Various molecular and physical mechanisms have been reported to contribute to tumor vascular dysfunction, the most prominent of which is the imbalance of angiogenic signaling mediated by pro- and anti-angiogenic molecules[11,23]. In normal tissue, this balance is precisely maintained to ensure normal vascular morphology and function[24]. However, during the process of carcinogenesis, this balance usually tends to angiogenesis, and the generated neo-vessels are immature abnormal vessels without complete structure[24]. In view of the key role of the VEGF/VEGFR axis in abnormal angiogenesis of HCC, rational targeting of this axis can promote the normalization of tissue vessels and limit the occurrence and development of HCC.

In the past few decades, the development of anti-angiogenesis therapy has mainly focused on blocking VEGF[17,18]. Several studies have also focused on blocking VEGF signaling by silencing VEGFA expression at the transcriptional and post-transcriptional levels. For example, Zou *et al*[25] identified emodin that could greatly increase seryl-tRNA synthetase expression in tripe-negative breast cancer (TNBC) cells, consequently reducing VEGFA transcription, and emodin potently inhibited vascular development of zebrafish and blocked tumor angiogenesis in TNBC-bearing mice, greatly improving the survival. Li *et al*[26] and Ding *et al*[27] raised that VEGF small interference RNA can precisely and efficiently silence VEGF expression and block VEGF signal pathway, leading to a significant decrease in tumor blood vessels and suppression of tumor growth and metastasis. However, these studies have only been tested in animals. Preclinical evidence suggests that monotherapy which blocks VEGF reduces micro-vessel density, inhibits tumor growth in many cancerous subcutaneous xenografts, and even inhibits tumor cell metastasis[28,29]. Ferrara *et al*[30] researched and developed the first anti-angiogenesis inhibitor (bevacizumab), a recombinant humanized monoclonal antibody that blocks VEGFA. Bevacizumab binds to VEGF in the bloodstream, thereby inhibiting the interaction between VEGF and VEGFR. In clinical trials of combination therapy for HCC, multiple lines of evidence suggest that bevacizumab has a potential therapeutic effect[31,32].

On the other hand, many anti-angiogenesis therapies in HCC focus on targeting VEGFR. Multikinase inhibitors (MKIs) and monoclonal antibodies (mAbs) were developed to inhibit VEGFR and its downstream targets to inhibit endothelial cell proliferation, thereby reducing the nutrient and oxygen supply required by tumors. Currently, the VEGFR-targeted MKIs and mAbs used in advanced HCC mainly include sorafenib, regorafenib, lenvatinib, cabozantinib, and ramucirumab (Table 1).

Sorafenib is an oral MKI that blocks VEGFR1-3, c-Kit, PDGF receptor (PDGFR)-b, and FMS-like tyrosine kinase-3 (FLT-3)[33]. The phase III clinical trial SHARP showed a 2.8-mo survival advantage for sorafenib over placebo in patients with advanced HCC. This recent study also showed that sorafenib can benefit patients with HCC regardless of etiology, and patients with hepatitis C appeared to experience greater benefit[34]. Treatment-related AEs were more common in the sorafenib group than in the placebo group (80% *vs* 52%), and the incidence of dose reductions and interruptions was high during treatment. The MKI regorafenib also targets VEGFR, RET, c-Kit, B-Raf, FGFR1 and PDGFR[33]. It is the first therapy to demonstrate a survival benefit in advanced HCC patients who have progressed on sorafenib[35]. Fatigue, hypertension, diarrhea and hand-foot skin reactions were common AEs in the regorafenib-treated group. Other analyses showed that the survival benefit of first line sorafenib and second line regorafenib was more than 24 mo[35]. The targets of lenvatinib include VEGFR1-3, FGFR1-4, PDGFRa, RET and c-Kit. Recently, a phase III study of lenvatinib *vs* sorafenib in patients with

Table 1 Currently approved anti-angiogenic therapy for advanced hepatocellular carcinoma

Therapy	Type	Line of therapy	Target	Study name	Primary outcome in the study (mo) (95%CI)	Adverse events in the study [affected/at risk (%)]
Anti-VEGFA						
Bevacizumab (combination with atezolizumab)	mAb	First line (plus atezolizumab)	VEGF-A	IMBrave150	OS at CCOD 30 mo: 19.2 (17.0-23.7); PFS: 6.8 (5.6-8.3)	Gastrointestinal perforation [1/329 (0.30%)], haemorrhage [40/329 (12.15%)], hypertension [2/329 (0.61%)] and proteinuria [100/329 (30.40%)], *etc.*
Anti-VEGFR						
Sorafenib	TKIs	First line	VEGFR1-3, c-Kit, PDGFR-b, and FLT-3	SHARP	OS: 10.8 (9.5-13.5); TTSP: 4.2 (3.5-4.2)	Diarrhea [166/297 (55.89%)], hand-foot skin reactions [2/297 (0.67%)], fatigue [145/297 (48.82%)], *etc.*
Lenvatinib	TKIs	First line	VEGFR1-3, FGFR1-4, PDGFRa, RET and c-Kit	REFLECT	OS: 13.6 (12.1–14.9); PFS: 7.4 (6.9–8.8)	Diarrhea [154/468 (33%)], decreased appetite [204/468 (44%)], *etc.*
Regorafenib	TKIs	Second line	VEGFR, RET, c-Kit, B-Raf, FGFR1 and PDGFR	RESORCE	OS: 10.7 (9.2-12.3); TTP:3.9 (2.9-4.26)	Toxicities were manageable this sorafenib-tolerant population and were similar to those observed with sorafenib, including diarrhea [163/374 (43.58%)], *etc.*
Cabozantinib	TKIs	Second and third line	VEGFR2, c-Kit, RET, FLT-3, Tie2, and Axl	CELESTIAL	OS: 10.2 (9.1-12.0)	Hypertension [137/467 (29.34%)]. Pneumonia [16/467 (3.43%)], *etc.*
Ramucirumab	mAb	Second line and AFP ≥ 400 ng/mL	VEGFR2	REACH-2	OS: 8.5 (7.0-10.6)	Hypertension [48/197 (24.37%)], hyponatremia [11/197 (5.58%)], *etc.*

TKIs: Tyrosine kinase inhibitor; CCOD: Clinical cut off date; OS: Overall survival; PFS: Progression free survival; TTSP: Time to symptomatic progression; TTP: Time to progression; CI: Confidence interval; AFP: Alpha fetoprotein; VEGFR: Vascular endothelial growth factor receptor; FLT: FMS related tyrosine kinase 1; FGFR: Fibroblast growth factor receptor; PDGFR: Platelet-derived growth factor receptor.

unresectable HCC showed that overall survival (OS) with lenvatinib was non-inferior to sorafenib[36]. The most common AEs in the lenvatinib group were diarrhea, fatigue, *etc*[36]. It should be noted that patients with tumors with more than 50% hepatic masses or involvement of branches of the main portal vein were excluded from the trial (NCT01761266); thus, further clinical trials should be conducted. Despite this problem, lenvatinib remains the only drug in first-line clinical trials that was positive against the proven active control, sorafenib. In addition to targeting VEGFR2, c-Kit, RET, FLT-3, Tie2, and Axl, cabozantinib has the unique property of inhibiting c-Met, and its potential activity was observed in phase II trials[37]. The subsequent phase III clinical trial, which compared cabozantinib to placebo in advanced HCC, met its primary endpoint of improved OS after up to two prior treatments, one of which included sorafenib[38]. Hypertension, pneumonia were common AEs in the cabozantinib group[38]. Ramucirumab, the mAb that antagonizes VEGFR2, improved OS in a phase III study in patients with sorafenib progression or intolerance with baseline alpha-fetoprotein (AFP) ≥ 400 ng/mL [39]. Hypertension and hyponatremia were the only over grade 3 AEs in patients of the test group[39]. Based on the results of the previous phase III study, patients can be selected for treatment based on baseline AFP values. A survival benefit was observed with ramucirumab in a subgroup of patients with higher baseline AFP (400 ng/mL), which is the first positive clinical trial in the biomarker-selected HCC population[39].

IMMUNOTHERAPY IN HCC

Driven by the success of ICB therapy in melanoma, ICB has been extensively studied in a variety of malignancies including HCC[40,41]. Long-term liver injury or chronic hepatitis infection often leaves the liver in a state of chronic inflammation[42]. Moderate inflammation can defend against pathogens and repair tissue damage, whereas persistent liver inflammation can disturb the microenvironment, thus favoring carcinogenesis. On the one hand, hepatic endocrine cytokines play a key role in tumorigenesis through regulating regulatory T cells (Tregs) that inhibit $CD8^+$ T cell activation[43]. It was previously reported that Tregs derived from hepatitis B virus-positive HCC tumors exhibited higher programmed cell death protein 1 (PD-1) expression and superior inhibitory capacity against $CD8^+$ T cells. On the other hand, cytotoxic immune populations frequently express markers of exhaustion such as PD-1, cytotoxic t-lymphocyte associated antigen 4 (CTLA-4) and lymphocyte activating gene 3[44].

Under normal conditions, these molecules inhibit T cell activation to maintain inflammatory homeostasis, protect tissue integrity, and prevent unnecessary autoimmunity[45]. However, in tumors, expression of these markers of exhaustion is inversely correlated with their function, making them a prime target for ICBs to revitalize and restore the cytotoxic capacity of $CD8^+$ T cells[43]. At the same time, the expression of PD-1 and its ligand (PD-L1) in tumor cells is upregulated, and when it binds to PD-1 expressed by T cells activated by tumor infiltration, it induces T cell exhaustion and suppresses the anti-tumor immune activity of these immune cells, thereby enabling tumor cells to evade immunity[46]. ICBs generate robust multitarget immune responses and can even induce long-lasting tumor remissions in some patients. Inhibition of the PD-1/PD-L1 interaction reverses the depleted state of these cytotoxic immune cells and reactivates their antitumor activity[46,47]. In HCC, the mAbs pembrolizumab and nivolumab that target PD-1, and nivolumab combined with ipilimumab (a mAb directed against CTLA-4), has been approved in the United States for sorafenib-treated patients, based on promising results from clinical trials[48-50]. A clinical trial confirmed the efficacy and safety of PD-1-targeting immunotherapy in HCC[51]. However, subsequent phase III trials of nivolumab *vs* sorafenib in first-line therapy failed to meet the primary survival endpoints[50,52]. The combination of phase III nivolumab and ipilimumab is currently under evaluation (NCT04039607).

In the current phase III clinical treatment of HCC, immune combination therapy has attracted considerable attention, especially the combination of ICIs and anti-angiogenic inhibitors (Table 2). Lenvatinib combined with pembrolizumab, bevacizumab combined with atezolizumab (PD-L1-targeting mAb) (T+A combination), and cabozantinib combined with atezolizumab have all obtained encouraging results in clinical studies[53-55]. Of these, the combination of bevacizumab and atezolizumab has been successful in phase III clinical trials of first-line treatment of HCC (IMbrave150). Compared with sorafenib, this combination improved the primary endpoints: OS and progression-free survival, and this combination was shown to be safe and improved quality of life[56]. Hypertension and proteinuria were typical side effects of bevacizumab and were the top two AEs in this test group. Upper gastrointestinal bleeding, another known side effect of bevacizumab, occurred in 7% of patients in this group, and was within the range of previous evaluations of bevacizumab AEs for the treatment of HCC[57,58]. Elevated transaminases and pruritus are common side effects of atezolizumab[32]. As this study applied the usual inclusion criteria in HCC clinical trials and included only Child-Pugh A patients, further clinical trials are pending[32].

Angiogenesis and immune checkpoint combination blockade in HCC

As shown above, the success of the phase III trial (IMbrave150) with the combination of atezolizumab and bevacizumab in advanced HCC is groundbreaking as it is the first treatment with a better survival rate than sorafenib since the approval of sorafenib in 2007 and is also the only successful first-line immunotherapy combination therapy for HCC in the world[32]. Antibodies targeting VEGF not only inhibit tumor growth but also reprogram the TME from immunosuppressive to immune activation[8,59]. Based on these findings, PD-1/PD-L1 inhibitors combined with VEGF/VEGFR inhibitors have attracted extensive attention in the treatment of HCC. Next, we will outline the mechanism and rationality of PD-1/PD-L1 inhibitors combined with VEGF/VEGFR inhibitor therapy, and the biomarkers of response to targeted immune combination therapy.

Mechanism and rationality

In the tumor area, VEGF released by hypoxic cancer cells promotes tumor cell growth and metastasis by angiogenesis[8]. On the other hand, VEGF can also promote the malignant progression of tumors by affecting the TME (Figure 1). The tumor immune cycle mainly includes seven steps, the release of tumor antigens, the uptake and presentation of tumor antigens by dendritic cells (DCs), the initiation and activation of T cells, the migration of T cells to tumors, the invasion of T cells against tumors, the recognition of tumor cells by T cells, and the attack of tumor cells by T cells[60]. VEGF is involved in almost every step of the tumor immune cycle and finally promotes tumor immune escape[61-64]. VEGF enhances the mobilization and proliferation of immunosuppressive cells, including Tregs, tumor-associated macrophages (TAMs), and myeloid-derived suppressor cells (MDSCs) *etc*, enhances the release of immunosuppressive cytokines[8,59], and promotes M1-TAMs to M2 type polarization. In addition, Tregs and TAMs release immunosuppressive factors, such as VEGF and angiopoietin 2, which form positive feedback to further promote tumor progression[65]. Furthermore, VEGF inhibits the maturation and antigen presentation of DCs. Thus, even in the presence of neoantigens, VEGF can reduce the proliferation and activation of naive CD8+ cells by inhibiting DCs[65]. VEGF prevents antigen activated CD8+ T cells from infiltrating tumor tissue by promoting the formation of abnormal tumor vessels. In addition, VEGF forms an immunosuppressive TME that inhibits the function of T cells in tumors during the effector phase of the immune response[65]. Therefore, inhibition of VEGF/VEGFR interaction not only normalizes vessels but also enhances antitumor immunity.

Previous studies have shown that inhibition of VEGF/VEGFR can enhance antitumor immunity. Gabrilovich *et al*[63] found that the targeted drugs which inhibit VEGF/VEGFR lead to an enhanced antigen-presenting capacity of DCs. In addition, studies also found that these drugs inhibit the production of Tregs, TAMs and MDSCs at tumor sites, and negatively regulate the expression of immunosuppressive cytokines such as transforming growth factor-beta and interleukin-10[66].

Table 2 Phase III clinical trials of combinations of anti-angiogenic inhibitors and immune checkpoint inhibitors in hepatocellular carcinoma

Trial name	Treatment	Setting	Primary endpoints	Current status	Enrollment, *n*
NCT03434379	Atezolizumab + bevacizumab	Advanced HCC; first line	OS, PFS	Active, not recruiting	558
NCT04770896	Atezolizumab + lenvatinib/sorafenib versus lenvatinib/sorafenib	Unresectable HCC; second line	OS	Recruiting	554
NCT03713593	Pembrolizumab + lenvatinib versus lenvatinib	Advanced HCC; first line	OS, PFS	Active, not recruiting	794
NCT03755791	Atezolizumab + cabozantinib versus sorafenib	Advanced HCC; first line	OS, PFS	Recruiting	740

OS: Overall survival; PFS: Progression free survival; HCC: Hepatocellular carcinoma.

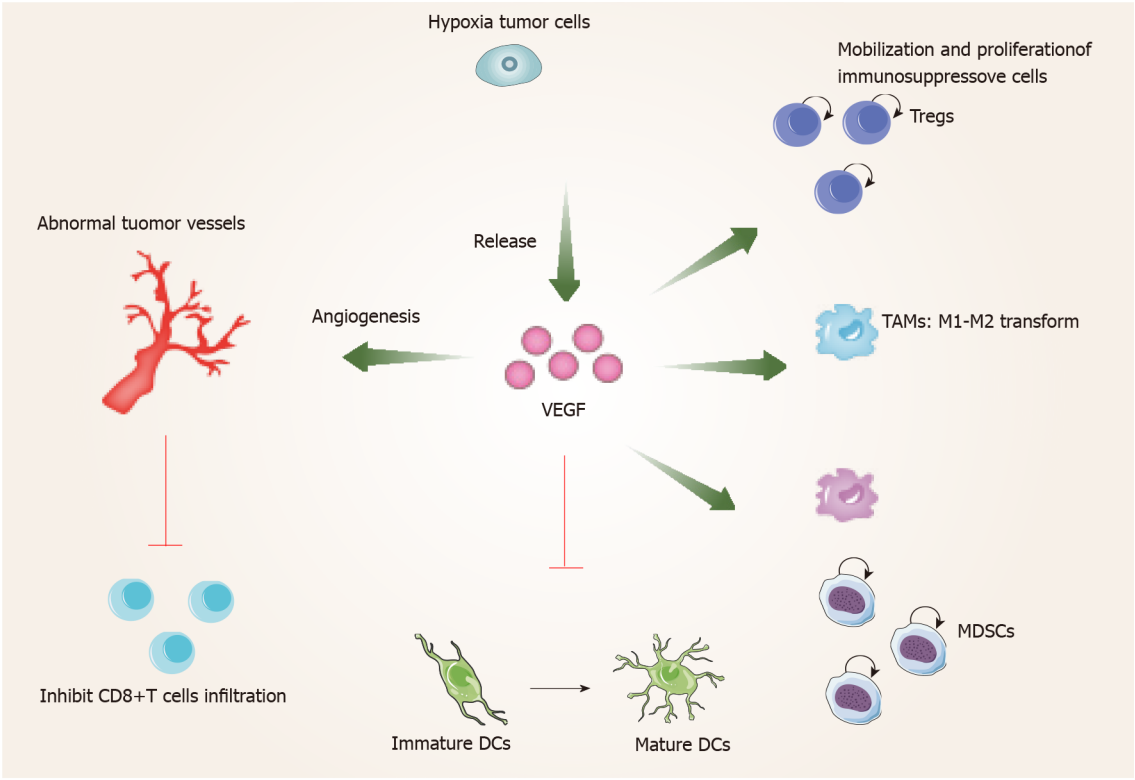

DOI: 10.3748/wjg.v28.i42.6034

Figure 1 Vascular endothelial growth factor promotes the formation of an immune suppressive microenvironment. VEGF: Vascular endothelial growth factor; DCs: Dendritic cells; MDSCs: Myeloid-derived suppressor cells; TAMs: Tumor-associated macrophages; Tregs: Regulatory T cells.

Therefore, blocking VEGF/VEGFR reprograms the immunosuppressive TME[67]. At the same time, the combination of PD-1/PD-L1 antibody can further enhance the antitumor activity of T cells. First, by reversing the VEGF-mediated suppression of DCs maturation resulting in efficient priming and activation of T cells[67,68]; second, by normalizing tumor vasculature and promoting efficient T cell infiltration into tumors[69]; and third, VEGF/VEGFR inhibitors inhibit the activity of MDSCs, Tregs, and TAMs, leading to the reprogramming of the immunosuppressive microenvironment to immune activation[61]. Finally, PD-1/PD-L1 inhibitors enhance the ability of T cells to attack tumor cells. These four aspects can lead to effective antitumor immunity and tumor growth inhibition. As described above, the use of molecularly targeted drugs against VEGF/VEGFR reactivates the aberrant immunosuppressive TME caused by VEGF, and finally allows the tumor cells to be effectively attacked[60,62]. A recent study of T+A therapy showed that the improved outcome of the combination of bevacizumab and atezolizumab compared with atezolizumab alone was mainly related to higher Tregs expression, suggesting that bevacizumab inhibits VEGF-enhanced antitumor immunity mainly related to inhibiting the function of Tregs[70]. Notably, previous studies have shown that anti-PD-1 therapy can increase tumor blood perfusion by normalizing blood vessels in breast and colorectal cancer models, which is

closely related to its antitumor efficacy[71]. These studies form the rationale for the combination of VEGF/VEGFR inhibitors and PD-1/PD-L1 inhibitors.

Biomarkers to assess the response of targeted immunotherapy

A major factor limiting the benefit of angiogenesis and immune checkpoint dual blockade for HCC is the lack of biomarkers to predict patients who can benefit from treatment. PD-L1 expression in tumor specimens was not associated with prognosis in HCC patients treated with nivolumab[48]. This study demonstrated that further comprehensive tumor and stromal immune scores, or tumor gene signatures should be explored. A recent study showed that pre-existing immunity (high expression of CD274, T-effector signature and intra-tumoral CD8+ T cell density) was positively associated with better clinical outcomes with the T+A combination and reduced clinical benefit was associated with a high Treg to effector T cell (Teff) ratio and expression of oncofetal genes (GPC3, AFP)[70]. Hatanaka *et al*[72] reported that C-reactive protein and AFP could be useful for predicting therapeutic outcomes and treatment-related AEs in HCC patients treated with the T+A combination. These results indicate that the clinical studies of bevacizumab combined with atezolizumab, lenvatinib combined with pembrolizumab, cabozantinib combined with atezolizumab and other combination therapies are a valuable platform for the analysis of other potential biomarkers of response to targeted immunotherapy and offer several new possibilities for identifying subpopulations of patients who benefit from these treatments. In several cancers, tumor mutational burden (TMB) and microsatellite instability (MSI) are associated with longer OS after ICB therapy. Considering the low frequency of TMB and MSI in HCC, their predictive applications in HCC are limited. However, it is worth noting that studies have shown that HCC with high TMB and low MSI responded to nivolumab for more than 2 years[73]. Thus, much more research is needed to determine the biomarkers of targeted immunotherapy in HCC.

CONCLUSION

The global disease burden of HCC is increasing year by year. According to statistics, the annual incidence of HCC may exceed 1 million cases in the near future, and most patients are in advanced stages at diagnosis. Currently, only reasonable systemic treatment can effectively delay the progression of HCC. This article describes the characteristics and treatment strategies of abnormal angiogenesis in HCC, and briefly reviews the immunotherapy of HCC. The strategy and rationality of angiogenesis and immune checkpoint dual blockade are further discussed. Among these combinatorial strategies, the success of the IMBrave150 clinical trial demonstrated that bevacizumab altered the tumor immune microenvironment, enabling greater responses to ICB, successfully transforming the immunosuppressive TME to an immune-activated microenvironment. Therefore, the efficacy achieved by the combination of anti-PD-1/PD-L1 antibody and VEGF/VEGFR inhibitor may be due to normalization of the TME. In addition to the combination of atezolizumab and bevacizumab, other combination therapies targeting the same mechanism have also received attention. While the clinical development of VEGF/VEGFR-targeted drugs is due to their anti-angiogenesis inhibitory effects, the potential of this class of drugs is as immunomodulators in combination with immunotherapy.

In the post-sorafenib era of advanced HCC treatment, a great number of combination therapies are being studied. However, one of the biggest challenges with combination therapy is the discovery of predictive biomarkers to accurately identify patients most likely to respond to treatment. In the study of HCC, anti-angiogenesis therapy has been used for more than a decade and ICB has been approved for several years, but these two therapies still lack convincing biomarkers. Therefore, for combination therapy, a better understanding of the mechanism of synergistic therapeutic effect and the discovery of predictive biomarkers will help to design more precise treatment regimens.

FOOTNOTES

Author contributions: Li SQ, Yang Y and Ye LS carried out the research for the manuscript and edited all drafts of the paper.

Supported by Guangdong Basic and Applied Basic Research Foundation, No. 2019A1515110654; the National Natural Science Foundation of China, No. 82103448; and China Organ Transplantation Development Foundation, No. YZLC-2021-003.

Conflict-of-interest statement: All the authors report no relevant conflicts of interest for this article.

Country/Territory of origin: China

ORCID number: Yang Yang 0000-0003-4981-4745; Lin-Sen Ye 0000-0001-9632-1949.

S-Editor: Wang JJ
L-Editor: A
P-Editor: Wang JJ

REFERENCES

1 **Xu XF**, Xing H, Han J, Li ZL, Lau WY, Zhou YH, Gu WM, Wang H, Chen TH, Zeng YY, Li C, Wu MC, Shen F, Yang T. Risk Factors, Patterns, and Outcomes of Late Recurrence After Liver Resection for Hepatocellular Carcinoma: A Multicenter Study From China. *JAMA Surg* 2019; **154**: 209-217 [PMID: 30422241 DOI: 10.1001/jamasurg.2018.4334]
2 **Lau WY**, Leung TW, Lai BS, Liew CT, Ho SK, Yu SC, Tang AM. Preoperative systemic chemoimmunotherapy and sequential resection for unresectable hepatocellular carcinoma. *Ann Surg* 2001; **233**: 236-241 [PMID: 11176130 DOI: 10.1097/00000658-200102000-00013]
3 **Topalian SL**, Taube JM, Anders RA, Pardoll DM. Mechanism-driven biomarkers to guide immune checkpoint blockade in cancer therapy. *Nat Rev Cancer* 2016; **16**: 275-287 [PMID: 27079802 DOI: 10.1038/nrc.2016.36]
4 **Mellman I**, Coukos G, Dranoff G. Cancer immunotherapy comes of age. *Nature* 2011; **480**: 480-489 [PMID: 22193102 DOI: 10.1038/nature10673]
5 **Chen X**, Xu R, He D, Zhang Y, Chen H, Zhu Y, Cheng Y, Liu R, Zhu R, Gong L, Xiao M, Wang Z, Deng L, Cao K. $CD8^+$ T effector and immune checkpoint signatures predict prognosis and responsiveness to immunotherapy in bladder cancer. *Oncogene* 2021; **40**: 6223-6234 [PMID: 34552192 DOI: 10.1038/s41388-021-02019-6]
6 **Zaremba A**, Eggermont AMM, Robert C, Dummer R, Ugurel S, Livingstone E, Ascierto PA, Long GV, Schadendorf D, Zimmer L. The concepts of rechallenge and retreatment with immune checkpoint blockade in melanoma patients. *Eur J Cancer* 2021; **155**: 268-280 [PMID: 34392069 DOI: 10.1016/j.ejca.2021.07.002]
7 **Keenan TE**, Tolaney SM. Role of Immunotherapy in Triple-Negative Breast Cancer. *J Natl Compr Canc Netw* 2020; **18**: 479-489 [PMID: 32259782 DOI: 10.6004/jnccn.2020.7554]
8 **Fukumura D**, Kloepper J, Amoozgar Z, Duda DG, Jain RK. Enhancing cancer immunotherapy using antiangiogenics: opportunities and challenges. *Nat Rev Clin Oncol* 2018; **15**: 325-340 [PMID: 29508855 DOI: 10.1038/nrclinonc.2018.29]
9 **Hanahan D**, Weinberg RA. Hallmarks of cancer: the next generation. *Cell* 2011; **144**: 646-674 [PMID: 21376230 DOI: 10.1016/j.cell.2011.02.013]
10 **Jain RK**. Normalizing tumor microenvironment to treat cancer: bench to bedside to biomarkers. *J Clin Oncol* 2013; **31**: 2205-2218 [PMID: 23669226 DOI: 10.1200/JCO.2012.46.3653]
11 **Jain RK**. Antiangiogenesis strategies revisited: from starving tumors to alleviating hypoxia. *Cancer Cell* 2014; **26**: 605-622 [PMID: 25517747 DOI: 10.1016/j.ccell.2014.10.006]
12 **Pinho SS**, Reis CA. Glycosylation in cancer: mechanisms and clinical implications. *Nat Rev Cancer* 2015; **15**: 540-555 [PMID: 26289314 DOI: 10.1038/nrc3982]
13 **Jain RK**, Koenig GC, Dellian M, Fukumura D, Munn LL, Melder RJ. Leukocyte-endothelial adhesion and angiogenesis in tumors. *Cancer Metastasis Rev* 1996; **15**: 195-204 [PMID: 8842491 DOI: 10.1007/BF00437472]
14 **Xiong XX**, Qiu XY, Hu DX, Chen XQ. Advances in Hypoxia-Mediated Mechanisms in Hepatocellular Carcinoma. *Mol Pharmacol* 2017; **92**: 246-255 [PMID: 28242743 DOI: 10.1124/mol.116.107706]
15 **Kim KR**, Moon HE, Kim KW. Hypoxia-induced angiogenesis in human hepatocellular carcinoma. *J Mol Med (Berl)* 2002; **80**: 703-714 [PMID: 12436347 DOI: 10.1007/s00109-002-0380-0]
16 **von Marschall Z**, Cramer T, Höcker M, Finkenzeller G, Wiedenmann B, Rosewicz S. Dual mechanism of vascular endothelial growth factor upregulation by hypoxia in human hepatocellular carcinoma. *Gut* 2001; **48**: 87-96 [PMID: 11115828 DOI: 10.1136/gut.48.1.87]
17 **Ferrara N**. VEGF and the quest for tumour angiogenesis factors. *Nat Rev Cancer* 2002; **2**: 795-803 [PMID: 12360282 DOI: 10.1038/nrc909]
18 **Ferrara N**, Gerber HP, LeCouter J. The biology of VEGF and its receptors. *Nat Med* 2003; **9**: 669-676 [PMID: 12778165 DOI: 10.1038/nm0603-669]
19 **Amini A**, Masoumi Moghaddam S, Morris DL, Pourgholami MH. The critical role of vascular endothelial growth factor in tumor angiogenesis. *Curr Cancer Drug Targets* 2012; **12**: 23-43 [PMID: 22111836 DOI: 10.2174/156800912798888956]
20 **Zhu AX**, Duda DG, Sahani DV, Jain RK. HCC and angiogenesis: possible targets and future directions. *Nat Rev Clin Oncol* 2011; **8**: 292-301 [PMID: 21386818 DOI: 10.1038/nrclinonc.2011.30]
21 **Poon RT**, Fan ST, Wong J. Clinical significance of angiogenesis in gastrointestinal cancers: a target for novel prognostic and therapeutic approaches. *Ann Surg* 2003; **238**: 9-28 [PMID: 12832961 DOI: 10.1097/01.sla.0000075047.47175.35]
22 **Poon RT**, Fan ST, Wong J. Clinical implications of circulating angiogenic factors in cancer patients. *J Clin Oncol* 2001; **19**: 1207-1225 [PMID: 11181687 DOI: 10.1200/JCO.2001.19.4.1207]
23 **Jain RK**, Martin JD, Stylianopoulos T. The role of mechanical forces in tumor growth and therapy. *Annu Rev Biomed Eng* 2014; **16**: 321-346 [PMID: 25014786 DOI: 10.1146/annurev-bioeng-071813-105259]
24 **Jain RK**. Normalization of tumor vasculature: an emerging concept in antiangiogenic therapy. *Science* 2005; **307**: 58-62 [PMID: 15637262 DOI: 10.1126/science.1104819]

25 **Zou G**, Zhang X, Wang L, Li X, Xie T, Zhao J, Yan J, Ye H, Jiao S, Xiang R, Shi Y. Herb-sourced emodin inhibits angiogenesis of breast cancer by targeting VEGFA transcription. *Theranostics* 2020; **10**: 6839-6853 [PMID: 32550907 DOI: 10.7150/thno.43622]

26 **Li F**, Wang Y, Chen WL, Wang DD, Zhou YJ, You BG, Liu Y, Qu CX, Yang SD, Chen MT, Zhang XN. Co-delivery of VEGF siRNA and Etoposide for Enhanced Anti-angiogenesis and Anti-proliferation Effect *via* Multi-functional Nanoparticles for Orthotopic Non-Small Cell Lung Cancer Treatment. *Theranostics* 2019; **9**: 5886-5898 [PMID: 31534526 DOI: 10.7150/thno.32416]

27 **Ding X**, Su Y, Wang C, Zhang F, Chen K, Wang Y, Li M, Wang W. Synergistic Suppression of Tumor Angiogenesis by the Co-delivering of Vascular Endothelial Growth Factor Targeted siRNA and Candesartan Mediated by Functionalized Carbon Nanovectors. *ACS Appl Mater Interfaces* 2017; **9**: 23353-23369 [PMID: 28617574 DOI: 10.1021/acsami.7b04971]

28 **Ferrara N**, Carver-Moore K, Chen H, Dowd M, Lu L, O'Shea KS, Powell-Braxton L, Hillan KJ, Moore MW. Heterozygous embryonic lethality induced by targeted inactivation of the VEGF gene. *Nature* 1996; **380**: 439-442 [PMID: 8602242 DOI: 10.1038/380439a0]

29 **Lieu CH**, Tran H, Jiang ZQ, Mao M, Overman MJ, Lin E, Eng C, Morris J, Ellis L, Heymach JV, Kopetz S. The association of alternate VEGF ligands with resistance to anti-VEGF therapy in metastatic colorectal cancer. *PLoS One* 2013; **8**: e77117 [PMID: 24143206 DOI: 10.1371/journal.pone.0077117]

30 **Ferrara N**, Hillan KJ, Novotny W. Bevacizumab (Avastin), a humanized anti-VEGF monoclonal antibody for cancer therapy. *Biochem Biophys Res Commun* 2005; **333**: 328-335 [PMID: 15961063 DOI: 10.1016/j.bbrc.2005.05.132]

31 **Cheng AL**, Qin S, Ikeda M, Galle PR, Ducreux M, Kim TY, Lim HY, Kudo M, Breder V, Merle P, Kaseb AO, Li D, Verret W, Ma N, Nicholas A, Wang Y, Li L, Zhu AX, Finn RS. Updated efficacy and safety data from IMbrave150: Atezolizumab plus bevacizumab vs. sorafenib for unresectable hepatocellular carcinoma. *J Hepatol* 2022; **76**: 862-873 [PMID: 34902530 DOI: 10.1016/j.jhep.2021.11.030]

32 **Finn RS**, Qin S, Ikeda M, Galle PR, Ducreux M, Kim TY, Kudo M, Breder V, Merle P, Kaseb AO, Li D, Verret W, Xu DZ, Hernandez S, Liu J, Huang C, Mulla S, Wang Y, Lim HY, Zhu AX, Cheng AL; IMbrave150 Investigators. Atezolizumab plus Bevacizumab in Unresectable Hepatocellular Carcinoma. *N Engl J Med* 2020; **382**: 1894-1905 [PMID: 32402160 DOI: 10.1056/NEJMoa1915745]

33 **Cheng AL**, Kang YK, Chen Z, Tsao CJ, Qin S, Kim JS, Luo R, Feng J, Ye S, Yang TS, Xu J, Sun Y, Liang H, Liu J, Wang J, Tak WY, Pan H, Burock K, Zou J, Voliotis D, Guan Z. Efficacy and safety of sorafenib in patients in the Asia-Pacific region with advanced hepatocellular carcinoma: a phase III randomised, double-blind, placebo-controlled trial. *Lancet Oncol* 2009; **10**: 25-34 [PMID: 19095497 DOI: 10.1016/S1470-2045(08)70285-7]

34 **Bruix J**, Cheng AL, Meinhardt G, Nakajima K, De Sanctis Y, Llovet J. Prognostic factors and predictors of sorafenib benefit in patients with hepatocellular carcinoma: Analysis of two phase III studies. *J Hepatol* 2017; **67**: 999-1008 [PMID: 28687477 DOI: 10.1016/j.jhep.2017.06.026]

35 **Bruix J**, Qin S, Merle P, Granito A, Huang YH, Bodoky G, Pracht M, Yokosuka O, Rosmorduc O, Breder V, Gerolami R, Masi G, Ross PJ, Song T, Bronowicki JP, Ollivier-Hourmand I, Kudo M, Cheng AL, Llovet JM, Finn RS, LeBerre MA, Baumhauer A, Meinhardt G, Han G; RESORCE Investigators. Regorafenib for patients with hepatocellular carcinoma who progressed on sorafenib treatment (RESORCE): a randomised, double-blind, placebo-controlled, phase 3 trial. *Lancet* 2017; **389**: 56-66 [PMID: 27932229 DOI: 10.1016/S0140-6736(16)32453-9]

36 **Llovet JM**, Hernandez-Gea V. Hepatocellular carcinoma: reasons for phase III failure and novel perspectives on trial design. *Clin Cancer Res* 2014; **20**: 2072-2079 [PMID: 24589894 DOI: 10.1158/1078-0432.CCR-13-0547]

37 **Schöffski P**, Gordon M, Smith DC, Kurzrock R, Daud A, Vogelzang NJ, Lee Y, Scheffold C, Shapiro GI. Phase II randomised discontinuation trial of cabozantinib in patients with advanced solid tumours. *Eur J Cancer* 2017; **86**: 296-304 [PMID: 29059635 DOI: 10.1016/j.ejca.2017.09.011]

38 **Abou-Alfa GK**, Meyer T, Cheng AL, El-Khoueiry AB, Rimassa L, Ryoo BY, Cicin I, Merle P, Chen Y, Park JW, Blanc JF, Bolondi L, Klümpen HJ, Chan SL, Zagonel V, Pressiani T, Ryu MH, Venook AP, Hessel C, Borgman-Hagey AE, Schwab G, Kelley RK. Cabozantinib in Patients with Advanced and Progressing Hepatocellular Carcinoma. *N Engl J Med* 2018; **379**: 54-63 [PMID: 29972759 DOI: 10.1056/NEJMoa1717002]

39 **Zhu AX**, Kang YK, Yen CJ, Finn RS, Galle PR, Llovet JM, Assenat E, Brandi G, Pracht M, Lim HY, Rau KM, Motomura K, Ohno I, Merle P, Daniele B, Shin DB, Gerken G, Borg C, Hiriart JB, Okusaka T, Morimoto M, Hsu Y, Abada PB, Kudo M; REACH-2 study investigators. Ramucirumab after sorafenib in patients with advanced hepatocellular carcinoma and increased α-fetoprotein concentrations (REACH-2): a randomised, double-blind, placebo-controlled, phase 3 trial. *Lancet Oncol* 2019; **20**: 282-296 [PMID: 30665869 DOI: 10.1016/S1470-2045(18)30937-9]

40 **Yang W**, Feng Y, Zhou J, Cheung OK, Cao J, Wang J, Tang W, Tu Y, Xu L, Wu F, Tan Z, Sun H, Tian Y, Wong J, Lai PB, Chan SL, Chan AW, Tan PB, Chen Z, Sung JJ, Yip KY, To KF, Cheng AS. A selective HDAC8 inhibitor potentiates antitumor immunity and efficacy of immune checkpoint blockade in hepatocellular carcinoma. *Sci Transl Med* 2021; **13** [PMID: 33827976 DOI: 10.1126/scitranslmed.aaz6804]

41 **Llovet JM**, Castet F, Heikenwalder M, Maini MK, Mazzaferro V, Pinato DJ, Pikarsky E, Zhu AX, Finn RS. Immunotherapies for hepatocellular carcinoma. *Nat Rev Clin Oncol* 2022; **19**: 151-172 [PMID: 34764464 DOI: 10.1038/s41571-021-00573-2]

42 **Medzhitov R**. Origin and physiological roles of inflammation. *Nature* 2008; **454**: 428-435 [PMID: 18650913 DOI: 10.1038/nature07201]

43 **Farhood B**, Najafi M, Mortezaee K. $CD8^+$ cytotoxic T lymphocytes in cancer immunotherapy: A review. *J Cell Physiol* 2019; **234**: 8509-8521 [PMID: 30520029 DOI: 10.1002/jcp.27782]

44 **Barber DL**, Wherry EJ, Masopust D, Zhu B, Allison JP, Sharpe AH, Freeman GJ, Ahmed R. Restoring function in exhausted CD8 T cells during chronic viral infection. *Nature* 2006; **439**: 682-687 [PMID: 16382236 DOI: 10.1038/nature04444]

45 **Pardoll DM**. The blockade of immune checkpoints in cancer immunotherapy. *Nat Rev Cancer* 2012; **12**: 252-264 [PMID: 22437870 DOI: 10.1038/nrc3239]

46 **Xie F**, Xu M, Lu J, Mao L, Wang S. The role of exosomal PD-L1 in tumor progression and immunotherapy. *Mol Cancer*

2019; **18**: 146 [PMID: 31647023 DOI: 10.1186/s12943-019-1074-3]

47 **Yao H**, Lan J, Li C, Shi H, Brosseau JP, Wang H, Lu H, Fang C, Zhang Y, Liang L, Zhou X, Wang C, Xue Y, Cui Y, Xu J. Inhibiting PD-L1 palmitoylation enhances T-cell immune responses against tumours. *Nat Biomed Eng* 2019; **3**: 306-317 [PMID: 30952982 DOI: 10.1038/s41551-019-0375-6]

48 **El-Khoueiry AB**, Sangro B, Yau T, Crocenzi TS, Kudo M, Hsu C, Kim TY, Choo SP, Trojan J, Welling TH Rd, Meyer T, Kang YK, Yeo W, Chopra A, Anderson J, Dela Cruz C, Lang L, Neely J, Tang H, Dastani HB, Melero I. Nivolumab in patients with advanced hepatocellular carcinoma (CheckMate 040): an open-label, non-comparative, phase 1/2 dose escalation and expansion trial. *Lancet* 2017; **389**: 2492-2502 [PMID: 28434648 DOI: 10.1016/S0140-6736(17)31046-2]

49 **Yau T**, Kang YK, Kim TY, El-Khoueiry AB, Santoro A, Sangro B, Melero I, Kudo M, Hou MM, Matilla A, Tovoli F, Knox JJ, Ruth He A, El-Rayes BF, Acosta-Rivera M, Lim HY, Neely J, Shen Y, Wisniewski T, Anderson J, Hsu C. Efficacy and Safety of Nivolumab Plus Ipilimumab in Patients With Advanced Hepatocellular Carcinoma Previously Treated With Sorafenib: The CheckMate 040 Randomized Clinical Trial. *JAMA Oncol* 2020; **6**: e204564 [PMID: 33001135 DOI: 10.1001/jamaoncol.2020.4564]

50 **Finn RS**, Ryoo BY, Merle P, Kudo M, Bouattour M, Lim HY, Breder V, Edeline J, Chao Y, Ogasawara S, Yau T, Garrido M, Chan SL, Knox J, Daniele B, Ebbinghaus SW, Chen E, Siegel AB, Zhu AX, Cheng AL; KEYNOTE-240 investigators. Pembrolizumab As Second-Line Therapy in Patients With Advanced Hepatocellular Carcinoma in KEYNOTE-240: A Randomized, Double-Blind, Phase III Trial. *J Clin Oncol* 2020; **38**: 193-202 [PMID: 31790344 DOI: 10.1200/JCO.19.01307]

51 **Scheiner B**, Kirstein MM, Hucke F, Finkelmeier F, Schulze K, von Felden J, Koch S, Schwabl P, Hinrichs JB, Waneck F, Waidmann O, Reiberger T, Müller C, Sieghart W, Trauner M, Weinmann A, Wege H, Trojan J, Peck-Radosavljevic M, Vogel A, Pinter M. Programmed cell death protein-1 (PD-1)-targeted immunotherapy in advanced hepatocellular carcinoma: efficacy and safety data from an international multicentre real-world cohort. *Aliment Pharmacol Ther* 2019; **49**: 1323-1333 [PMID: 30980420 DOI: 10.1111/apt.15245]

52 **Yau T**, Hsu C, Kim TY, Choo SP, Kang YK, Hou MM, Numata K, Yeo W, Chopra A, Ikeda M, Kuromatsu R, Moriguchi M, Chao Y, Zhao H, Anderson J, Cruz CD, Kudo M. Nivolumab in advanced hepatocellular carcinoma: Sorafenib-experienced Asian cohort analysis. *J Hepatol* 2019; **71**: 543-552 [PMID: 31176752 DOI: 10.1016/j.jhep.2019.05.014]

53 **Finn RS**, Ikeda M, Zhu AX, Sung MW, Baron AD, Kudo M, Okusaka T, Kobayashi M, Kumada H, Kaneko S, Pracht M, Mamontov K, Meyer T, Kubota T, Dutcus CE, Saito K, Siegel AB, Dubrovsky L, Mody K, Llovet JM. Phase Ib Study of Lenvatinib Plus Pembrolizumab in Patients With Unresectable Hepatocellular Carcinoma. *J Clin Oncol* 2020; **38**: 2960-2970 [PMID: 32716739 DOI: 10.1200/JCO.20.00808]

54 **Castet F**, Willoughby CE, Haber PK, Llovet JM. Atezolizumab plus Bevacizumab: A Novel Breakthrough in Hepatocellular Carcinoma. *Clin Cancer Res* 2021; **27**: 1827-1829 [PMID: 33472912 DOI: 10.1158/1078-0432.CCR-20-4706]

55 **Llovet JM**, Montal R, Sia D, Finn RS. Molecular therapies and precision medicine for hepatocellular carcinoma. *Nat Rev Clin Oncol* 2018; **15**: 599-616 [PMID: 30061739 DOI: 10.1038/s41571-018-0073-4]

56 **Galle PR**, Finn RS, Qin S, Ikeda M, Zhu AX, Kim TY, Kudo M, Breder V, Merle P, Kaseb A, Li D, Mulla S, Verret W, Xu DZ, Hernandez S, Ding B, Liu J, Huang C, Lim HY, Cheng AL, Ducreux M. Patient-reported outcomes with atezolizumab plus bevacizumab versus sorafenib in patients with unresectable hepatocellular carcinoma (IMbrave150): an open-label, randomised, phase 3 trial. *Lancet Oncol* 2021; **22**: 991-1001 [PMID: 34051880 DOI: 10.1016/S1470-2045(21)00151-0]

57 **Pinter M**, Ulbrich G, Sieghart W, Kölblinger C, Reiberger T, Li S, Ferlitsch A, Müller C, Lammer J, Peck-Radosavljevic M. Hepatocellular Carcinoma: A Phase II Randomized Controlled Double-Blind Trial of Transarterial Chemoembolization in Combination with Biweekly Intravenous Administration of Bevacizumab or a Placebo. *Radiology* 2015; **277**: 903-912 [PMID: 26131911 DOI: 10.1148/radiol.2015142140]

58 **Siegel AB**, Cohen EI, Ocean A, Lehrer D, Goldenberg A, Knox JJ, Chen H, Clark-Garvey S, Weinberg A, Mandeli J, Christos P, Mazumdar M, Popa E, Brown RS Jr, Rafii S, Schwartz JD. Phase II trial evaluating the clinical and biologic effects of bevacizumab in unresectable hepatocellular carcinoma. *J Clin Oncol* 2008; **26**: 2992-2998 [PMID: 18565886 DOI: 10.1200/JCO.2007.15.9947]

59 **Chouaib S**, Messai Y, Couve S, Escudier B, Hasmim M, Noman MZ. Hypoxia promotes tumor growth in linking angiogenesis to immune escape. *Front Immunol* 2012; **3**: 21 [PMID: 22566905 DOI: 10.3389/fimmu.2012.00021]

60 **Chen DS**, Mellman I. Oncology meets immunology: the cancer-immunity cycle. *Immunity* 2013; **39**: 1-10 [PMID: 23890059 DOI: 10.1016/j.immuni.2013.07.012]

61 **Hegde PS**, Wallin JJ, Mancao C. Predictive markers of anti-VEGF and emerging role of angiogenesis inhibitors as immunotherapeutics. *Semin Cancer Biol* 2018; **52**: 117-124 [PMID: 29229461 DOI: 10.1016/j.semcancer.2017.12.002]

62 **Ferrara N**, Hillan KJ, Gerber HP, Novotny W. Discovery and development of bevacizumab, an anti-VEGF antibody for treating cancer. *Nat Rev Drug Discov* 2004; **3**: 391-400 [PMID: 15136787 DOI: 10.1038/nrd1381]

63 **Gabrilovich DI**, Chen HL, Girgis KR, Cunningham HT, Meny GM, Nadaf S, Kavanaugh D, Carbone DP. Production of vascular endothelial growth factor by human tumors inhibits the functional maturation of dendritic cells. *Nat Med* 1996; **2**: 1096-1103 [PMID: 8837607 DOI: 10.1038/nm1096-1096]

64 **Gabrilovich D**, Ishida T, Oyama T, Ran S, Kravtsov V, Nadaf S, Carbone DP. Vascular endothelial growth factor inhibits the development of dendritic cells and dramatically affects the differentiation of multiple hematopoietic lineages in vivo. *Blood* 1998; **92**: 4150-4166 [PMID: 9834220]

65 **Voron T**, Marcheteau E, Pernot S, Colussi O, Tartour E, Taieb J, Terme M. Control of the immune response by pro-angiogenic factors. *Front Oncol* 2014; **4**: 70 [PMID: 24765614 DOI: 10.3389/fonc.2014.00070]

66 **Elovic AE**, Ohyama H, Sauty A, McBride J, Tsuji T, Nagai M, Weller PF, Wong DT. IL-4-dependent regulation of TGF-alpha and TGF-beta1 expression in human eosinophils. *J Immunol* 1998; **160**: 6121-6127 [PMID: 9637529]

67 **Tamura R**, Tanaka T, Akasaki Y, Murayama Y, Yoshida K, Sasaki H. The role of vascular endothelial growth factor in the hypoxic and immunosuppressive tumor microenvironment: perspectives for therapeutic implications. *Med Oncol* 2019; **37**: 2 [PMID: 31713115 DOI: 10.1007/s12032-019-1329-2]

68 **Zhao H**, Wu L, Yan G, Chen Y, Zhou M, Wu Y, Li Y. Inflammation and tumor progression: signaling pathways and targeted intervention. *Signal Transduct Target Ther* 2021; **6**: 263 [PMID: 34248142 DOI: 10.1038/s41392-021-00658-5]

69 **Goel S**, Duda DG, Xu L, Munn LL, Boucher Y, Fukumura D, Jain RK. Normalization of the vasculature for treatment of cancer and other diseases. *Physiol Rev* 2011; **91**: 1071-1121 [PMID: 21742796 DOI: 10.1152/physrev.00038.2010]

70 **Zhu AX**, Abbas AR, de Galarreta MR, Guan Y, Lu S, Koeppen H, Zhang W, Hsu CH, He AR, Ryoo BY, Yau T, Kaseb AO, Burgoyne AM, Dayyani F, Spahn J, Verret W, Finn RS, Toh HC, Lujambio A, Wang Y. Molecular correlates of clinical response and resistance to atezolizumab in combination with bevacizumab in advanced hepatocellular carcinoma. *Nat Med* 2022; **28**: 1599-1611 [PMID: 35739268 DOI: 10.1038/s41591-022-01868-2]

71 **Zheng X**, Fang Z, Liu X, Deng S, Zhou P, Wang X, Zhang C, Yin R, Hu H, Chen X, Han Y, Zhao Y, Lin SH, Qin S, Kim BY, Jiang W, Wu Q, Huang Y. Increased vessel perfusion predicts the efficacy of immune checkpoint blockade. *J Clin Invest* 2018; **128**: 2104-2115 [PMID: 29664018 DOI: 10.1172/JCI96582]

72 **Hatanaka T**, Kakizaki S, Hiraoka A, Tada T, Hirooka M, Kariyama K, Tani J, Atsukawa M, Takaguchi K, Itobayashi E, Fukunishi S, Tsuji K, Ishikawa T, Tajiri K, Ochi H, Yasuda S, Toyoda H, Ogawa C, Nishimura T, Shimada N, Kawata K, Kosaka H, Tanaka T, Ohama H, Nouso K, Morishita A, Tsutsui A, Nagano T, Itokawa N, Okubo T, Arai T, Imai M, Naganuma A, Koizumi Y, Nakamura S, Joko K, Kaibori M, Iijima H, Hiasa Y, Kumada T; Real-life Practice Experts for HCC (RELPEC) Study Group, and HCC 48 Group (hepatocellular carcinoma experts from 48 clinics in Japan). Prognostic impact of C-reactive protein and alpha-fetoprotein in immunotherapy score in hepatocellular carcinoma patients treated with atezolizumab plus bevacizumab: a multicenter retrospective study. *Hepatol Int* 2022; **16**: 1150-1160 [PMID: 35749019 DOI: 10.1007/s12072-022-10358-z]

73 **Ang C**, Klempner SJ, Ali SM, Madison R, Ross JS, Severson EA, Fabrizio D, Goodman A, Kurzrock R, Suh J, Millis SZ. Prevalence of established and emerging biomarkers of immune checkpoint inhibitor response in advanced hepatocellular carcinoma. *Oncotarget* 2019; **10**: 4018-4025 [PMID: 31258846 DOI: 10.18632/oncotarget.26998]

World Journal of Gastroenterology

Submit a Manuscript: https://www.f6publishing.com

World J Gastroenterol 2022 November 14; 28(42): 6045-6055

DOI: 10.3748/wjg.v28.i42.6045

ISSN 1007-9327 (print) ISSN 2219-2840 (online)

ORIGINAL ARTICLE

Retrospective Cohort Study

Clinical value of predictive models based on liver stiffness measurement in predicting liver reserve function of compensated chronic liver disease

Rui-Min Lai, Miao-Miao Wang, Xiao-Yu Lin, Qi Zheng, Jing Chen

Specialty type: Infectious diseases

Provenance and peer review: Unsolicited article; Externally peer reviewed.

Peer-review model: Single blind

Peer-review report's scientific quality classification

Grade A (Excellent): 0
Grade B (Very good): B
Grade C (Good): C
Grade D (Fair): 0
Grade E (Poor): 0

P-Reviewer: Enomoto H, Japan; Rodrigues AT, Brazil

Received: July 1, 2022
Peer-review started: July 1, 2022
First decision: August 1, 2022
Revised: August 13, 2022
Accepted: October 14, 2022
Article in press: October 14, 2022
Published online: November 14, 2022

Rui-Min Lai, Xiao-Yu Lin, Qi Zheng, Jing Chen, Department of Hepatology, Hepatology Research Institute, The First Affiliated Hospital, Fujian Medical University, Fuzhou 350005, Fujian Province, China

Miao-Miao Wang, Department of Endocrinology, The 910th Hospital of The Joint Service Support Force, Quanzhou 362000, Fujian Province, China

Corresponding author: Jing Chen, MD, Chief Physician, Professor, Department of Hepatology, Hepatology Research Institute, The First Affiliated Hospital, Fujian Medical University, No. 20 Chazhong Road, Taijiang District, Fuzhou 350005, Fujian Province, China.
mykelchen@sina.com

Abstract

BACKGROUND

Assessment of liver reserve function (LRF) is essential for predicting the prognosis of patients with chronic liver disease (CLD) and determines the extent of liver resection in patients with hepatocellular carcinoma.

AIM

To establish noninvasive models for LRF assessment based on liver stiffness measurement (LSM) and to evaluate their clinical performance.

METHODS

A total of 360 patients with compensated CLD were retrospectively analyzed as the training cohort. The new predictive models were established through logistic regression analysis and were validated internally in a prospective cohort (132 patients).

RESULTS

Our study defined indocyanine green retention rate at 15 min (ICGR15) ≥ 10% as mildly impaired LRF and ICGR15 ≥ 20% as severely impaired LRF. We constructed predictive models of LRF, named the mLPaM and sLPaM, which involved only LSM, prothrombin time international normalized ratio to albumin ratio (PTAR), age and model for end-stage liver disease (MELD). The area under the curve of the mLPaM model (0.855, 0.872, respectively) and sLPaM model (0.869, 0.876, respectively) were higher than that of the methods for MELD, albumin-

bilirubin grade and PTAR in the two cohorts, and their sensitivity and negative predictive value were the highest among these methods in the training cohort. In addition, the new models showed good sensitivity and accuracy for the diagnosis of LRF impairment in the validation cohort.

CONCLUSION

The new models had a good predictive performance for LRF and could replace the indocyanine green (ICG) clearance test, especially in patients who are unable to undergo ICG testing.

Key Words: Liver stiffness measurement; Chronic liver disease; Liver reserve function; Indocyanine green clearance test; Predictive model

Core Tip: This study aimed to establish predictive models of liver stiffness measurement (LSM) in patients with compensated chronic liver disease based on LSM and evaluate their clinical value. The results showed that the new models had a good predictive performance for liver reserve function (LRF). The area under the curve of the models was higher than that of the model for end-stage liver disease, albumin-bilirubin grade and prothrombin time international normalized ratio to albumin ratio. Moreover, the predictive performance of the new models was validated in a prospective cohort. We believe that these models could replace the indocyanine green (ICG) clearance test to assess LRF, especially in patients who are unable to undergo ICG testing.

Citation: Lai RM, Wang MM, Lin XY, Zheng Q, Chen J. Clinical value of predictive models based on liver stiffness measurement in predicting liver reserve function of compensated chronic liver disease. *World J Gastroenterol* 2022; 28(42): 6045-6055

URL: https://www.wjgnet.com/1007-9327/full/v28/i42/6045.htm

DOI: https://dx.doi.org/10.3748/wjg.v28.i42.6045

INTRODUCTION

The high prevalence of chronic liver disease (CLD) in China has become a severe public health problem. Cirrhosis, hepatocellular carcinoma (HCC), hepatic encephalopathy and other decompensated complications are the leading causes of mortality in CLD patients without treatment. Liver reserve function (LRF) is defined as the compensated ability of the liver to maintain normal physiological functions in the presence of injury, which mainly depends on the quality and quantity of hepatocytes in the remnant liver[1,2]. There are no obvious clinical symptoms in CLD patients in the early stage, but their LRF may be impaired. Early evaluation of LRF is of great help in identifying disease progression, timely implementation of interventions and appropriate treatment strategies in CLD patients. Several scoring systems, including the Child-Turcotte-Pugh (CTP), model for end-stage liver disease (MELD), albumin-bilirubin (ALBI) and APRI, can be used to evaluate LRF[1,3-5]. Although the CTP score is widely used to assess LRF, it includes subjective criteria, such as ascites and hepatic encephalopathy. The MELD score is initially used as a standard model to assess the prognosis of patients with decompensated cirrhosis, but its creatinine (Cr) value can be significantly affected by age and gender.

The indocyanine green (ICG) clearance test is commonly used for LRF assessment, which is considered the most valuable method for evaluating LRF. ICGR15 had become a standard dynamic preoperative instrument to evaluate the hepatic functional reserve before liver resection and predict post-hepatectomy liver failure[6,7]. However, the ICG clearance test process is tedious and requires a technical operator; thus, most of these tests can only be carried out in major hospitals. In addition, some patients are allergic to ICG, which can lead to failure of the test. Due to impossible implementation of the ICG clearance test in CLD patients, a new method to accurately assess LRF is needed.

Liver stiffness measurement (LSM) is commonly used to evaluate the degree of liver fibrosis, and due to its non-invasiveness, cost-efficiency and safety, it has been widely applied in clinical treatment. Previous studies have shown that LSM can predict the occurrence of liver failure after HCC resection[8-10]. Therefore, LSM has potential value in evaluating hepatic functional reserve.

The purpose of this study was to analyze the association between LSM and ICGR15 in evaluating LRF. We constructed the predictive models based on LSM and examined their clinical application value in evaluating LRF in compensated CLD patients.

MATERIALS AND METHODS

Research population

All patients with CLD (≥ 18 years old) consecutively observed in the inpatient department of the Hepatology Research Institute of the First Affiliated Hospital, Fujian Medical University, China, from March 2016 to June 2019 were retrospectively analyzed as the training cohort. From September 2019 to August 2020, patients with CLD were prospectively evaluated to validate the new models. Information regarding the patients' demographics, ICG clearance test, laboratory data and Fibro-scan examination was abstracted from the electronic medical record system of the First Affiliated Hospital of Fujian Medical University. Patients with the following conditions were excluded: (1) Decompensated cirrhosis with CTP grade B and C; (2) insufficient data; and (3) complicated with other tumors, or gestation. After exclusion, 492 patients were identified for study inclusion, comprising 389 chronic hepatitis B patients, 35 fatty liver disease patients, 21 autoimmune liver disease patients, 8 hepatitis C virus patients and 39 patients with other etiologies. All enrolled patients were divided into the training cohort (360 patients) and validation cohort (132 patients), including 105 HCC patients who met the diagnostic criteria in the guidelines for diagnosis and treatment of primary liver cancer in China (2019 edition)[11].

Clinical and laboratory parameters

The demographic data collected included age and gender. The clinical laboratory information included prothrombin time (PT), international normalized ratio (INR), total bilirubin (TBIL), aspartate aminotransferase, alanine aminotransferase, albumin (ALB), glomerular filtration rate, alkaline phosphatase, gamma-glutamyltransferase, cholinesterase, platelet count, and hemoglobin. The parameters were detected using an Olympus AU2700 automatic biochemical analyzer. The calculation of CTP score included five items, namely ALB, TBIL, PT, hepatic encephalopathy and ascites[12]. The CTP classifications were defined as grade A (5-6 points), grade B (7-9 points), and grade C (10-15 points). The MELD score was calculated by the formula 3.78 × ln[TBIL (mg/dL)] + 11.2 × ln (INR) + 9.57 × ln[Cr (mg/dL)] + 6.43 × etiology (0 for cholestasis and alcohol, and 1 for others)[13]. The prothrombin time international normalized ratio to albumin ratio (PTAR) score was calculated by the formula INR/ALB (g/dL)[14]. The ALBI score was calculated by the formula ln[TBIL (mol/L)] × 0.66 + ln[ALB (g/L)]-0.0852[15].

All patients received the ICG clearance test after overnight fasting, a dose of 0.5 mg/kg of ICG was rapidly injected into patients *via* a peripheral vein in the forearm. An optical probe attached to the patient's nose was used to monitor plasma ICG concentrations, and the value of ICGR15 was calculated by a Pulse Dye Densito-Graph Analyzer (DDG-3300K, Nihon Kohden, Tokyo, Japan)[16]. The LRF was defined as normal if ICGR15 < 10%, mild impairment if ICGR15 ≥ 10%, and severe impairment if ICGR15 ≥ 20%.

The Fibro-Scan 502 Touch (Echosens, Paris, France) was performed by the same trained operator according to the manufacturer's instructions. LSM was performed on the right lobe of the liver through the intercostal spaces. Ten successful acquisitions were performed for each patient. The success rate (≥ 60%) was calculated as the number of successful measurements divided by the total number of measurements recorded[17]. LSM was expressed as the median and IQR [in kilopascals (kPa)] of all valid measurements obtained. A LSM was considered reliable if 10 valid acquisitions were obtained. Patients with poorly reliable measurements (IQR/median ratio > 0.30 with a median LSM > 7.1 kPa) were excluded[18]. This retrospective study was approved by the ethics committee of the First Affiliated Hospital of Fujian Medical University, China.

Statistical analysis

Statistical analyses were performed using SPSS 23.0. The normally distributed continuous variables are presented as mean ± SD, which were further evaluated by Student's *t*-test in the different groups. Whereas, variables showing skewed distributions were evaluated by the Mann-Whitney *U* test, and are presented as median (interquartile range). Categorical variables are described using frequencies and proportions, and the Pearson's chi-squared test was used to compare categorical variables.

Multivariable analyses were conducted on variables that reached $P < 0.1$ at univariate analysis. Multivariate analysis was performed using the logistic regression analysis, and we established regression prediction models to predict the hepatic functional reserve. The continuous variables (cut-off value of LSM was 12.4 and PTAR was 0.280) were transformed into dichotomous variables. In order to avoid collinearity of some clinical indicators, stepwise forward regression was used in multivariate analysis. The optimal cut-off level of the model was determined by a receiver operator characteristic curve analysis. The areas under the curve (AUCs) were measured and compared to evaluate the discrimination ability of different models. The final predictive model was fitted on an internal validation dataset and on the entire prospective population. A two sided *P* value less than 0.05 was considered significant.

RESULTS

Summary of baseline clinical and demographic data of chronic liver disease patients

Overall, 492 patients were included in the study, including 103 patients with HCC (Table 1). 350 (71.14%) of 492 patients were male, the predominant etiology of liver disease was related to HBV (n = 389, 79.07%). Patients in the validation cohort were older than those in the training cohort (mean age, 54.84 ± 27.70 *vs* 48.71 ± 13.34, $P < 0.001$), and there was a statistically significant difference in ALB and TBIL levels. However, the two cohorts had a similar level of LSM and MELD ($P = 0.066$, $P = 0.241$, respectively).

Construction of the LRF predictive model based on LSM

With ICGR15 ≥ 10% and ICGR15 ≥ 20% as the predictive points, the new models of mildly impaired LRF (mLPaM) and severely impaired LRF (sLPaM) were constructed based on LSM. In the training cohort, 360 patient variables were included in the multivariate logistic stepwise regression analysis. LSM (OR = 4.357, 95%CI: 2.248-8.445), PTAR (OR = 3.544, 95%CI: 1.838-6.835), age (OR = 1.048, 95%CI: 1.024-1.073) and MELD score (OR = 1.340, 95%CI: 1.150-1.562) were independent influencing factors of ICGR15 ≥ 10% (Table 2). LSM (OR = 3.120, 95%CI: 1.125-8.656), PTAR (OR = 3.524, 95%CI: 1.267-9.801), age (OR = 1.059, 95%CI: 1.024-1.096) and MELD score (OR = 1.377, 95%CI: 1.146-1.655) were independent influencing factors of ICGR15 ≥ 20% (Table 3). The predictive models using the above 4 variables were constructed as follows: mLPaM = 1.472 LSM (LSM ≥ 12.4 = 2, LSM < 12.4 = 1) + 1.265 PTAR (PTAR ≥ 0.280 = 2, PTAR < 0.280 = 1) + 0.047 age (years) + 0.291 MELD-7.600 and sLPaM = 1.138 LSM (LSM ≥ 12.4 = 2, LSM < 12.4 = 1) + 1.260 PTAR (PTAR ≥ 0.280 = 2, PTAR < 0.280 = 1) + 0.058 age (years) + 0.320 MELD-9.750.

A comparison of the predictive performance of the constructed model and other methods in the training cohort

The AUC values of the mLPaM model (0.855) and sLPaM model (0.872) were greater than that of MELD score, PTAR and ALBI evaluation tools, and their sensitivity and negative predictive values were better than these evaluation methods (Table 4 and Figure 1).

Internal validation of the new predictive model in the validation cohort

132 CLD patients were prospectively considered for enrollment in the internal validation cohort. The performance of the various methods at predicting LRF is reported in Table 5. The AUC values of the mLPaM model (0.869) and sLPaM model (0.876) were greater than other LRF predictive methods. The mLPaM model showed good sensitivity (89.1%) and optimal accuracy (78.94%) for the diagnosis of mild LRF impairment, and the sLPaM model showed optimal sensitivity (92.9%) for the diagnosis of severe LRF impairment (Table 5 and Figure 2).

DISCUSSION

To date, accurate evaluation of LRF has been a hot topic in national and international research. As classic scoring systems, the CTP score and MELD score have been widely used in clinical practice. The CTP has introduced an element of bias into the scoring system due to the subjective nature of how clinical encephalopathy and ascites variables may be graded[19]. The MELD score is a continuous variable, and each indicator is given a corresponding weight through statistical analysis, which has further accuracy in evaluating LRF. In recent years, the ALBI and PTAR models have been gradually applied in clinical practice, which better evaluated LRF[20,21]. However, the ICG clearance test is currently considered the most valuable test in assessing LRF.

Although the ICG clearance test is a simple and helpful tool to assess individual LRF, it is an invasive and complex procedure, and the result is influenced by many factors (such as biliary excretion disorder and low proteinemia). In particular, the ICG clearance test is not applicable in pregnant women, patients with a history of iodine allergy or hyperthyroidism[22]. Transient elastography (TE) is a non-invasive and reproducible technique for assessing liver fibrosis, and is even a replacement for liver biopsy[23, 24]. The Baveno VII Consensus showed that TE was an accurate tool for the prediction of CSPH[25]. In a previous study, it was found that LSM could predict postoperative liver failure in patients with HCC [26]. Therefore, LSM is considered to have a strong relationship with liver function.

As liver function impairment is the primary determinant of the development of post-hepatectomy liver failure, the vast majority of candidates for liver resection had CTP grade A[27]. According to the CTP classification, the majority of patients with HCC were classified as grade A, but their liver function may vary significantly[15]. A previous study revealed that ICGR15 was more accurate than the CTP score and MELD score in predicting hepatic functional reserve before hepatectomy[3]. The study showed that ICGR15 > 15% was an accurate method of predicting postoperative hepatic decompensation in patients with CTP grade A[28]. In patients with an ICGR15 > 20%, a previous study

Table 1 Comparison of demographic and clinical characteristics of chronic liver disease patients in the training cohort and validation cohort

	Validation cohort, *n* = 132	Training cohort, *n* = 360	*P* value
Gender (male/female, *n*)	90/42	260/100	0.381
Age (yr)	54.84 ± 27.70	48.71 ± 13.34	0.001
Etiology			0.097
HBV	111	278	
Others	21	82	
HCC (*n*)	42	63	**0.001**
HB (g/dL)	14.28 ± 10.86	13.71 ± 2.16	0.346
PLT (× 10^9/L)	174.96 ± 83.93	170.95 ± 74.69	0.610
PT (s)	13.21 ± 1.66	12.84 ± 1.67	**0.030**
APTT (s)	33.28 ± 7.73	32.54 ± 6.14	0.273
INR	1.16 ± 0.16	1.09 ± 0.16	**0.000**
AST (U/L)	72.14 ± 78.19	86.16 ± 135.81	0.264
ALT (U/L)	106.35 ± 166.60	136.73 ± 247.37	0.192
ALB (g/L)	38.03 ± 5.22	40.03 ± 5.08	**0.000**
TBIL (μmol/L)	28.29 ± 31.05	19.94 ± 16.99	**0.000**
CHE (U/L)	6163.11 ± 2647.19	6748.44 ± 2127.44	**0.015**
ALP (U/L)	118.60 ± 95.93	179.64 ± 721.94	0.334
GGT (U/L)	128.91 ± 201.79	116.89 ± 188.75	0.539
GLO (g/L)	28.70 ± 4.81	29.02 ± 5.19	0.534
Cr (μmol/L)	65.36 ± 23.23	65.68 ± 15.38	0.860
MELD	8.14 ± 3.46	7.80 ± 2.56	0.241
ALBI	-2.36 ± 0.54	-2.60 ± 0.48	**0.000**
PTAR	0.31 ± 0.07	0.28 ± 0.07	**0.000**
ICGR15 (%)	11.55 ± 11.82	8.16 ± 8.56	**0.000**
LSM (kPa)	19.54 ± 18.28	16.34 ± 16.62	0.066

HBV: Hepatitis B virus; HCC: Hepatocellular carcinoma; HB: Hemoglobin; PLT: Platelet count; PT: Prothrombin time; APTT: Active prothrombin time; INR: International normalized ratio; AST: Aspartate transaminase; ALT: Alanine aminotransaminase; ALB: Albumin; TBIL: Total bilirubin; CHE: Cholinesterase; ALP: Alkaline phosphatase; GGT: Gamma-glutamyltransferase; GLO: Globulin; Cr: Creatinine; MELD: Model for end-stage liver disease; ALBI: Albumin-bilirubin grade; PTAR: Prothrombin time international normalized ratio to albumin ratio; ICGR15: Indocyanine green retention rate at 15 min; LSM: Liver stiffness measurement.

recommended non-anatomical resection rather than anatomical resection for the treatment of a solitary 2–5-cm-diameter HCC without macroscopic vascular invasion[29]. Therefore, it is essential to assess LRF before HCC hepatectomy, thereby assisting clinical decision-making.

Our research constructed new models for clinical prediction of LRF impairment based on LSM, and the models were superior to other existing methods for predicting LRF (Table 4 and Figure 1). Moreover, compared to the other four methods, the models also showed better performance for predicting LRF in the prospective validation cohort (Table 5 and Figure 2). Therefore, based on the analysis of the above research results, these models could be an alternative tool for LRF assessment, especially in evaluating a population almost entirely stratified as CTP grade A.

Limitations of the study

Despite the significant findings in this study, our research also had a few limitations. First, the study was limited by its single-center prospective cohort nature. The patients were recruited from the same medical facility, and not all patients with complete clinical data were obtained from a treatment database. Second, most of the patients in this study were Asians with B viral hepatitis. Therefore, the performance of the model in patients of other ethnicities (*e.g.*, Caucasians, Africans, *etc.*) still needs

Table 2 Multivariate logistic stepwise regression analysis of indocyanine green retention rate at 15 min ≥ 10% in the training cohort

Variable	*B*	SE	Wald	*P* value	OR (95%CI)
LSM (kPa)	1.472	0.338	19.008	< 0.001	4.357 (2.248-8.445)
PTAR	1.265	0.335	14.260	< 0.001	3.544 (1.838-6.835)
Age (yr)	0.047	0.012	15.329	< 0.001	1.048 (1.024-1.073)
MELD	0.291	0.078	13.844	< 0.001	1.337 (1.147-1.558)
Constant	-7.600	1.022	55.302	< 0.001	0.007

LSM: Liver stiffness measurement; PTAR: Prothrombin time international normalized ratio to albumin ratio; MELD: Model for end-stage liver disease.

Table 3 Multivariate logistic stepwise regression analysis of indocyanine green retention rate at 15 min ≥ 20% in the training cohort

Variable	*B*	SE	Wald	*P* value	OR (95%CI)
LSM (kPa)	1.138	0.520	4.778	0.029	3.120 (1.125-8.656)
PTAR	1.260	0.521	5.825	0.016	3.524 (1.267-9.801)
Age (yr)	0.058	0.017	11.226	0.001	1.059 (1.024-1.096)
MELD	0.320	0.094	11.652	0.001	1.377 (1.146-1.655)
Constant	-9.750	-1.454	44.963	< 0.001	0.001

LSM: Liver stiffness measurement; PTAR: Prothrombin time international normalized ratio to albumin ratio; MELD: Model for end-stage liver disease.

Table 4 Comparison of the predictive performance of the new constructed models (mLPaM and sLPaM) and other models in the assessment of impaired liver reserve function in the training cohort

	AUC (95%CI)	Optimal cut-off	Sensitivity (%)	Specificity (%)	PPV (%)	NPV (%)	Accuracy (%)
mLPaM	0.855 (0.809-0.901)	0.135	91.3	66.4	36.09	97.35	70.68
MELD	0.752 (0.688-0.817)	7.662	80.0	61.4	31.25	93.33	54.75
ALBI	0.776 (0.717-0.835)	-2.557	76.3	67.9	37.67	91.85	69.90
PTAR	0.728 (0.664-0.791)	0.150	73.8	71.8	42.11	90.79	72.24
LSM (kPa)	0.733 (0.672-0.794)	1.50	78.8	67.9	37.67	92.86	70.05
sLPaM	0.872 (0.823-0.921)	0.046	96.8	64.6	14.83	99.69	66.53
MELD	0.786 (0.687-0.886)	9.380	71.0	85.2	35.45	96.25	83.74
ALBI	0.798 (0.706-0.890)	-2.220	64.5	87.4	39.81	95.01	84.78
PTAR	0.731 (0.644-0.818)	0.150	80.6	65.5	15.33	97.76	66.59
LSM (kPa)	0.706 (0.618-0.795)	1.50	80.6	60.6	12.79	97.76	61.94

MELD: Model for end-stage liver disease; ALBI: Albumin-bilirubin grade; PTAR: Prothrombin time international normalized ratio to albumin ratio; LSM: Liver stiffness measurement; AUC: Area under the cure; CI: Confidence interval; NPV: Negative predictive value; PPV: Positive predictive value; mLPaM: Mildly impaired liver reserve function model; sLPaM: Severely impaired liver reserve function model.

further investigation. Third, the models were mainly used to evaluate LRF in patients with compensated CLD, and their predictive value in patients with decompensated stage needs further evaluation. Finally, although the formula for the models was relatively complex, a mobile app or web-based calculator could calculate the score easily and rapidly in the current high-tech era. Despite these limitations, this study provided the first accurate models for evaluating LRF based on LSM in China.

Table 5 Comparison of the predictive performance of the new constructed models (mLPaM and sLPaM) and other models in the assessment of impaired liver reserve function in the prospective validation cohort

	AUC (95%CI)	Optimal cut-off	Sensitivity (%)	Specificity (%)	PPV (%)	NPV (%)	Accuracy (%)
mLPaM	0.869 (0.810-0.929)	0.240	89.1	74.4	60.85	93.86	78.94
MELD	0.729 (0.633-0.824)	9.743	43.5	96.5	93.65	59.01	67.74
ALBI	0.824 (0.749-0.900)	-2.315	78.3	76.7	63.78	87.09	77.25
PTAR	0.672 (0.580-0.765)	1.500	89.1	45.3	30.70	93.86	54.66
LSM (kPa)	0.782 (0.702-0.862)	1.500	91.3	65.1	49.93	95.15	72.33
sLPaM	0.876 (0.812-0.940)	0.073	92.9	68.3	49.94	95.15	72.33
MELD	0.803 (0.701-0.904)	9.187	64.3	85.6	61.54	87.00	79.98
ALBI	0.836 (0.743-0.929)	-1.897	71.4	88.5	67.44	90.27	84.22
PTAR	0.666 (0.566-0.767)	1.500	92.9	59.6	28.43	97.98	64.50
LSM (kPa)	0.743 (0.653-0.833)	1.500	92.9	55.8	25.37	97.98	60.96

MELD: Model for end-stage liver disease; ALBI: Albumin-bilirubin grade; PTAR: Prothrombin time international normalized ratio to albumin ratio; LSM: Liver stiffness measurement; AUC: Area under the cure; CI: Confidence interval; NPV: Negative predictive value; PPV: Positive predictive value; mLPaM: Mildly impaired liver reserve function model; sLPaM: Severely impaired liver reserve function model.

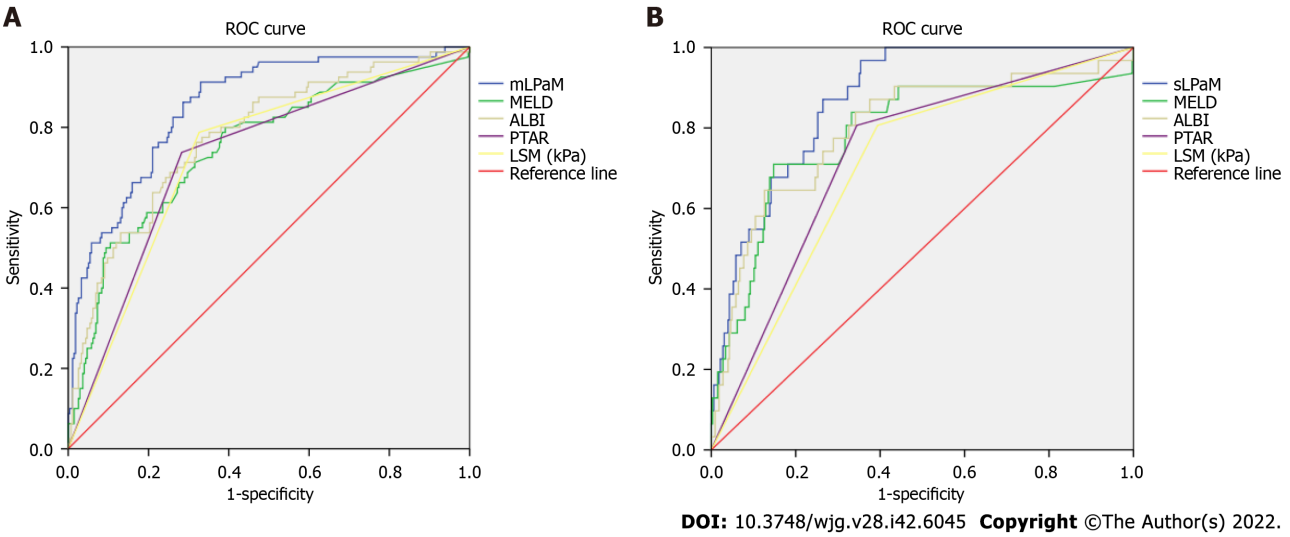

DOI: 10.3748/wjg.v28.i42.6045

Figure 1 Comparison of different liver reserve function assessment methods by receiver operator characteristic curves in the training cohort. A: mLPaM is indocyanine green retention rate at 15 min (ICGR15) ≥ 10%; B: sLPaM is ICGR15 ≥ 20%. ROC: Receiver operator characteristic; MELD: Model for end-stage liver disease; ALBI: Albumin-bilirubin grade; PTAR: Prothrombin time international normalized ratio to albumin ratio; LSM: Liver stiffness measurement; mLPaM: Mildly impaired liver reserve function model; sLPaM: Severely impaired liver reserve function model.

CONCLUSION

The first predicted models based on LSM could facilitate accurate, reliable and simple-to-use prediction of LRF irrespective of etiology. They are entirely objective based on routine clinical and laboratory parameters. These models would be a useful tool for realizing individualized LRF evaluation to improve the popularity of testing and avoid possible risks during the ICG clearance test, ultimately achieving a clinically feasible and safe LRF test.

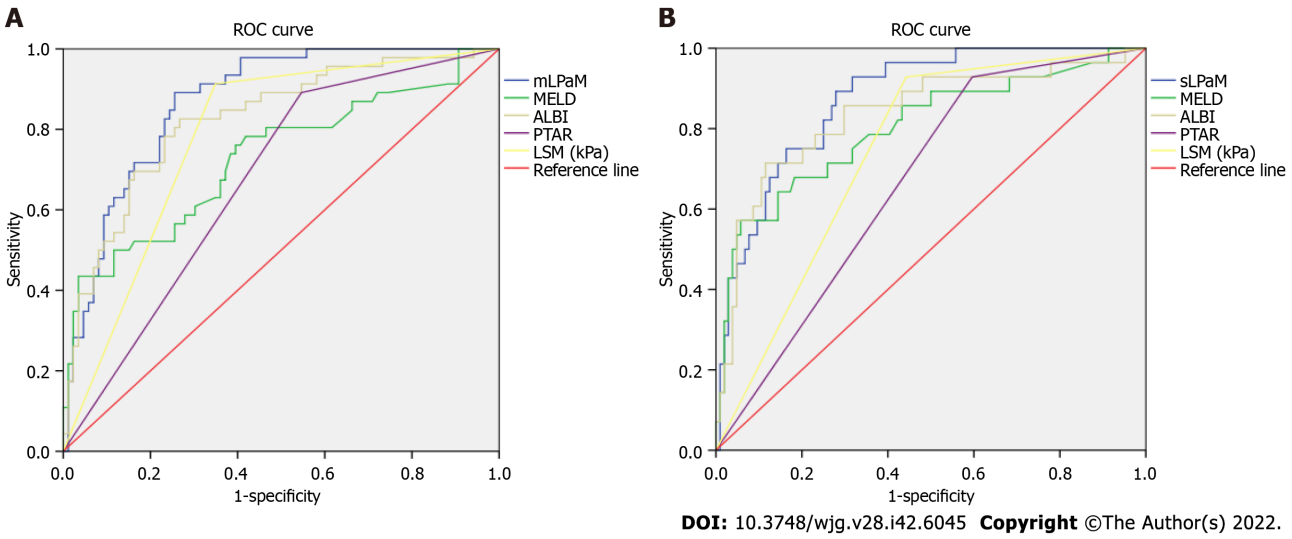

DOI: 10.3748/wjg.v28.i42.6045

Figure 2 Comparison of different liver reserve function assessment methods by area under the curves in the validation cohort. A: mLPaM is indocyanine green retention rate at 15 min (ICGR15) ≥ 10%; B: sLPaM is ICGR15 ≥ 20%. ROC: Receiver operator characteristic; MELD: Model for end-stage liver disease; ALBI: Albumin-bilirubin grade; PTAR: Prothrombin time international normalized ratio to albumin ratio; LSM: Liver stiffness measurement; mLPaM: Mildly impaired liver reserve function model; sLPaM: Severely impaired liver reserve function model.

ARTICLE HIGHLIGHTS

Research background

There are no obvious clinical symptoms in chronic liver disease (CLD) patients at the early stage, but their liver reserve function (LRF) may be impaired. Early evaluation of LRF is of great help in identifying disease progression. Assessment of LRF is essential for predicting the prognosis of patients with CLD and determines the extent of liver resection in patients with hepatocellular carcinoma (HCC).

Research motivation

Liver function impairment is the primary determinant in the development of post-hepatectomy liver failure. There are no obvious clinical symptoms in CLD patients at Child-Turcotte-Pugh A stage, but their LRF may be impaired. Due to impossible implementation of the indocyanine green (ICG) clearance test in some CLD patients, a new method to accurately assess LRF is needed.

Research objectives

This study aimed to establish noninvasive models of LRF assessment based on LSM. The new predictive models were established through logistic regression analysis and were validated internally in a prospective cohort. The new models had a good predictive performance on LRF and could replace the ICG clearance test, especially in the patients who are unable to undergo ICG testing.

Research methods

Clinical data from 360 patients with compensated CLD were retrospectively collected and analyzed in the training cohort. The new predictive models were established through logistic regression analysis and were validated internally in a prospective cohort (132 patients). The areas under the ROC curve (AUCs) were measured and compared to evaluate the discrimination ability of different models.

Research results

Our study defined the indocyanine green retention rate at 15 min (ICGR15) ≥ 10% as mildly impaired LRF and ICGR15 ≥ 20% as severely impaired LRF. We constructed predictive models of LRF, named the mLPaM and sLPaM, which involved only LSM, prothrombin time international normalized ratio to albumin ratio, age and model for end-stage liver disease. The AUC of the mLPaM model (0.855, 0.872, respectively) and sLPaM model (0.869, 0.876, respectively) were higher than that of other methods in the two cohorts. In addition, the new models showed good sensitivity and accuracy for the diagnosis of LRF impairment in the validation cohort.

Research conclusions

Our study found that the new models had a good predictive performance for LRF and could replace the ICG clearance test, especially in patients who are unable to undergo ICG testing.

Research perspectives

This was not a multicenter study and most of the CLD patients in this study were Asians. Therefore, a multi-center prospective cohort study could further evaluate the performance of the predictive models, and the models in patients of other ethnicities need further investigation. The predictive value of the models in patients with a decompensated stage need further evaluation.

ACKNOWLEDGEMENTS

We would like to thank the patients who participated in this study.

FOOTNOTES

Author contributions: Lai RM and Zheng Q conceived and designed the study; Wang MM and Lin XY collected clinical data of the patients and contributed to the data analysis; Lai RM and Chen J wrote the manuscript; and all authors approved the final version of the manuscript.

Supported by Startup Fund for Scientific Research of Fujian Medical University, No. 2018QH1052; and Fujian Health Research Talents Training Program, No. 2019-1-42.

Institutional review board statement: This retrospective study was approved by the ethics committee at the First Affiliated Hospital of Fujian Medical University, China.

Informed consent statement: Patients were not required to give informed consent to the study as the analysis used anonymous data that were obtained after each patient agreed to treatment by written consent.

Conflict-of-interest statement: All the authors report no relevant conflicts of interest for this article.

Data sharing statement: The original anonymous dataset is available on request from the corresponding author at mykelchen@sina.com.

STROBE statement: The authors have read the STROBE Statement—checklist of items, and the manuscript was prepared and revised according to the STROBE Statement—checklist of items.

Country/Territory of origin: China

ORCID number: Rui-Min Lai 0000-0003-2911-0273; Qi Zheng 0000-0001-8006-7069; Jing Chen 0000-0001-5602-1554.

S-Editor: Gong ZM
L-Editor: Webster JR
P-Editor: Gong ZM

REFERENCES

1 **Mai RY**, Zeng J, Lu HZ, Liang R, Lin Y, Piao XM, Gao X, Wu GB, Wu FX, Ma L, Xiang BD, Li LQ, Ye JZ. Combining Aspartate Aminotransferase-to-Platelet Ratio Index with Future Liver Remnant to Assess Preoperative Hepatic Functional Reserve in Patients with Hepatocellular Carcinoma. *J Gastrointest Surg* 2021; **25**: 688-697 [PMID: 32274631 DOI: 10.1007/s11605-020-04575-w]

2 **Cieslak KP**, Runge JH, Heger M, Stoker J, Bennink RJ, van Gulik TM. New perspectives in the assessment of future remnant liver. *Dig Surg* 2014; **31**: 255-268 [PMID: 25322678 DOI: 10.1159/000364836]

3 **Wang YY**, Zhao XH, Ma L, Ye JZ, Wu FX, Tang J, You XM, Xiang BD, Li LQ. Comparison of the ability of Child-Pugh score, MELD score, and ICG-R15 to assess preoperative hepatic functional reserve in patients with hepatocellular carcinoma. *J Surg Oncol* 2018; **118**: 440-445 [PMID: 30259515 DOI: 10.1002/jso.25184]

4 **Lin ZH**, Xin YN, Dong QJ, Wang Q, Jiang XJ, Zhan SH, Sun Y, Xuan SY. Performance of the aspartate aminotransferase-to-platelet ratio index for the staging of hepatitis C-related fibrosis: an updated meta-analysis. *Hepatology* 2011; **53**: 726-736 [PMID: 21319189 DOI: 10.1002/hep.24105]

5 **Demirtas CO**, D'Alessio A, Rimassa L, Sharma R, Pinato DJ. ALBI grade: Evidence for an improved model for liver

functional estimation in patients with hepatocellular carcinoma. *JHEP Rep* 2021; **3**: 100347 [PMID: 34505035 DOI: 10.1016/j.jhepr.2021.100347]

6 **De Gasperi A**, Mazza E, Prosperi M. Indocyanine green kinetics to assess liver function: Ready for a clinical dynamic assessment in major liver surgery? *World J Hepatol* 2016; **8**: 355-367 [PMID: 26981173 DOI: 10.4254/wjh.v8.i7.355]

7 **Sato N**, Kenjo A, Suzushino S, Kimura T, Okada R, Ishigame T, Kofunato Y, Marubashi S. Predicting Post-Hepatectomy Liver Failure Using Intra-Operative Measurement of Indocyanine Green Clearance in Anatomical Hepatectomy. *World J Surg* 2021; **45**: 3660-3667 [PMID: 34392399 DOI: 10.1007/s00268-021-06289-9]

8 **Lei Q**, Zhang Y, Ke C, Yan C, Huang P, Shen H, Lei H, Chen Y, Luo J, Meng Z. Value of the albumin-bilirubin score in the evaluation of hepatitis B virus-related acute-on-chronic liver failure, liver cirrhosis, and hepatocellular carcinoma. *Exp Ther Med* 2018; **15**: 3074-3079 [PMID: 29456711 DOI: 10.3892/etm.2018.5748]

9 **Huang Z**, Huang J, Zhou T, Cao H, Tan B. Prognostic value of liver stiffness measurement for the liver-related surgical outcomes of patients under hepatic resection: A meta-analysis. *PLoS One* 2018; **13**: e0190512 [PMID: 29324802 DOI: 10.1371/journal.pone.0190512]

10 **Serenari M**, Han KH, Ravaioli F, Kim SU, Cucchetti A, Han DH, Odaldi F, Ravaioli M, Festi D, Pinna AD, Cescon M. A nomogram based on liver stiffness predicts postoperative complications in patients with hepatocellular carcinoma. *J Hepatol* 2020; **73**: 855-862 [PMID: 32360997 DOI: 10.1016/j.jhep.2020.04.032]

11 **Department of Medical Administration, National Health and Health Commission of the People's Republic of China**. [Guidelines for diagnosis and treatment of primary liver cancer in China (2019 edition)]. *Zhonghua Gan Zang Bing Za Zhi* 2020; **28**: 112-128 [PMID: 32164061 DOI: 10.3760/cma.j.issn.1007-3418.2020.02.004]

12 **Durand F**, Valla D. Assessment of the prognosis of cirrhosis: Child-Pugh versus MELD. *J Hepatol* 2005; **42** Suppl: S100-S107 [PMID: 15777564 DOI: 10.1016/j.jhep.2004.11.015]

13 **Perdigoto DN**, Figueiredo P, Tomé L. The Role of the CLIF-C OF and the 2016 MELD in Prognosis of Cirrhosis with and without Acute-on-Chronic Liver Failure. *Ann Hepatol* 2019; **18**: 48-57 [PMID: 31113608 DOI: 10.5604/01.3001.0012.7862]

14 **Haruki K**, Shiba H, Saito N, Horiuchi T, Shirai Y, Fujiwara Y, Furukawa K, Sakamoto T, Yanaga K. Risk stratification using a novel liver functional reserve score of combination prothrombin time-international normalized ratio to albumin ratio and albumin in patients with hepatocellular carcinoma. *Surgery* 2018; **164**: 404-410 [PMID: 29754978 DOI: 10.1016/j.surg.2018.02.022]

15 **Johnson PJ**, Berhane S, Kagebayashi C, Satomura S, Teng M, Reeves HL, O'Beirne J, Fox R, Skowronska A, Palmer D, Yeo W, Mo F, Lai P, Iñarrairaegui M, Chan SL, Sangro B, Miksad R, Tada T, Kumada T, Toyoda H. Assessment of liver function in patients with hepatocellular carcinoma: a new evidence-based approach-the ALBI grade. *J Clin Oncol* 2015; **33**: 550-558 [PMID: 25512453 DOI: 10.1200/JCO.2014.57.9151]

16 **Wang L**, Xie L, Zhang N, Zhu W, Zhou J, Pan Q, Mao A, Lin Z, Wang L, Zhao Y. Predictive Value of Intraoperative Indocyanine Green Clearance Measurement on Postoperative Liver Function After Anatomic Major Liver Resection. *J Gastrointest Surg* 2020; **24**: 1342-1351 [PMID: 31197694 DOI: 10.1007/s11605-019-04262-5]

17 **Naveau S**, Voican CS, Lebrun A, Gaillard M, Lamouri K, Njiké-Nakseu M, Courie R, Tranchart H, Balian A, Prévot S, Dagher I, Perlemuter G. Controlled attenuation parameter for diagnosing steatosis in bariatric surgery candidates with suspected nonalcoholic fatty liver disease. *Eur J Gastroenterol Hepatol* 2017; **29**: 1022-1030 [PMID: 28570343 DOI: 10.1097/MEG.0000000000000919]

18 **Boursier J**, Zarski JP, de Ledinghen V, Rousselet MC, Sturm N, Lebail B, Fouchard-Hubert I, Gallois Y, Oberti F, Bertrais S, Calès P; Multicentric Group from ANRS/HC/EP23 FIBROSTAR Studies. Determination of reliability criteria for liver stiffness evaluation by transient elastography. *Hepatology* 2013; **57**: 1182-1191 [PMID: 22899556 DOI: 10.1002/hep.25993]

19 **Kok B**, Abraldes JG. Child-Pugh Classification: Time to Abandon? *Semin Liver Dis* 2019; **39**: 96-103 [PMID: 30634187 DOI: 10.1055/s-0038-1676805]

20 **Feng D**, Wang M, Hu J, Li S, Zhao S, Li H, Liu L. Prognostic value of the albumin-bilirubin grade in patients with hepatocellular carcinoma and other liver diseases. *Ann Transl Med* 2020; **8**: 553 [PMID: 32411776 DOI: 10.21037/atm.2020.02.116]

21 **Levesque E**, Martin E, Dudau D, Lim C, Dhonneur G, Azoulay D. Current use and perspective of indocyanine green clearance in liver diseases. *Anaesth Crit Care Pain Med* 2016; **35**: 49-57 [PMID: 26477363 DOI: 10.1016/j.accpm.2015.06.006]

22 **Gao F**, Cai MX, Lin MT, Xie W, Zhang LZ, Ruan QZ, Huang ZM. Prognostic value of international normalized ratio to albumin ratio among critically ill patients with cirrhosis. *Eur J Gastroenterol Hepatol* 2019; **31**: 824-831 [PMID: 30601338 DOI: 10.1097/MEG.0000000000001339]

23 **Singh S**, Muir AJ, Dieterich DT, Falck-Ytter YT. American Gastroenterological Association Institute Technical Review on the Role of Elastography in Chronic Liver Diseases. *Gastroenterology* 2017; **152**: 1544-1577 [PMID: 28442120 DOI: 10.1053/j.gastro.2017.03.016]

24 **Park CC**, Nguyen P, Hernandez C, Bettencourt R, Ramirez K, Fortney L, Hooker J, Sy E, Savides MT, Alquiraish MH, Valasek MA, Rizo E, Richards L, Brenner D, Sirlin CB, Loomba R. Magnetic Resonance Elastography *vs* Transient Elastography in Detection of Fibrosis and Noninvasive Measurement of Steatosis in Patients With Biopsy-Proven Nonalcoholic Fatty Liver Disease. *Gastroenterology* 2017; **152**: 598-607.e2 [PMID: 27911262 DOI: 10.1053/j.gastro.2016.10.026]

25 **de Franchis R**, Bosch J, Garcia-Tsao G, Reiberger T, Ripoll C; Baveno VII Faculty. Baveno VII - Renewing consensus in portal hypertension. *J Hepatol* 2022; **76**: 959-974 [PMID: 35120736 DOI: 10.1016/j.jhep.2021.12.022]

26 **Shen Y**, Zhou C, Zhu G, Shi G, Zhu X, Huang C, Zhou J, Fan J, Ding H, Ren N, Sun HC. Liver Stiffness Assessed by Shear Wave Elastography Predicts Postoperative Liver Failure in Patients with Hepatocellular Carcinoma. *J Gastrointest Surg* 2017; **21**: 1471-1479 [PMID: 28510795 DOI: 10.1007/s11605-017-3443-9]

27 **Maluccio M**, Covey A. Recent progress in understanding, diagnosing, and treating hepatocellular carcinoma. *CA Cancer J Clin* 2012; **62**: 394-399 [PMID: 23070690 DOI: 10.3322/caac.21161]

28 **Le Roy B**, Grégoire E, Cossé C, Serji B, Golse N, Adam R, Cherqui D, Mabrut JY, Le Treut YP, Vibert E. Indocyanine Green Retention Rates at 15 min Predicted Hepatic Decompensation in a Western Population. *World J Surg* 2018; **42**: 2570-2578 [PMID: 29340728 DOI: 10.1007/s00268-018-4464-6]

29 **Yamamoto Y**, Ikoma H, Morimura R, Konishi H, Murayama Y, Komatsu S, Shiozaki A, Kuriu Y, Kubota T, Nakanishi M, Ichikawa D, Fujiwara H, Okamoto K, Sakakura C, Ochiai T, Otsuji E. Clinical analysis of anatomical resection for the treatment of hepatocellular carcinoma based on the stratification of liver function. *World J Surg* 2014; **38**: 1154-1163 [PMID: 24305927 DOI: 10.1007/s00268-013-2369-y]

World Journal of Gastroenterology

Submit a Manuscript: https://www.f6publishing.com

World J Gastroenterol 2022 November 14; 28(42): 6056-6067

DOI: 10.3748/wjg.v28.i42.6056

ISSN 1007-9327 (print) ISSN 2219-2840 (online)

ORIGINAL ARTICLE

Retrospective Study

Novel management indications for conservative treatment of chylous ascites after gastric cancer surgery

Peng-Fei Kong, Yong-Hu Xu, Zhi-Hua Lai, Ming-Zhe Ma, Yan-Tao Duan, Bo Sun, Da-Zhi Xu

Specialty type: Food Science and technology

Provenance and peer review: Unsolicited article; Externally peer reviewed.

Peer-review model: Single blind

Peer-review report's scientific quality classification

Grade A (Excellent): 0
Grade B (Very good): B, B
Grade C (Good): 0
Grade D (Fair): 0
Grade E (Poor): 0

P-Reviewer: Aoki H, Japan; Ilhan E, Turkey

Received: June 27, 2022
Peer-review started: June 27, 2022
First decision: August 1, 2022
Revised: August 15, 2022
Accepted: October 26, 2022
Article in press: October 26, 2022
Published online: November 14, 2022

Peng-Fei Kong, Yong-Hu Xu, Ming-Zhe Ma, Yan-Tao Duan, Bo Sun, Da-Zhi Xu, Department of Gastric Surgery, Fudan University Shanghai Cancer Center, Shanghai 200032, China

Zhi-Hua Lai, Department of the General Surgery, Suzhou Industrial Park Xinghai Hospital, Suzhou 215124, Jiangsu Province, China

Corresponding author: Da-Zhi Xu, MD, PhD, Chief Doctor, Professor, Surgeon, Department of Gastric Surgery, Fudan University Shanghai Cancer Center, No. 270 Dong'an Road, Shanghai 200032, China. xudzh@shca.org.cn

Abstract

BACKGROUND

Chylous ascites (CA) presents a challenge as a relatively common postoperative complication in gastric cancer (GC). Primary conservative therapy involved total parenteral nutrition, continuous low-pressure drainage, somatostatin, and a low-fat diet. Drainage tube (DT) clamping has been presented as a potential alternative conservative treatment for GC patients with CA.

AIM

To propose novel conservative treatment strategies for CA following GC surgery.

METHODS

The data of patients with CA after GC surgery performed at the Fudan University Shanghai Cancer Center between 2006 and 2021 were evaluated retrospectively.

RESULTS

53 patients underwent surgery for GC and exhibited postoperative CA during the study period. Postoperative hospitalization and time of DT removal showed a significant positive association (R^2 = 0.979, P < 0.001). We further observed that delayed DT removal significantly extended the total and postoperative hospitalization, antibiotic usage duration, and hospitalization cost (postoperative hospitalization: 25.8 d *vs* 15.5 d, P < 0.001; total hospitalization: 33.2 d *vs* 24.7 d, P < 0.01; antibiotic usage duration: 10.8 d *vs* 6.2 d, P < 0.01; hospitalization cost: ¥9.2 × 10^4 *vs* ¥6.5 × 10^4, P < 0.01). Multivariate analysis demonstrated that postoperative infection and antibiotic usage were independent factors for delayed DT removal. Furthermore, DT removal times were shorter in seven patients who underwent DT clamping (clamped DT *vs* normal group, 11.8 d *vs* 13.6 d, P = 0.047; clamped DT *vs* delayed group, 13.6 d *vs* 27.4 d, P < 0.001). In addition, our results indicated

that removal of the DT may be possible after three consecutive days of drainage volumes less than 300 mL in GC patients with CA.

CONCLUSION

Infection and antibiotic usage were vital independent factors that influenced delayed DT removal in patients with CA. Appropriate standards for DT removal can significantly reduce the duration of hospitalization. Furthermore, DT clamping might be a recommended option for conservative treatment of postoperative CA.

Key Words: Gastric cancer; Chylous ascites; Conservative treatment; Drainage tube

Core Tip: Chylous ascites (CA) is one of uncommon postoperative complication in the patients received gastric cancer (GC) surgery. Previously, the primary treatment for CA was conservative therapy, which mainly involved total parenteral nutrition, continuous low-pressure drainage, somatostatin, and a low-fat diet. Therefore, we retrospectively analyzed the patients with CA after GC surgery in our center, aiming to explore the vital factors that influence CA treatment and recommend novel conservative treatment strategies for postoperative CA in GC.

Citation: Kong PF, Xu YH, Lai ZH, Ma MZ, Duan YT, Sun B, Xu DZ. Novel management indications for conservative treatment of chylous ascites after gastric cancer surgery. *World J Gastroenterol* 2022; 28(42): 6056-6067

URL: https://www.wjgnet.com/1007-9327/full/v28/i42/6056.htm

DOI: https://dx.doi.org/10.3748/wjg.v28.i42.6056

INTRODUCTION

Chylous ascites (CA) was first reported by Morton in 1691 and is defined as the leakage of milk-like fluid that contains high level of triglyceride (TG)[1,2]. Gastric cancer (GC) is one of the most common malignant tumors worldwide, and a standardized protocol for radical surgical resection has been widely accepted as a safe and effective treatment[3,4]. CA generally occurs following abdominal surgery, the incidence of postoperative CA ranges from 2.06% to 11.80% in GC patients[5-7], as a result of disturbance of the cisterna chyli or its major tributaries[8,9]. The increased incidence of CA is considered to be likely due to the increased number of cancer patients undergoing more aggressive surgical interventions in addition to laparoscopic surgery[10]. CA presents a challenge as a relatively common postoperative complication and impacts subsequent adjuvant treatments in GC. In addition, massive and prolonged CA may lead to infection, malnutrition and immunodeficiency[11].

To date, treatment options for CA have included dietary measures, use of pharmacological agents and surgical or percutaneous interventions. A high-protein and low-fat diet with medium-chain triglycerides is often recommended for patients with CA[12]. Patients who do not respond to dietary restriction should receive total parenteral nutrition (TPN), which bypasses the bowel and may thus reduce lymph flow[13]. Continuous low-pressure drainage and somatostatin also represent effective conservative treatment for postoperative CA[6,14]. CA can be cured by lymphangiography and adjunctive embolization techniques that include direct percutaneous injection of glue into the leakage site or into the surrounding lymphoid tissue[15]. Furthermore, the use of surgical measures to successfully treat CA has been reported in patients with cirrhosis and CA that is resistant to conservative therapy[1].

In this study, we retrospectively analyzed 53 patients with CA after GC surgery, aiming to explore the vital factors that influence CA treatment and recommend novel conservative treatment strategies for postoperative CA in GC.

MATERIALS AND METHODS

Patients

We retrospectively reviewed all patients with CA who had undergone surgery for GC at our institution from 1 March 2006 to 31 May 2021. Three investigators performed a thorough review of all available data from the Fudan University Shanghai Cancer Center (FUSCC) medical record system, using RED

Cap electronic data capture tools. In this cohort, 53 patients were admitted for gastric resection and lymphadenectomy: 2 underwent palliative resection and 51 underwent radical gastric resection with curative intent. This study was approved by the FUSCC review board in accordance with Chinese bioethical regulations, and all enrolled patients signed informed consent forms.

Definitions

CA was defined as the presence of milky or creamy peritoneal fluid in the drainage tubes, at a volume of ≥ 200 mL/d and a TG levels ≥ 110 mg/dL[1,11]. Additionally, the chyle test was routinely performed if the milky peritoneal fluid was suspected to be CA[16]. Clinical and pathological data, including the age, gender, AJCC (American Joint Committee on Cancer) stage, surgical procedure, lymph node dissection, drainage tube (DT) removal, time of oral feeding, time to CA onset, drainage duration, and hospitalization duration were collected and analyzed. All patients with CA were managed conservatively; the conservative treatments included TPN, continuous low-pressure drainage, somatostatin, DT clamping, and a low-fat diet. The time to CA onset was defined as the interval between the surgical procedure and the appearance of CA. Delay DT removal was defined as a DT removal time > 16 d after surgery for all patients or patients discharge with DT. Additionally, white blood cell counts, body temperature measurement, and germiculture were performed to diagnose CA combined with infection. DT clamping is defined as physical closing of the abdominal DT, with a daily open drainage time of about 2 h.

Statistical analysis

Categorical variable analysis was performed using the χ^2 test or Fisher's exact test, and continuous variables were compared using Student's t test. We used univariate logistic regression models to evaluate the risk factors of delayed DT removal in GC patients with postoperative CA, and a Cox regression model was used to perform multivariable analysis to calculate relative risk. All values were categorized into groups according to medians. All results were considered clinically significant at a P value < 0.05. Statistical analyses were performed using SPSS software version 19.0.

RESULTS

Clinical characteristics of gastric cancer patients with postoperative chylous ascites

Between 1 March 2006 and 31 May 2021, 16074 GC patients were hospitalized in our department and 7081 patients underwent gastrectomy and lymphadenectomy. Of these patients, 53 underwent surgical resection for GC and developed CA. The main characteristics and patient selection are shown in Table 1 and Figure 1. The patients had an average age of 61.0 ± 11.3 years, a high ratio of male and advanced stage of disease (Male *vs* female: 77.40% *vs* 22.60%, early stage *vs* advanced stage: 39.6% *vs* 60.4%), 51 underwent radical surgery, 43 underwent D2 lymph node dissection, and 13 were discharged with DT. The average oral feeding and CA onset times after surgery were 3.8 and 7.5 d, respectively. The average durations of DT drainage and postoperative hospitalization were 14.3 and 21.9 d, respectively.

Delayed drainage tube removal has an important influence on gastric cancer patients with postoperative chylous ascites

In our data, 40 patients (75%) had their DTs removed during the hospitalization period, and 13 patients (25%) were discharged with DT (Figure 2A). As shown in Figure 2B and Supplementary Figure 1, both postoperative (R^2 = 0.979, P < 0.001) and total hospitalization time (R^2 = 0.791, P < 0.001) had a significant positive association with DT removal time. Moreover, the median postoperative DT removal time of the patients discharged with or without DT was 30 and 16 d, respectively (Figure 2C and Supplementary Figure 2). We defined the patients' DT removal time > the median time (16 d) or the patients discharged with DT as delayed DT removal, and the patients were categorized into either the delayed DT removal or normal group (Figure 2D). Comparing the delayed and normal groups, delayed DT removal significantly extended the total and postoperative hospitalization times, duration of antibiotic usage, and hospitalization costs in the GC patients (postoperative hospitalization duration: 25.8 d *vs* 15.5 d, P < 0.001; total hospitalization duration: 33.2 d *vs* 24.7 d, P < 0.01; antibiotic usage: 10.8 d *vs* 6.2 d, P < 0.01; hospitalization cost: ¥9.2 × 10^4 *vs* ¥6.5 × 10^4, P < 0.01) (Figure 2E).

Characteristic differences between the normal and delayed drainage tube removal groups in gastric cancer patients with postoperative chylous ascites

We present the characteristic differences between the normal and delayed DT removal groups in Figure 3, Table 2 and Supplementary Table 1. First, we evaluated the clinical characteristics and detected that there were no differences between the two groups regarding gender, age, tumor size or location, lymphadenectomy, and AJCC stage. Second, the treatment-related features were further explored. Of note, the patients in the normal group were more likely to undergo DT clamping than the delayed DT removal group (35.0% *vs* 0%, P < 0.001). In addition, compared with the patients in the delayed group, a

Table 1 Clinical characteristics of gastric cancer patients with postoperative chylous ascites

Characteristics	Cases
Age, yr	61.0 ± 11.3
Gender, *n* (%)	
Male	41 (77.4)
Female	12 (22.6)
Tumor location, *n* (%)	
Upper	18 (40.0)
Middle	11 (20.6)
Bottom	24 (45.3)
AJCC 8th stage, *n* (%)	
I	21 (39.6)
II	11 (20.8)
III	18 (34.0)
IV	3 (5.7)
Type of surgery, *n* (%)	
Radical	51 (96.2)
Non-radical	2 (3.8)
LN dissection, *n* (%)	
D1	8 (15.1)
D2	43 (81.1)
D3	2 (3.8)
Discharged without DT, *n* (%)	
Yes	40 (75.5)
No	13 (24.5)
Postoperative time of oral feeding (d)	3.8 ± 1.0
Postoperative time of CA appearance (d)	7.5 ± 2.4
DT removal duration (d)	14.3 ± 12.6
Postoperative hospitalization duration (d)	21.9 ± 11.1

SD: Standard deviation; AJCC: American Joint Committee on Cancer; LN: Lymph node; DT: Drainage tube; CA: Chylous ascites.

shorter duration of low-fat diet were slightly shared in the normal group patients (40.0% *vs* 63.6%, P = 0.082). Third, we estimated the DT drainage variation between the two groups. Obviously, the delayed DT removal group generally had a longer duration of DT drainage than the normal group; however, the CA onset time and maximum drainage volumes were not significantly different between the two groups.

Infection and antibiotic usage were key independent factors influencing the delay of drainage tube removal

As shown in Table 3 and Figure 4, the univariate analysis revealed that early postoperative intake (RR: 2.22, 1.10–4.48, P = 0.031), postoperative infection (RR: 2.20, 1.21-4.61, P = 0.003), and antibiotic usage (RR: 0.45, 0.22–0.91, P = 0.009) were significantly associated with delayed DT removal in GC patients with CA. However, the baseline characteristics (age, gender, and AJCC stage), lymph node dissection, CA onset time, maximum drainage volume, postoperative albumin, postoperative hemoglobin, and DT clamping were not significantly associated with delayed DT removal (all P > 0.05). Furthermore, multivariate analysis demonstrated that postoperative infection (HR: 2.40, 1.63-4.14, P = 0.007) and antibiotic usage (HR: 0.86, 0.76-0.96, P = 0.009) were independent factors that influenced delayed DT removal in GC patients with postoperative CA.

Table 2 Clinical characteristics differences between the normal and delayed drainage tube removal groups

Subgroup	No. of patients	
	Normal (*n* = 20)	Delayed DT removal (*n* = 33)
Clamp DT		
Yes	7	0
No	13	0
Preoperative HGB, g/L		
≤ 130	12	15
> 130	8	18
Preoperative ALB, g/L		
≤ 41	9	17
> 41	11	16
Maximum drainage, mL		
≤ 540	13	13
> 540	7	20
Postoperative intake[1], d		
≤ 3	10	17
> 3	10	16
CA onset time, d		
≤ 7	15	16
> 7	5	17
Antibiotic usage, d		
≤ 5	12	16
> 5	8	17
Postoperative infection		
Yes	8	12
No	12	21
AJCC stage		
Early	8	13
Advanced	12	20
LN dissection		
D1	6	2
D2+	14	31
Age, yr		
≤ 60	8	15
> 60	12	18
Gender		
Male	15	26
Female	5	7

[1]Time of oral feeding after gastric surgery.
HGB: Hemoglobin; ALB: Albumin; AJCC: American Joint Committee on Cancer; LN: Lymph node; DT: Drainage tube; CA: Chylous ascites.

Table 3 Postoperative infection-related complications significantly affect gastric cancer patients with postoperative chylous ascites to remove abdominal drainage tubes in time

	Univariate analysis		Multivariate analysis	
	HR (95%CI)	*P* value	HR (95%CI)	*P* value
DT clamping	0.39 (0.11-1.72)	0.281	-	-
Postoperative HGB	1.49 (0.72-3.08)	0.283	-	-
Postoperative ALB	1.82 (0.88-3.76)	0.303	1.09 (0.98-1.21)	0.127
Maximum drainage	0.98 (0.47-2.05)	0.367	-	-
Postoperative intake time	2.22 (1.10-4.48)	0.031	1.86 (0.94-4.21)	0.234
CA onset time	0.81 (0.40-1.62)	0.486	-	-
Duration of antibiotic usage	0.45 (0.22-0.91)	0.009	0.86 (0.76-0.96)	0.009
Postoperative infection	2.20 (1.21-4.61)	0.003	2.40 (1.63-4.14)	0.007
AJCC Stage	0.95 (0.75-1.21)	0.676	-	-
LN dissection	0.87 (0.53-1.42)	0.595	-	-
Age	1.34 (0.66-2.70)	0.471	-	-
Gender	2.02 (0.85-4.78)	0.141	3.13 (0.85-11.1)	0.187

HR: Hazard ratio; CI: Confidence interval; HGB: Hemoglobin; ALB: Albumin; AJCC: American Joint Committee on Cancer; LN: Lymph node; DT: Drainage tube; CA: Chylous ascites.

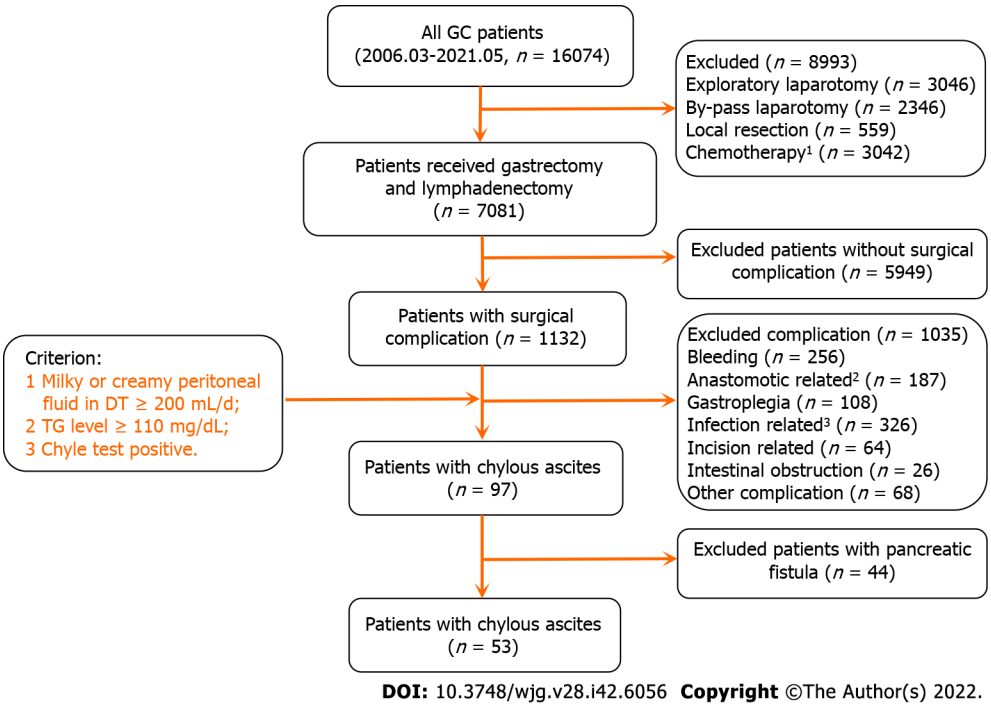

DOI: 10.3748/wjg.v28.i42.6056

Figure 1 Flowchart of study included patients. [1]Include the patients underwent neo-adjuvant, adjuvant, and palliative chemotherapy. [2]Include the patients with anastomotic stenosis and fistula, except for the patients with anastomotic bleeding. [3]The patients with all infection events except abdominal infection. GC: Gastric cancer; DT: Drainage tube; TG: Triglyceride.

Drainage tube clamping is a favorable method for the gastric cancer patients with postoperative chylous ascites

In Figure 5A, we describe comprehensive treatment for GC patients with postoperative CA; the therapies included DT clamping, somatostatin, antibiotic, TPN, low-fat diet, and continuous low-pressure drainage. DT clamping was performed for seven patients during the hospitalization period when postoperative CA occurred, and the clamped DT patients had a shorter DT removal time than the nor-

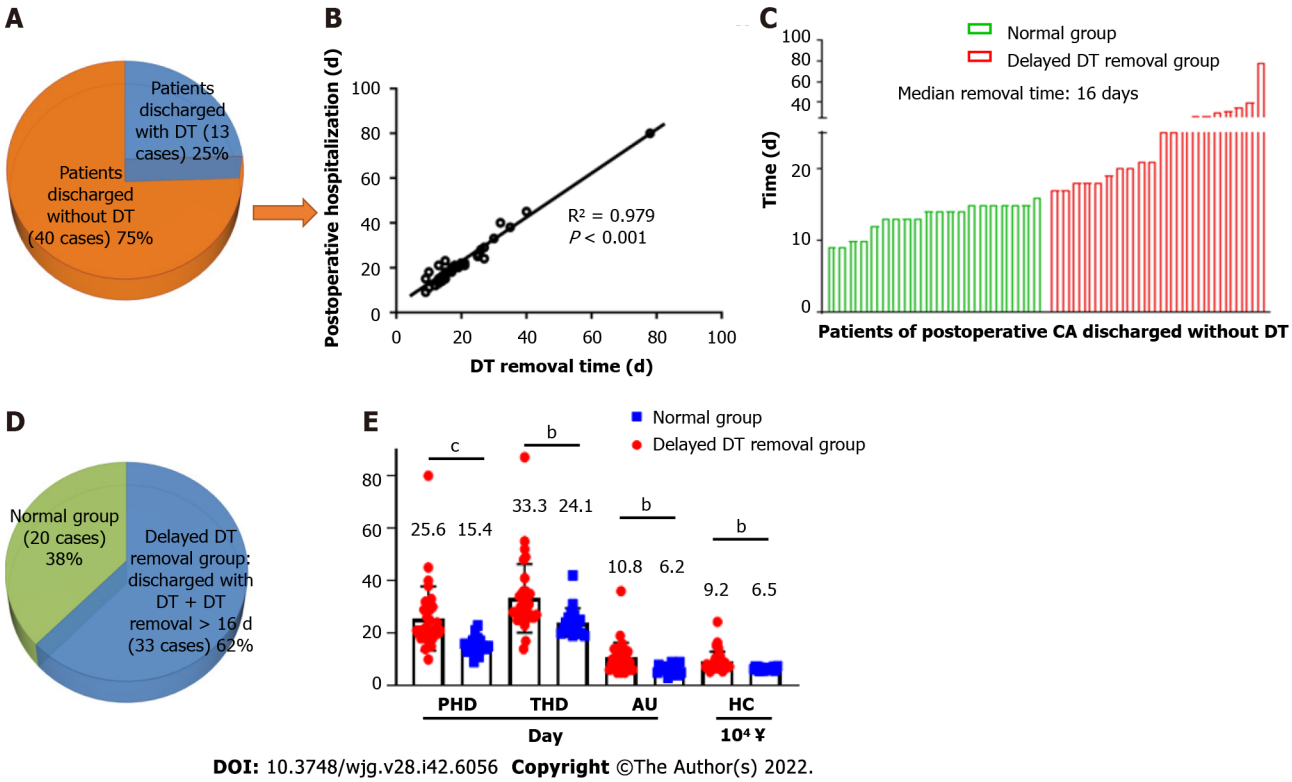

DOI: 10.3748/wjg.v28.i42.6056

Figure 2 Delayed drainage tube removal has an important influence on gastric cancer patients with postoperative chylous ascites. $^{b}P < 0.01$. $^{c}P < 0.001$. A: The status of drainage tube (DT) after discharged in gastric cancer (GC) patients with postoperative chylous ascites (CA); B: Postoperative hospitalization have a significantly positive correlation with the time of removal DT in GC patients discharged without DT; C: Time of removal DT in GC patients with postoperative CA who discharged without DT; D: The definition of delayed DT removal in GC patients with postoperative CA; E: Delayed DT removal obviously increase medical resources consumption and economic burden in GC patients with postoperative CA. GC: Gastric cancer; CA: Chylous ascites; DT: Drainage tube; PHD: Postoperative hospitalization duration; THD: Total hospitalization duration; AU: time of antibiotic usage; HC: Hospitalization cost.

mal and delayed removal groups (clamped DT group *vs* normal group, 11.8 d *vs* 13.6 d, $P = 0.047$; clamped DT group *vs* delayed group, 13.6 d *vs* 27.4 d, $P < 0.001$) (Figure 5B and Supplementary Figure 3). Moreover, similar clinical characteristics and treatment strategies were present in the three sub-groups (Supplementary Table 2). Our result further indicated that DT clamping significantly decreased total and postoperative hospitalization time, duration of antibiotic usage, and hospitalization costs in the GC patients with CA (Supplementary Figure 4). In Figure 5C, we dynamically observed the variation in daily drainage volume before DT removal (day 1 to day 7). Compared with the delayed removal group, start from day 3 before remove DT, the normal group and the clamped-DT group had relatively high drainage volumes. Additionally, the results of the drainage variation analysis indicated that 3 consecutive days of drainage volume less than 300 mL may be a suitable remove DT threshold in the GC patients with postoperative CA. Among two patients underwent DT clamping, computed tomography imaging of the abdomen showed that, after about 1 wk of DT clamping, the fluid in the abdominal cavity was reduced (Figure 5D).

Novel conservative therapeutic strategies for gastric cancer patients with postoperative chylous ascites

As the results mentioned above, we subsequently summarized the experiences of the GC patients with postoperative CA treatment in our department (Figure 6). First, the CA patients were divided into two sub-groups according to their postoperative infection status. Second, in the patients with infection, based on traditional treatments, antibiotic therapy was a vital supplement. Third, in the patients without infection, DT clamping was a viable option. Finally, for patients with 3 consecutive days of drainage less than 300 mL, DT removal might be the appropriate management.

DISCUSSION

In this study, we retrospectively analyzed 53 cases of GC with postoperative CA at the FUSCC. Our results indicated that hospitalization duration was closely associated with DT removal time. Furthermore, postoperative infection and antibiotic usage were important independent factors that

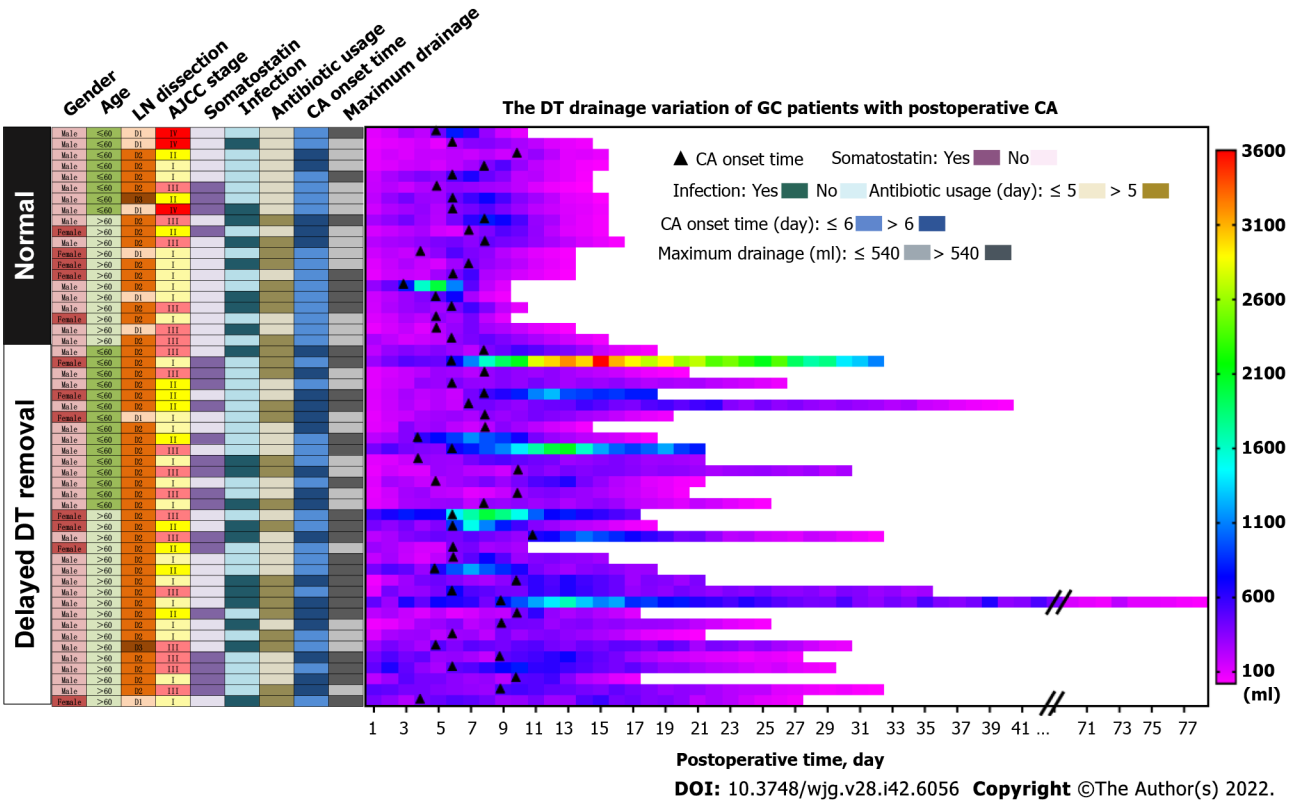

Figure 3 Overview of characteristic differences between the normal and delayed drainage tube removal groups in gastric cancer patients with postoperative chylous ascites. GC: Gastric cancer; DT: Drainage tube; LN: Lymph node; CA: Chylous ascites.

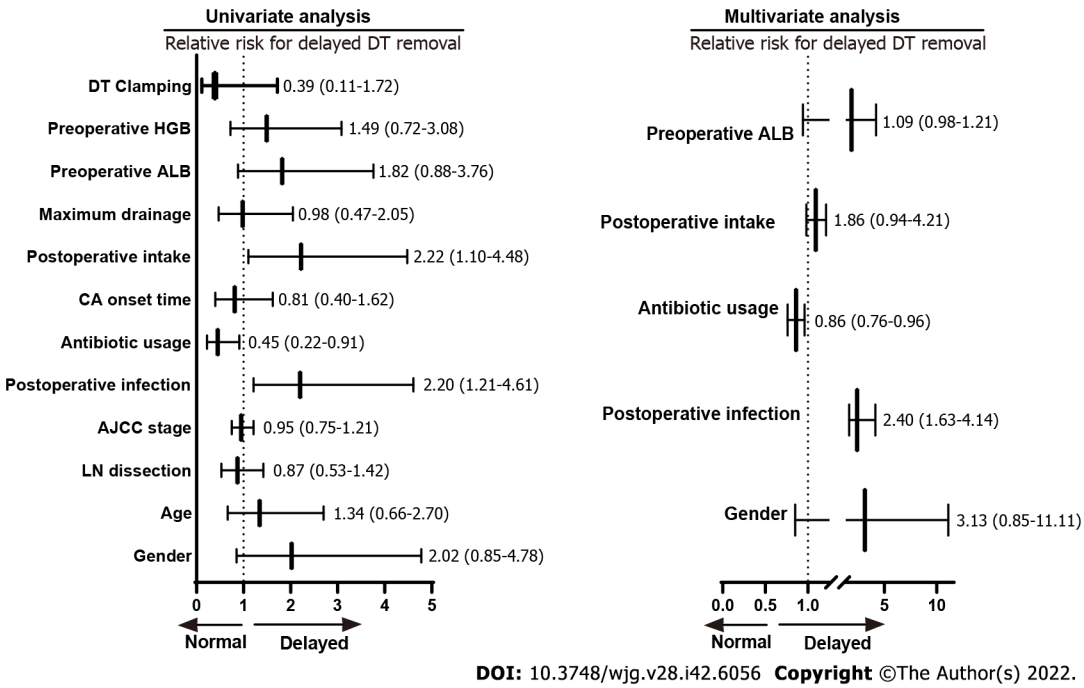

Figure 4 Exploration of multiple factors influence drainage tube removal in gastric cancer patients with postoperative chylous ascites. GC: Gastric cancer; DT: Drainage tube; LN: Lymph node; CA: Chylous ascites.

influenced delayed DT removal in GC patients with postoperative CA. Our study also implied that DT clamping was an appropriate method of postoperative CA treatment for patients without postoperative infection. More importantly, appropriate and lenient indications for DT removal can significantly reduce the duration of hospitalization.

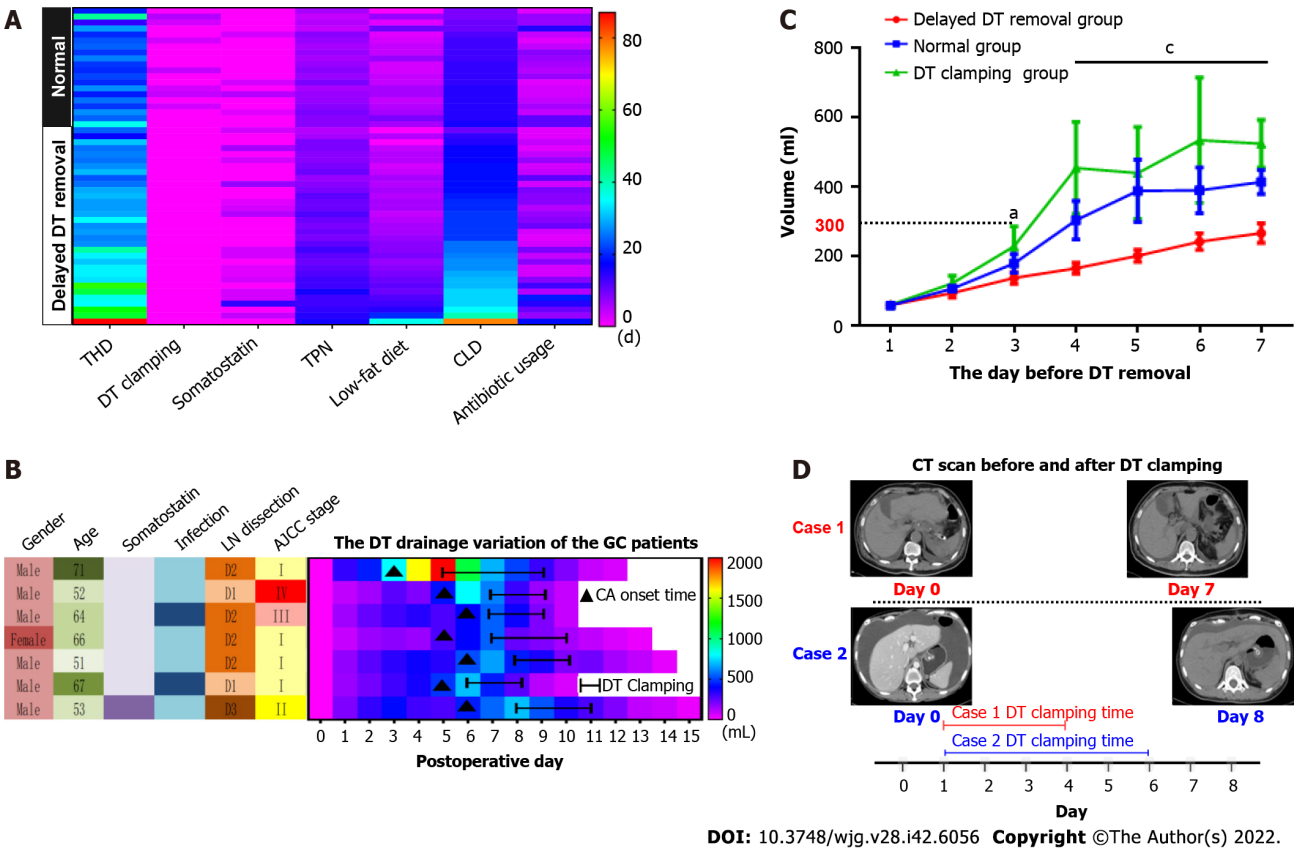

DOI: 10.3748/wjg.v28.i42.6056

Figure 5 Drainage tube clamping is a favorable method for the gastric cancer patients with postoperative chylous ascites. A: Overview of overall treatment in the gastric cancer (GC) patients with postoperative chylous ascites; B: The drainage tube (DT) drainage variation of the GC patients underwent the treatment of DT clamping; C: The drainage of GC patients with postoperative chylous ascites in different groups before DT removal; D: Computed tomography scan indicate that the fluid in abdominal cavity was clearly reduced after the DT was clamped. THD: Total hospitalization duration; TPN: Total parenteral nutrition; CLD: Continuous low-pressure drainage; GC: Gastric cancer; DT: Drainage tube; CA: Chylous ascites; LN: Lymph node. $^{a}P < 0.05$. $^{c}P < 0.001$.

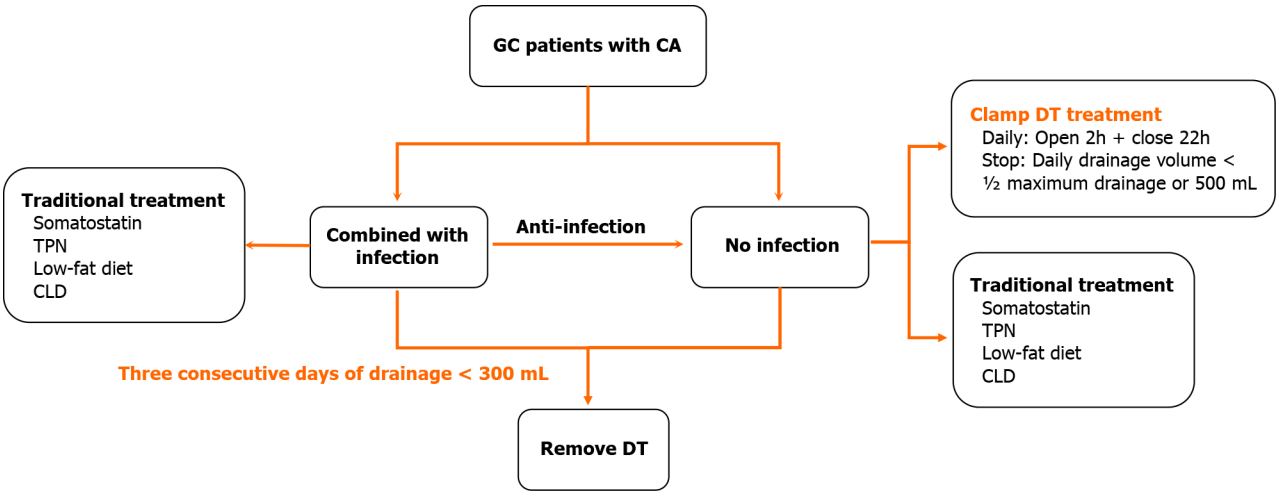

DOI: 10.3748/wjg.v28.i42.6056

Figure 6 Novel conservative therapeutic strategies for gastric cancer patients with postoperative chylous ascites. TPN: Total parenteral nutrition; CLD: Continuous low-pressure drainage; GC: Gastric cancer; DT: Drainage tube; CA: Chylous ascites.

In most of the GC patients, postoperative CA cannot be discharged at a routine time and have a significant impact on subsequent adjuvant treatment[6,7]. Normally, patients are discharged within 7 d after undergoing GC surgery and most start adjuvant treatment within 30 d at our center. However, in the 53 patients with postoperative CA in our study, the average postoperative hospitalization duration was 21.9 d, and 8 patients' postoperative hospital stays were longer than 30 d. As previously reported, lymphadenectomy was a key influencing factor in GC patients with postoperative CA[5,9]. As shown in

Supplementary Table 3, the clinical characteristics of patients with CA tended to be consistent among those who underwent variety of lymphadenectomy, similar with previous studies that CA was found to be a rare complication even for gastric carcinoma patients undergoing D3 dissection[5,17].

Our results clearly indicated that hospitalization duration is mainly dependent on the time of DT removal in GC patients with CA. A multi-center prospective study recommended the criterion for DT removal be drainage flow between 500 and 1000 mL/d[6]. In fact, we previous performed relatively rigorous standards for DT removal in the patients with CA. Usually, while the volume of drainage less than 100 mL/d, the DT removal will be truly considered. Although all the patients' DTs were removed until the flow volume less than 300 mL/d, and the delayed removal group preferred to perform a significantly high criterion. Therefore, we have a sufficient reason to conclude that, after excluding the influence of postoperative infection, early DT removal is a better choice in GC patients with CA. Moreover, our study found that postoperative infection and antibiotic usage were vital independent factors that influenced delayed DT removal in patients with CA, and clearly clarified anti-infection were an effective supplemental therapy for conservative treatment of postoperative CA. Similarly, Lu *et al*[7] reported the patients with CA had a certain higher level of postoperative white blood cell counts than the other patients in GC.

Previously, the primary treatment for CA was conservative therapy, which mainly involved TPN, continuous low-pressure drainage, somatostatin, and a low-fat diet[18]. Recently, DT clamping has been presented as a potential alternative for patients with CA in other malignancies[19]. In this study, the DTs of 7 patients were clamped until the daily drainage was less than 500 mL/d (or ½ the maximum drainage). After DT clamping, the flow amount was significantly reduced, and the patients were successfully discharged without DT. For the reason of clamping DT facilitates DT removal, previous research has demonstrated absorption and lymphatic drainage increase along with the interstitial hydrostatic pressure[20]. Furthermore, DT clamping could help to evaluate the feasibility of DT removal by conveniently simulating the removal and conversion back to drainage[21]. Several studies have suggested DT clamping as an important alternative, and the detailed suggestion was daily drainage ranging from 1000 to 1500 mL[6,22]. However, a consensus on the threshold of drainage volume for DT clamping has not yet been reached. Therefore, determination of an appropriate criterion for DT removal and DT clamping is urgently needed for GC patients with postoperative CA.

There are certain limitations to our study. First, due to the retrospective study design, it was difficult to individually balance a variety of influencing factors; thus, various biases were unavoidable. Second, despite routine chyle test and TG were measured, the definition of CA is slightly less rigorous. In particular, CA with co-infection cannot fully rule-out the influence of pancreatic and anastomotic leakage, and other infection-related complications. In addition, small-volume CA (*i.e.*, daily drainage volume ranging from 30 to 200 mL) was not considered in this study.

CONCLUSION

In conclusion, postoperative infection and antibiotic usage were vital independent factors that influenced delayed DT removal in GC patients with CA. Appropriate and lenient standards for DT removal can significantly reduce the duration of hospitalization. Furthermore, DT clamping might be a recommend alternative for conservative treatment of postoperative CA.

ARTICLE HIGHLIGHTS

Research background

Chylous ascites (CA) is relatively common postoperative complication in patients undergoing received gastric cancer (GC) surgery that obviously prolongs hospitalization and has a major impacts on subsequent adjuvant treatments.

Research motivation

Drainage tube (DT) clamping has been presented as a potential alternative conservative treatment for GC patients with CA.

Research objectives

This study aimed to explore key factors influencing CA treatment and recommend novel conservative treatment strategies for postoperative CA in GC patients.

Research methods

Data from patients with CA after GC surgery performed at the Fudan University Shanghai Cancer Center between 2006 and 2021 were retrospectively evaluated. Patients were classified into two distinct

groups with respect to DT removal time. We further explored the differences in clinical-pathological features of the different DT removal groups.

Research results

Fifty-three patients underwent surgery for GC and experienced postoperative CA during the study period. Postoperative hospitalization and DT removal time showed a significant positive association (R^2 = 0.979, P < 0.001), while delayed DT removal significantly extended total and postoperative hospitalization times, antibiotic usage duration, and hospitalization cost. In addition, postoperative infection and antibiotic usage were independent factors for delayed DT removal.

Research conclusions

Postoperative infection and antibiotic usage were vital independent factors that influenced delayed DT removal in GC patients with CA. Appropriate and lenient standards for DT removal may significantly reduce the duration of hospitalization.

Research perspectives

DT clamping could be recommended as an alternative for conservative treatment of postoperative CA.

ACKNOWLEDGEMENTS

We thank Dr. Xuan Li for statistical advising and review of the manuscript.

FOOTNOTES

Author contributions: Kong PF and Xu YH contributed equally to this work; Xu DZ designed the research study; Kong PF, Xu YH, Lai ZH and Sun B performed the research; Kong PF, Xu YH, Ma MZ and Duan YT analyzed the data and wrote the manuscript; all authors have read and approve the final manuscript.

Institutional review board statement: The study was reviewed and approved by Ethics Committee of Fudan University Shanghai Cancer Center Review Board [Approval No. FUSCC-D-2021-164].

Informed consent statement: All study participants provided informed written consent prior to study enrollment.

Conflict-of-interest statement: All the authors report no relevant conflicts of interest for this article.

Data sharing statement: Dataset available from the corresponding author at xudzh@shca.org.cn. Participants gave informed consent for data sharing.

Country/Territory of origin: China

ORCID number: Ming-Zhe Ma 0000-0001-8858-0983; Da-Zhi Xu 0000-0002-2265-1272.

S-Editor: Gong ZM
L-Editor: A
P-Editor: Yuan YY

REFERENCES

1 **Cárdenas A**, Chopra S. Chylous ascites. *Am J Gastroenterol* 2002; **97**: 1896-1900 [PMID: 12190151 DOI: 10.1111/j.1572-0241.2002.05911.x]
2 **Huang Q**, Jiang ZW, Jiang J, Li N, Li JS. Chylous ascites: treated with total parenteral nutrition and somatostatin. *World J Gastroenterol* 2004; **10**: 2588-2591 [PMID: 15300913 DOI: 10.3748/wjg.v10.i17.2588]
3 **Siegel RL**, Miller KD, Goding Sauer A, Fedewa SA, Butterly LF, Anderson JC, Cercek A, Smith RA, Jemal A. Colorectal cancer statistics, 2020. *CA Cancer J Clin* 2020; **70**: 145-164 [PMID: 32133645 DOI: 10.3322/caac.21601]
4 **Sasako M**, Sano T, Yamamoto S, Kurokawa Y, Nashimoto A, Kurita A, Hiratsuka M, Tsujinaka T, Kinoshita T, Arai K, Yamamura Y, Okajima K; Japan Clinical Oncology Group. D2 lymphadenectomy alone or with para-aortic nodal

dissection for gastric cancer. *N Engl J Med* 2008; **359**: 453-462 [PMID: 18669424 DOI: 10.1056/NEJMoa0707035]
5 **Yol S**, Bostanci EB, Ozogul Y, Ulas M, Akoglu M. A rare complication of D3 dissection for gastric carcinoma: chyloperitoneum. *Gastric Cancer* 2005; **8**: 35-38 [PMID: 15747172 DOI: 10.1007/s10120-004-0312-5]
6 **Ilhan E**, Demir U, Alemdar A, Ureyen O, Eryavuz Y, Mihmanli M. Management of high-output chylous ascites after D2-lymphadenectomy in patients with gastric cancer: a multi-center study. *J Gastrointest Oncol* 2016; **7**: 420-425 [PMID: 27284475 DOI: 10.21037/jgo.2016.02.03]
7 **Lu J**, Wei ZQ, Huang CM, Zheng CH, Li P, Xie JW, Wang JB, Lin JX, Chen QY, Cao LL, Lin M. Small-volume chylous ascites after laparoscopic radical gastrectomy for gastric cancer: results from a large population-based sample. *World J Gastroenterol* 2015; **21**: 2425-2432 [PMID: 25741151 DOI: 10.3748/wjg.v21.i8.2425]
8 **Pabst TS 3rd**, McIntyre KE Jr, Schilling JD, Hunter GC, Bernhard VM. Management of chyloperitoneum after abdominal aortic surgery. *Am J Surg* 1993; **166**: 194-8; discussion 198 [PMID: 8352415 DOI: 10.1016/s0002-9610(05)81055-4]
9 **Barchi LC**, Charruf AZ, de Oliveira RJ, Jacob CE, Cecconello I, Zilberstein B. Management of postoperative complications of lymphadenectomy. *Transl Gastroenterol Hepatol* 2016; **1**: 92 [PMID: 28138657 DOI: 10.21037/tgh.2016.12.05]
10 **Bhardwaj R**, Vaziri H, Gautam A, Ballesteros E, Karimeddini D, Wu GY. Chylous Ascites: A Review of Pathogenesis, Diagnosis and Treatment. *J Clin Transl Hepatol* 2018; **6**: 105-113 [PMID: 29577037 DOI: 10.14218/JCTH.2017.00035]
11 **Aalami OO**, Allen DB, Organ CH Jr. Chylous ascites: a collective review. *Surgery* 2000; **128**: 761-778 [PMID: 11056439 DOI: 10.1067/msy.2000.109502]
12 **Lizaola B**, Bonder A, Trivedi HD, Tapper EB, Cardenas A. Review article: the diagnostic approach and current management of chylous ascites. *Aliment Pharmacol Ther* 2017; **46**: 816-824 [PMID: 28892178 DOI: 10.1111/apt.14284]
13 **Lopez-Gutierrez JC**, Tovar JA. Chylothorax and chylous ascites: management and pitfalls. *Semin Pediatr Surg* 2014; **23**: 298-302 [PMID: 25459015 DOI: 10.1053/j.sempedsurg.2014.09.011]
14 **Shibuya Y**, Asano K, Hayasaka A, Shima T, Akagi K, Ozawa N, Wada Y. A novel therapeutic strategy for chylous ascites after gynecological cancer surgery: a continuous low-pressure drainage system. *Arch Gynecol Obstet* 2013; **287**: 1005-1008 [PMID: 23224652 DOI: 10.1007/s00404-012-2666-y]
15 **Kim J**, Won JH. Percutaneous Treatment of Chylous Ascites. *Tech Vasc Interv Radiol* 2016; **19**: 291-298 [PMID: 27993325 DOI: 10.1053/j.tvir.2016.10.006]
16 **Kaas R**, Rustman LD, Zoetmulder FA. Chylous ascites after oncological abdominal surgery: incidence and treatment. *Eur J Surg Oncol* 2001; **27**: 187-189 [PMID: 11289756 DOI: 10.1053/ejso.2000.1088]
17 **Kim DW**, Kim MH, Kim CG. Lymphoscintigraphy revealed chyloperitoneum after gastrectomy for gastric cancer. *Clin Nucl Med* 2015; **40**: 41-44 [PMID: 25310405 DOI: 10.1097/RLU.0000000000000609]
18 **Adler E**, Bloyd C, Wlodarczyk S. Chylous Ascites. *J Gen Intern Med* 2020; **35**: 1586-1587 [PMID: 31720957 DOI: 10.1007/s11606-019-05532-3]
19 **Thiel FC**, Parvanta P, Hein A, Mehlhorn G, Lux MP, Renner SP, Preisner A, Beckmann MW, Schrauder MG. Chylous ascites after lymphadenectomy for gynecological malignancies. *J Surg Oncol* 2016; **114**: 613-618 [PMID: 27378217 DOI: 10.1002/jso.24354]
20 **Miserocchi G**. Physiology and pathophysiology of pleural fluid turnover. *Eur Respir J* 1997; **10**: 219-225 [PMID: 9032518 DOI: 10.1183/09031936.97.10010219]
21 **Yan S**, Wang X, Wang Y, Lv C, Wang J, Yang Y, Wu N. Intermittent chest tube clamping may shorten chest tube drainage and postoperative hospital stay after lung cancer surgery: a propensity score matching analysis. *J Thorac Dis* 2017; **9**: 5061-5067 [PMID: 29312711 DOI: 10.21037/jtd.2017.11.08]
22 **Scaletta G**, Quagliozzi L, Cianci S, Vargiu V, Mele MC, Scambia G, Fagotti A. Management of postoperative chylous ascites after surgery for ovarian cancer: a single-institution experience. *Updates Surg* 2019; **71**: 729-734 [PMID: 31006086 DOI: 10.1007/s13304-019-00656-x]

World Journal of Gastroenterology

Submit a Manuscript: https://www.f6publishing.com

World J Gastroenterol 2022 November 14; 28(42): 6068-6077

DOI: 10.3748/wjg.v28.i42.6068

ISSN 1007-9327 (print) ISSN 2219-2840 (online)

ORIGINAL ARTICLE

Clinical Trials Study

Computed tomography perfusion in liver and spleen for hepatitis B virus-related portal hypertension: A correlation study with hepatic venous pressure gradient

Lei Wang, Yu Zhang, Yi-Fan Wu, Zhen-Dong Yue, Zhen-Hua Fan, Chun-Yan Zhang, Fu-Quan Liu, Jian Dong

Specialty type: Gastroenterology and hepatology

Provenance and peer review: Unsolicited article; Externally peer reviewed.

Peer-review model: Single blind

Peer-review report's scientific quality classification

Grade A (Excellent): A
Grade B (Very good): B, B
Grade C (Good): 0
Grade D (Fair): 0
Grade E (Poor): 0

P-Reviewer: Fakhreddine AY; Kim E, United States; van Kester MS, The Netherlands

Received: August 7, 2022
Peer-review started: August 7, 2022
First decision: August 31, 2022
Revised: October 14, 2022
Accepted: October 31, 2022
Article in press: October 31, 2022
Published online: November 14, 2022

Lei Wang, Department of Intervention Therapy, Beijing Shijitan Hospital, Capital Medical University, Beijing 100038, China

Yu Zhang, Yi-Fan Wu, Zhen-Dong Yue, Zhen-Hua Fan, Fu-Quan Liu, Interventional Radiology, Beijing Shijitan Hospital, Capital Medical University, Beijing 100038, China

Chun-Yan Zhang, Jian Dong, Department of Radiology, Beijing Shijitan Hospital, Capital Medical University, Beijing 100038, China

Corresponding author: Jian Dong, MD, Doctor, Department of Radiology, Beijing Shijitan Hospital, Capital Medical University, No. 10 Tieyi Street, Haidian District, Beijing 100038, China. dongjianradiology@163.com

Abstract

BACKGROUND

Hepatic venous pressure gradient (HVPG) is the gold standard for diagnosis of portal hypertension (PH). However, its use can be limited because it is an invasive procedure. Therefore, it is necessary to explore a non-invasive method to assess PH.

AIM

To investigate the correlation of computed tomography (CT) perfusion of the liver with HVPG and Child-Pugh score in hepatitis B virus (HBV)-related PH.

METHODS

Twenty-eight patients (4 female, 24 male) with gastroesophageal variceal bleeding induced by HBV-related PH were recruited in our study. All patients received CT perfusion of the liver before transjugular intrahepatic portosystemic stent-shunt (TIPS) therapy. Quantitative parameters of CT perfusion of the liver, including liver blood flow (LBF), liver blood volume (LBV), hepatic artery fraction, splenic blood flow and splenic blood volume were measured. HVPG was recorded during TIPS therapy. Correlation of liver perfusion with Child-Pugh score and HVPG were analyzed, and the receiver operating characteristic curve was analyzed. Based on HVPG (> 12 mmHg *vs* ≤ 12 mmHg), patients were divided into moderate and severe groups, and all parameters were compared.

RESULTS

Based on HVPG, 18 patients were classified into the moderate group and 10 patients were classified into the severe group. The Child-Pugh score, HVPG, LBF and LBV were significantly higher in the moderate group compared to the severe group (all $P < 0.05$). LBF and LBV were negatively associated with HVPG ($r = -0.473$, $P < 0.05$ and $r = -0.503$, $P < 0.01$, respectively), whereas splenic blood flow was positively associated with hepatic artery fraction ($r = 0.434$, $P < 0.05$). LBV was negatively correlated with Child-Pugh score. Child-Pugh score was not related to HVPG. Using a cutoff value of 17.85 mL/min/100 g for LBV, the sensitivity and specificity of HVPG ≥ 12 mmHg for diagnosis were 80% and 89%, respectively.

CONCLUSION

LBV and LBF were negatively correlated with HVPG and Child-Pugh scores. CT perfusion imaging is a potential non-invasive quantitative predictor for PH in HBV-related liver cirrhosis.

Key Words: Hepatic venous pressure gradient; Portal hypertension; Computed tomography perfusion; Hepatitis B; Liver cirrhosis

Core Tip: Hepatic venous pressure gradient (HVPG) is the gold standard for the diagnosis of portal hypertension (PH), but its use is limited because it is an invasive procedure. Non-invasive assessment of HVPG requires further research. Computed tomography perfusion of the liver may be a useful tool for the evaluation of HVPG. Our results showed that a cutoff of 17.85 mL/min/100 g for liver blood volume yielded an 80% sensitivity and 89% specificity for severe PH. Therefore, computed tomography perfusion of the liver has the potential as a non-invasive quantitative predictor for PH in hepatitis B virus-related liver cirrhosis.

Citation: Wang L, Zhang Y, Wu YF, Yue ZD, Fan ZH, Zhang CY, Liu FQ, Dong J. Computed tomography perfusion in liver and spleen for hepatitis B virus-related portal hypertension: A correlation study with hepatic venous pressure gradient. *World J Gastroenterol* 2022; 28(42): 6068-6077

URL: https://www.wjgnet.com/1007-9327/full/v28/i42/6068.htm

DOI: https://dx.doi.org/10.3748/wjg.v28.i42.6068

INTRODUCTION

Gastroesophageal variceal bleeding is a common complication of portal hypertension (PH) in decompensated liver cirrhosis. There is a 60% recurrence rate and 20% mortality rate in the 1st year, and it is the leading cause of liver transplantation and mortality[1-4]. The diagnostic criteria for PH include hepatic venous pressure gradient (HVPG) ≥ 5 mmHg. Notably, when HVPG is higher than 12 mmHg, patients have a significantly increased risk of gastroesophageal bleeding. It was reported that HVPG was positively associated with individual risk of gastroesophageal variceal bleeding, and the incidence of variceal bleeding increased proportionally with an increase in HVPG[1,5-8]. In addition, HVPG can be applied clinically for risk stratification, therapeutic adoption, drug efficacy and adverse events for PH [4,9-12]. However, HVPG is an invasive procedure, which has limited its wide application for the evaluation of therapeutic effects or long-term follow-up. Therefore, studies continue to focus on non-invasive evaluation of HVPG, including anatomy (*e.g.*, liver volume, maximal diameter of spleen), lab results (*e.g.*, platelet level, coagulation function), liver function (*e.g.*, Child-Pugh score, model for end-stage liver disease [commonly known as MELD] score), liver and spleen stiffness (*e.g.*, FibroScan, FibroTouch, magnetic resonance elastography), and even computation simulation modeling. However, none of these methods has demonstrated satisfactory accuracy and reproducibility.

Computed tomography (CT) perfusion of the liver is traditionally utilized to evaluate liver cancer, metastatic tumors, and liver cirrhosis. Decreased blood flow perfusion from the portal vein system and increased blood flow perfusion from the hepatic artery system can be identified with CT perfusion of the liver[13-16]. Furthermore, liver blood perfusion after transjugular intrahepatic portosystemic stent-shunt (TIPS) can be quantitatively assessed with CT perfusion[17]. However, very few reports have focused on the correlation between HVPG and CT perfusion in gastroesophageal bleeding. Talakić *et al* [13] reported that HVPG had no correlation with CT perfusion in end-stage cirrhosis. Therefore, we aimed to explore the relationship between quantitative indices of CT perfusion with HVPG and the Child-Pugh score and to investigate the feasibility of CT perfusion as a non-invasive imaging tool for

HVPG in gastroesophageal variceal bleeding induced by hepatitis B virus (HBV)-related PH.

MATERIALS AND METHODS

Patients

This prospective study was approved by the Institutional Ethics Committee at our hospital, and all written informed consents were obtained from each participant. Patients with recurrent gastroesophageal variceal bleeding resulting from HBV-related PH were randomly recruited from January 1, 2019 to June 30, 2019. All patients previously underwent drug and/or endoscopic therapy and were prepared for the TIPS procedure. The inclusion criteria were as follows: (1) Gastroesophageal bleeding as a consequence of HBV-related PH; (2) CT perfusion and Child-Pugh score available 1 wk before TIPS surgery; and (3) HVPG measured during TIPS and HVPG ≥ 5 mmHg. The exclusion criteria were as follows: (1) Gastroesophageal bleeding caused by any other etiology; (2) liver tumors, including primary and metastatic; (3) any other conditions leading to hemodynamic changes in the liver, such as partial hepatectomy, splenectomy, hepatic tumor surgery, TIPS, *etc*; (4) any factors affecting liver blood perfusion, such as portal vein thrombosis, cavernous transformation, Budd-Chiari syndrome, *etc*; (5) dysfunction in vital organs, such as cardiac, renal or respiratory damage/failure; and (6) any factors that reduced the quality of CT images, such as motion and metal artifacts.

CT perfusion and post-processing

CT perfusion was performed by a Revolution CT scanner (GE Healthcare, Chicago, IL, United States) with 16 cm Z-axis coverage axial scanning mode to cover most parts of the liver. Scanning parameters were set as tube voltage 100 kVp, automatic tube current from 50 mA to 200 mA with noise index as 14, slice thickness of 5 mm, rotation speed of 1.0 sec, helical pitch of 0.992:1.000 and 80% adaptive statistical iterative reconstruction (commonly known as ASIR). Initially, 50 mL nonionic contrast media (Omnipaque 350; GE Healthcare) followed by a 50-mL saline chaser were injected through the antecubital vein at a rate of 5 mL/sec, using a dual-head pump injector (Stellant; Medtron, Saarbrucken, Germany). The scanning was fixed with a 9-sec time delay after injection. Then, CT perfusion was performed. The CT perfusion was compromised of 26 pass acquisitions and 25 interscan gap without table movement, including 10 early acquisitions with an interscan gap of 1 sec, 12 acquisitions with an interscan gap of 2 sec, and 4 acquisitions with an interscan gap of 4 sec. Thus, total scanning time was 80 sec. All patients were instructed to avoid deep and irregular breathing during the procedure. A band compressing the upper abdomen was used to reduce respiratory motion artifacts.

Raw data generated by CT perfusion were reconstructed with a thickness of 2.5 mm. Post-processing was performed separately by two radiologists with 11 years and 7 years respectively of experience in the CT perfusion procedure. First, iterative registration reconstruction was performed to correct respiratory motion between each dynamic acquisition. Second, corrected data were post-processed with a commercial software (CT Perfusion 4D AW 4.7; GE Healthcare). Third, regions of interest were placed in the abdominal aorta and portal vein separately for liver perfusion (Figure 1). The region of interest was placed in the abdominal aorta only for splenic perfusion (Figure 2). Then, the perfusion map would be generated automatically for the liver and spleen (Figures 1 and 2). Finally, three volumes-of-interest would be selected in the left and right liver parenchyma without any hepatic vessels. By contrast, three volumes-of-interest were also selected in the superior, medial and inferior splenic parenchyma. Then, average values of perfusion parameters, including liver blood volume (LBV) (mL/100 mL), liver blood flow (LBF) (mL/100 mL/min), hepatic arterial fraction (HAF) (%), splenic blood volume (SBV) (mL/100 mL/min) and splenic blood flow (SBF) (mL/100 mL/min) were calculated and recorded.

HVPG measurement

HVPG was measured according to established standards[18,19] during the TIPS procedure. After fasting for more than 8 h, all patients underwent local anesthesia. The right internal jugular vein was cannulated using the Seldinger technique, and a 5-French balloon catheter (Edwards Lifesciences LLC, Irvine, CA, United States) was placed into the right hepatic vein, and the wedged and free hepatic venous pressure was measured three times in each patient. Then, HVPG was calculated as the difference between average wedged and free hepatic venous pressure.

Statistical analysis

Statistical analysis was performed with SPSS 24.0 software (IBM Corp., Armonk, NY, United States). All data were described as mean ± SD or range [95% confidence interval (CI)]. Kolmogorov-Smirnov was performed for the normal distribution test. Pearson or Spearman was used to evaluate the relationship among quantitative indices. Kappa was applied to analyze the agreement between observers. Patients were classified into two groups according to the HVPG value [> 12 mmHg (moderate) *vs* ≤ 12 mmHg (severe)]. Quantitative indices, including LBV, HAF, LBF, and SBV, were compared between the two groups. Receiver operating characteristic (ROC) was performed to calculate a cutoff value for differen-

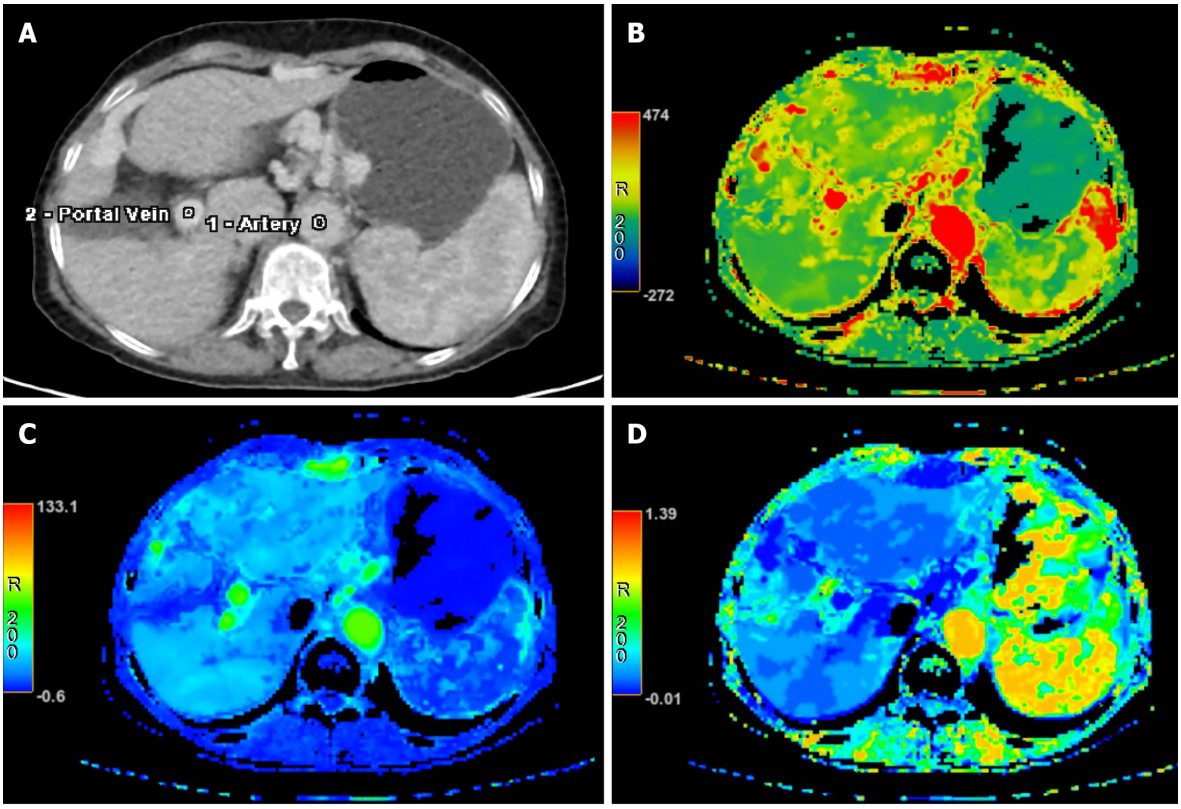

DOI: 10.3748/wjg.v28.i42.6068

Figure 1 Computed tomography perfusion of the liver post-processing data. A: Regions of interest were placed in the abdominal aorta and main portal vein as the input blood vessels for calculation of liver computed tomography perfusion; B-D: The parameters of liver computed tomography perfusion were calculated automatically to include hepatic artery fraction (B), liver blood flow (C), and liver blood volume (D).

tiation between moderate and severe PH. A P value of less than 0.05 was considered significant.

RESULTS

General data analysis

Initially, 35 patients had portal vein thrombosis. Then, 13 patients with splenectomy, 3 patients with liver tumors and 2 patients with motion artifacts (leading to unavailable CT perfusion) were excluded. Finally, 28 patients (4 female and 24 male) were included in our study, with an age range of 28-years-old to 68-years-old and an average age of 53.7 years ± 10.4 years. Patient characteristics are summarized in Table 1, including demographics, medical history, Child-Pugh class, and HVPG.

Comparisons of Child-Pugh scores in different types of PH

Ten patients had moderate PH (HVPG < 12 mmHg), and the remaining eighteen patients had severe PH (HVPG ≥ 12 mmHg). The median HVPG was 10 mmHg (interquartile range: 9.0 mmHg; range: 8.0-11.0 mmHg) in the moderate PH group and 21 mmHg (interquartile range: 17.5 mmHg; range: 14.0-31.0 mmHg) in the severe PH group. In the moderate PH group, 6 patients were Child-Pugh A and 4 patients were Child-Pugh B. In the severe PH group, 5 patients were Child-Pugh A, 12 patients were Child-Pugh B, and 1 patient was Child-Pugh C. For the moderate PH group, HVPG and Child-Pugh scores were lower than those in the severe PH group (9.6 mmHg ± 1.3 mmHg *vs* 18.9 mmHg ± 4.4 mmHg, P < 0.001) (Table 2).

Correlation of CT perfusion parameters with HVPG

The two radiologists demonstrated good agreement (Kappa = 0.821, P < 0.01) in the evaluation of the CT perfusion parameters. Quantitative parameters of CT perfusion of the liver are summarized in Table 2. Both LBF and LBV in moderate PH were higher than in severe PH (114.6 ± 36.0 *vs* 87.9 ± 24.8 and 19.7 ± 3.0 *vs* 15.5 ± 2.2, respectively, all P < 0.05). No significant difference was observed between the two groups for the other indices (Table 2).

LBF was negatively associated with HVPG (r = -0.398, P < 0.05). LBV was negatively related to HVPG (r = -0.504, P < 0.01) and Child-Pugh (r = -0.563, P < 0.01). SBF was positively related to HAF (r = 0.498, P

Table 1 Characteristics of the patients

Characteristic	Value
Sex as female/male, *n*	4/24
Age, yr, mean ± SD	53.7 ± 10.4
Height, cm, mean ± SD	169.4 ± 5.8
Weight, kg, mean ± SD	62.9 ± 11.6
Previous episodes of variceal bleeding, mean ± SD	3 ± 2
Treatment history, *n* (%)	
β blockade only	3 (10.7)
Sclera therapy only	4 (14.3)
β blockade and sclerotherapy	21 (75.0)
Child-Pugh stage, *n* (%)	
A	11 (39.3)
B	16 (57.1)
C	1 (3.6)
Ascites, *n* (%)	
None	17 (60.7)
Mild	2 (7.1)
Severe	9 (32.1)
HVPG, mmHg, *n* (%)	
< 12	10 (35.7)
≥ 12	18 (64.3)

HVPG: Hepatic venous pressure gradient; SD: Standard deviation.

< 0.01). No association was observed among HAF, SBV, SBF, Child-Pugh score and HVPG. The ROC of LBV for differentiation between moderate and severe PH resulted in an area under the curve of 0.864 with a standard error of 0.075 (95%CI: 0.72-1.00) (Figure 3). Using a cutoff value of 17.85 mL/min/100 mL for LBV, the sensitivity and specificity for detection of severe PH was 80% and 89%, respectively. ROC of LBF resulted in an area under the curve of 0.797 with a standard error of 0.100 (95%CI: 0.60-1.00) (Figure 3). Using a cutoff value of 111.3 mL/min/100 mL for LBF, the sensitivity and specificity for detection of severe PH was 60% and 94%, respectively.

DISCUSSION

HVPG is the gold standard for diagnosis of liver cirrhosis-induced PH and is an independent risk factor for evaluating the prognosis of decompensated liver cirrhosis[5,19,20]. However, as an invasive measurement requiring a complex operation, wide clinical application of HVPG has been limited. It was reported that quantitative parameters (*e.g.*, LBF, LBV) from CT perfusion of the liver can be used to evaluate the blood supply changes in the liver and spleen with good sensitivity and specificity[13,21,22]. Therefore, our study investigated the correlation of CT perfusion for quantitative assessment of PH in HBV-related PH. Our results suggested that LBV and LBF were negatively correlated with HVPG and Child-Pugh scores, and CT perfusion imaging is a potential non-invasive quantitative predictor for PH in HBV-related liver cirrhosis.

In our study, LBV and LBF were negatively correlated with HVPG. This was explained by a significant decrease in hepatic flow[20-22] after hepatitis B infection when patients were suffering from cirrhosis-induced PH. A decrease in hepatic flow results from hepatocyte damage caused by HBV, deconstruction in normal liver structure, deposition of collagen fibers in the perisinusoidal space and formation of pseudo-lobules and fibroses, which together remarkably increases the resistance of the portal vein blood flow into the liver[1,4]. In this study, LBV and LBF were negatively related to HVPG. It is possible that the decrease of LBV and LBF is the consequence of the increase of HVPG, suggesting significantly reduced blood perfusion in the liver as PH increases. Therefore, CT perfusion is potentially

Table 2 Comparison of the moderate and severe portal hypertension groups

Index	Moderate PH	Severe PH	*P* value
Sex as female/male	2/8	2/16	0.520
Age, yr	54.2 ± 10.9	53.4 ± 10.5	0.848
Height, cm	168.0 ± 6.0	170.1 ± 5.6	0.362
Weight, kg	64.8 ± 12.3	61.8 ± 11.4	0.528
Child-Pugh score	7.1 ± 1.9	7.8 ± 1.8	0.023
HVPG	9.6 ± 1.3	18.9 ± 4.4	0.000
Perfusion CT			
LBF	114.6 ± 36.0	87.9 ± 24.8	0.029
LBV	19.7 ± 3.0	15.5 ± 2.2	0.000
HAF as $\times 10^{-2}$	8.2 ± 2.3	8.7 ± 4.7	0.731
SBF	96.0 ± 30.0	108.7 ± 31.4	0.308
SBV	13.9 ± 2.9	11.9 ± 2.5	0.084

Data are presented as *n* or mean ± SD. CT: Computed tomography; HAF: Hepatic arterial fraction; HVPG: Hepatic venous pressure gradient; LBF: Liver blood flow; LBV: Liver blood volume; PH: Portal hypertension; SBF: Splenic blood flow; SBV: Splenic blood volume.

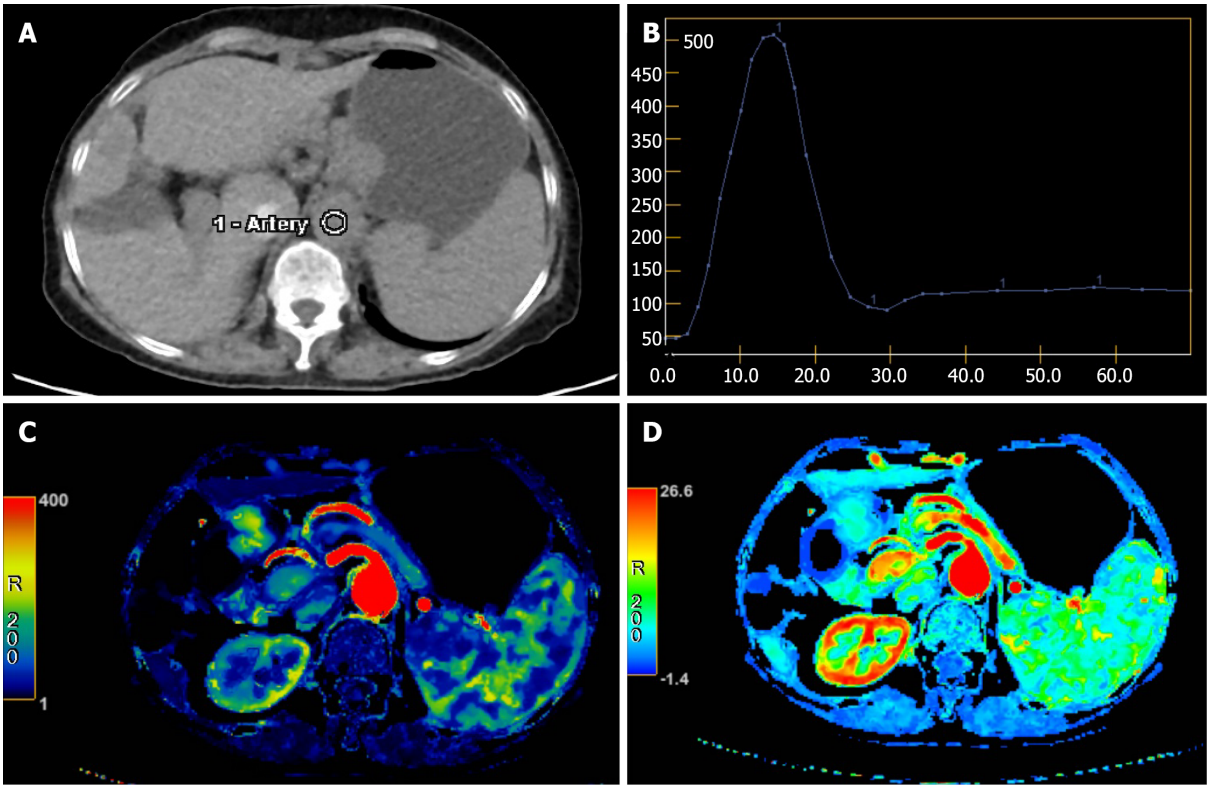

DOI: 10.3748/wjg.v28.i42.6068

Figure 2 Computed tomography perfusion of the spleen post-processing data. A: Regions of interest were placed in the abdominal aorta as the input blood vessel; B: The time-density curve was generated automatically for calculation of splenic perfusion; C and D: The parameters of computed tomography perfusion of the spleen were calculated automatically, including splenic blood flow (C) and splenic blood volume (D).

feasible for the non-invasive evaluation of HVPG using LBV and LBF in patients with HBV-related PH.

In this study, liver blood perfusion parameters (*e.g.*, LBV and LBF) in the moderate PH group were significantly higher than those in the severe PH group. For distinguishing moderate PH from severe PH, LBV had a ROC curve with a sensitivity and specificity of 80% and 89%, respectively. LBF had a sensitivity and specificity of 60% and 94%, respectively. Therefore, CT perfusion parameters (LBV and

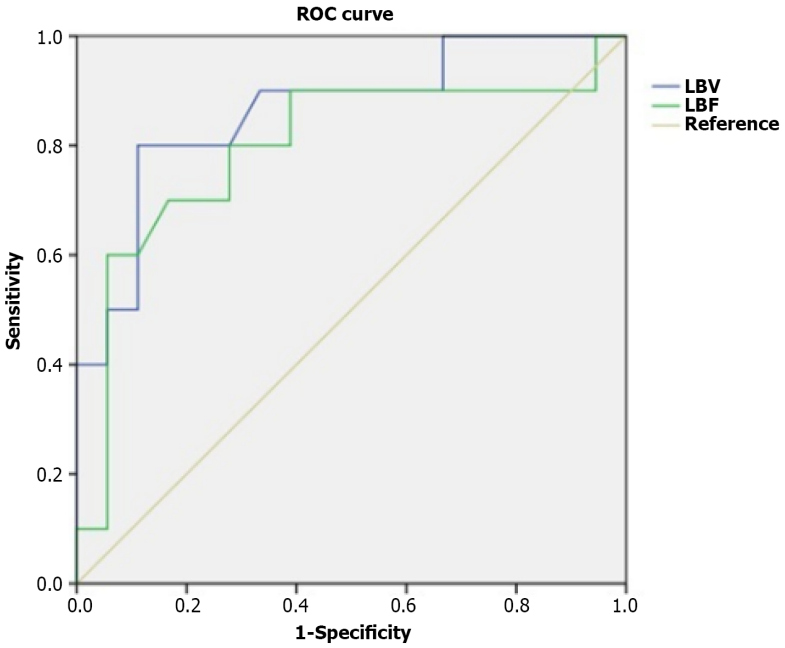

DOI: 10.3748/wjg.v28.i42.6068

Figure 3 Receiver operating characteristic curves to differentiate moderate and severe portal hypertension. For discriminating severe portal hypertension, liver blood volume had an area under the curve of 0.864 with a standard error of 0.075 [95% confidence interval (CI): 0.72-1.00], while liver blood flow had an area under the curve of 0.797 with a standard error of 0.100 (95%CI: 0.60-1.00). LBF: Liver blood flow; LBV: Liver blood volume; ROC: Receiver operating characteristic.

LBF) can be used to distinguish moderate PH and severe PH in PH-induced gastroesophageal variceal bleeding in patients with HBV-related PH.

LBV was negatively correlated with Child-Pugh score, suggesting that liver reserve function decreases with reduced LBV. Moreover, the Child-Pugh score in the moderate PH group was significantly lower than that in the severe PH group. Similarly, liver reserve function was better in the moderate PH group than the severe PH group. This was related to pathophysiological mechanisms underlying hepatitis B cirrhosis and PH. In addition, HVPG in the severe PH group was significantly higher than the moderate PH group. The intrahepatic portal venous system pressure in severe PH may increase, leading to progressively decreased blood flow and gradually weakening the reserve capacity of liver function. However, in this study, the Child-Pugh score was not associated with HVPG, which was consistent with previous studies[3,7,10,23]. The Child-Pugh score is mainly used to evaluate liver reserve function, which can only provide a crude evaluation of PH.

HAF was not related to HVPG, suggesting no correlation between the hepatic artery perfusion ratio and PH in liver cirrhosis. HAF mainly indicates the proportion of hepatic artery blood supply to the total liver blood supply in cirrhosis. When cirrhosis occurs due to damage in the liver sinusoid and liver lobule structure, the blood in the portal vein meets increasing resistance against its return to the liver. When portal vein pressure increases, the blood supply flowing to the liver is reduced. Likewise, compensatory hepatic artery blood perfusion can increase. However, the portal vein blood supply accounts for about three-quarters of the total liver blood supply[24]. The compensatory increase in hepatic artery blood supply could not compensate for a substantial decrease in blood flow in the liver caused by reduced portal vein blood supply. This buffering effect is not enough to maintain the hepatic blood supply[22-24]. In addition, HAF is affected by various factors, such as blood pressure, blood volume and cardiac function. This might explain why HAF was not correlated with HVPG.

The perfusion parameters of the spleen (*e.g.*, SBF, SBV) were not related to HVPG and Child-Pugh classification. This was consistent with a previous study. However, in that cohort, blood flow and blood volume of the liver were not associated with HVPG[13]. This may be related to different samples included in our study, where patients suffering from liver cirrhosis caused by hepatitis B were classified as relatively moderate cases. Among them, according to the Child-Pugh classification, 11 cases were defined as grade A, 16 cases as grade B, and 1 case as grade C. By contrast, patients included in the previous study were primarily suffering from alcoholic cirrhosis with Child-Pugh grade B and C. Furthermore, in the previous study, all patients were suffering from more severe diseases and were planning for liver transplantation as treatment. Moreover, our study excluded factors that may affect portal vein hemodynamics (such as splenic resection, portal vein thrombosis), which may explain the differences between the two studies.

Limitations existed in our study. First, our study only included cases of HBV-related PH, with a remarkable disproportion in patient sex. The majority of patients were Child-Pugh A and Child-Pugh B. A larger sample size is required to identify the clinical application of CT perfusion in patients with different causes of cirrhosis and higher Child-Pugh scores, including alcoholic cirrhosis, drug-induced metabolic liver disease and autoimmune liver disease. Second, our study primarily targeted patients who were suffering from gastric fundus esophageal variceal bleeding as a consequence of PH and excluded other factors like thrombosis, cavernous transformation and splenectomy that could affect liver hemodynamics. Nonetheless, further research is required to determine its application in PH with multiple complications. Finally, our study did not focus on pathology, laboratory and comparative imaging evaluation (such as volume and elasticity of the liver and spleen). Thus, further research is required.

CONCLUSION

Quantitative parameters of CT perfusion imaging, in particular LBV and LBF, were negatively correlated with HVPG and Child-Pugh scores. Therefore, CT perfusion imaging is a potential application for non-invasive quantitative evaluation of HVPG in patients with HBV-related PH.

ARTICLE HIGHLIGHTS

Research background

Hepatic venous pressure gradient (HVPG) is the gold standard for diagnosis of portal hypertension (PH), but the measurement of HVPG is an invasive procedure, which has limited its widespread use. Therefore, we aimed to investigate the feasibility of computed tomography (CT) perfusion as a non-invasive imaging tool for HVPG in PH.

Research motivation

To date, no satisfactory non-invasive method has been proposed as an alternative for HVPG. Determining the feasibility of CT perfusion indices as a non-invasive tool to assess HVPG would be beneficial to patients.

Research objectives

To investigate the correlation of CT perfusion of the liver with HVPG and Child-Pugh score in hepatitis B virus (HBV)-related PH.

Research methods

We prospectively selected 28 HBV-related PH patients in our hospital from January 2019 to June 2019. CT perfusion was performed in all patients, and quantitative parameters of CT perfusion were applied to evaluate HVPG non-invasively. Quantitative indices, including liver blood volume (LBV), liver blood flow (LBF), hepatic artery fraction, splenic blood volume and splenic blood flow, were calculated. The correlation analysis was calculated, and receiver operating characteristic curve analysis was performed.

Research results

Quantitative parameters of CT perfusion imaging, in particular LBV and LBF, were negatively correlated with HVPG and Child-Pugh scores.

Research conclusions

Our findings showed that CT perfusion parameters, LBV and LBF, were negatively correlated with HVPG and Child-Pugh scores. CT perfusion imaging showed potential as a non-invasive quantitative method for the evaluation of HVPG in HBV-related PH.

Research perspectives

Non-invasive assessment of HVPG has been an area of interest for decades, and multi-modality research should be explored in the future, including CT perfusion, anatomical information, lab results, liver and spleen stiffness and computation simulation modeling.

FOOTNOTES

Author contributions: Dong J, Liu FQ, and Wang L designed the report; Zhang Y, Wu YF, Yue ZD, Fan ZH, and

Zhang CY collected the clinical data; Wang L and Zhang Y analyzed and wrote the paper; Dong J and Liu FQ performed quality control; Liu FQ contributed to administrative and financial support; all authors have read and approved the final version of the manuscript.

Supported by the National Natural Science Foundation of China General Program, No. 81871461.

Institutional review board statement: This study was reviewed and approved by the Ethics Committee of the Beijing Shijitan Hospital, Capital Medical University (Approval No. 201801).

Clinical trial registration statement: This study is registered at ClinicalTrials.gov: http://www.chictr.org.cn/edit.aspx?pid=26048&htm=4. The registration identification number is ChiCTR1800015268.

Informed consent statement: Written informed consent was obtained from each patient.

Conflict-of-interest statement: There are no conflicts of interest to report.

Data sharing statement: No additional data are available.

Country/Territory of origin: China

ORCID number: Lei Wang 0000-0002-4374-059X; Jian Dong 0000-0002-2643-0370.

S-Editor: Chen YL
L-Editor: A
P-Editor: Chen YL

REFERENCES

1 **Bosch J**, García-Pagán JC. Prevention of variceal rebleeding. *Lancet* 2003; **361**: 952-954 [PMID: 12648985 DOI: 10.1016/S0140-6736(03)12778-X]
2 **García-Pagán JC**, Caca K, Bureau C, Laleman W, Appenrodt B, Luca A, Abraldes JG, Nevens F, Vinel JP, Mössner J, Bosch J; Early TIPS (Transjugular Intrahepatic Portosystemic Shunt) Cooperative Study Group. Early use of TIPS in patients with cirrhosis and variceal bleeding. *N Engl J Med* 2010; **362**: 2370-2379 [PMID: 20573925 DOI: 10.1056/NEJMoa0910102]
3 **Ripoll C**. Hepatic venous pressure gradient and outcomes in cirrhosis. *J ClinGastroenterol* 2007; **41** Suppl 3: S330-S335 [PMID: 17975485 DOI: 10.1097/MCG.0b013e318150d0f4]
4 **Tsochatzis EA**, Bosch J, Burroughs AK. Liver cirrhosis. *Lancet* 2014; **383**: 1749-1761 [PMID: 24480518 DOI: 10.1016/S0140-6736(14)60121-5]
5 **La Mura V**, Garcia-Guix M, Berzigotti A, Abraldes JG, García-Pagán JC, Villanueva C, Bosch J. A Prognostic Strategy Based on Stage of Cirrhosis and HVPG to Improve Risk Stratification After Variceal Bleeding. *Hepatology* 2020; **72**: 1353-1365 [PMID: 31960441 DOI: 10.1002/hep.31125]
6 **Villanueva C**, Graupera I, Aracil C, Alvarado E, Miñana J, Puente Á, Hernandez-Gea V, Ardevol A, Pavel O, Colomo A, Concepción M, Poca M, Torras X, Reñe JM, Guarner C. A randomized trial to assess whether portal pressure guided therapy to prevent variceal rebleeding improves survival in cirrhosis. *Hepatology* 2017; **65**: 1693-1707 [PMID: 28100019 DOI: 10.1002/hep.29056]
7 **D'Amico G**, Garcia-Pagan JC, Luca A, Bosch J. Hepatic vein pressure gradient reduction and prevention of variceal bleeding in cirrhosis: a systematic review. *Gastroenterology* 2006; **131**: 1611-1624 [PMID: 17101332 DOI: 10.1053/j.gastro.2006.09.013]
8 **Abraldes JG**, Villanueva C, Bañares R, Aracil C, Catalina MV, Garci A-Pagán JC, Bosch J; Spanish Cooperative Group for Portal Hypertension and Variceal Bleeding. Hepatic venous pressure gradient and prognosis in patients with acute variceal bleeding treated with pharmacologic and endoscopic therapy. *J Hepatol* 2008; **48**: 229-236 [PMID: 18093686 DOI: 10.1016/j.jhep.2007.10.008]
9 **Vorobioff J**, Groszmann RJ, Picabea E, Gamen M, Villavicencio R, Bordato J, Morel I, Audano M, Tanno H, Lerner E, Passamonti M. Prognostic value of hepatic venous pressure gradient measurements in alcoholic cirrhosis: a 10-year prospective study. *Gastroenterology* 1996; **111**: 701-709 [PMID: 8780575 DOI: 10.1053/gast.1996.v111.pm8780575]
10 **Ripoll C**, Groszmann R, Garcia-Tsao G, Grace N, Burroughs A, Planas R, Escorsell A, Garcia-Pagan JC, Makuch R, Patch D, Matloff DS, Bosch J; Portal Hypertension Collaborative Group. Hepatic venous pressure gradient predicts clinical decompensation in patients with compensated cirrhosis. *Gastroenterology* 2007; **133**: 481-488 [PMID: 17681169 DOI: 10.1053/j.gastro.2007.05.024]
11 **Takuma Y**, Nouso K, Morimoto Y, Tomokuni J, Sahara A, Takabatake H, Matsueda K, Yamamoto H. Portal Hypertension

in Patients with Liver Cirrhosis: Diagnostic Accuracy of Spleen Stiffness. *Radiology* 2016; **279**: 609-619 [PMID: 26588019 DOI: 10.1148/radiol.2015150690]

12 **Villanueva C**, Albillos A, Genescà J, Abraldes JG, Calleja JL, Aracil C, Bañares R, Morillas R, Poca M, Peñas B, Augustin S, Garcia-Pagan JC, Pavel O, Bosch J. Development of hyperdynamic circulation and response to β-blockers in compensated cirrhosis with portal hypertension. *Hepatology* 2016; **63**: 197-206 [PMID: 26422126 DOI: 10.1002/hep.28264]

13 **Talakić E**, Schaffellner S, Kniepeiss D, Mueller H, Stauber R, Quehenberger F, Schoellnast H. CT perfusion imaging of the liver and the spleen in patients with cirrhosis: Is there a correlation between perfusion and portal venous hypertension? *EurRadiol* 2017; **27**: 4173-4180 [PMID: 28321540 DOI: 10.1007/s00330-017-4788-x]

14 **Miles KA**, Hayball MP, Dixon AK. Functional images of hepatic perfusion obtained with dynamic CT. *Radiology* 1993; **188**: 405-411 [PMID: 8327686 DOI: 10.1148/radiology.188.2.8327686]

15 **Annet L**, Materne R, Danse E, Jamart J, Horsmans Y, Van Beers BE. Hepatic flow parameters measured with MR imaging and Doppler US: correlations with degree of cirrhosis and portal hypertension. *Radiology* 2003; **229**: 409-414 [PMID: 12970464 DOI: 10.1148/radiol.2292021128]

16 **Pandharipande PV**, Krinsky GA, Rusinek H, Lee VS. Perfusion imaging of the liver: current challenges and future goals. *Radiology* 2005; **234**: 661-673 [PMID: 15734925 DOI: 10.1148/radiol.2343031362]

17 **Weidekamm C**, Cejna M, Kramer L, Peck-Radosavljevic M, Bader TR. Effects of TIPS on liver perfusion measured by dynamic CT. *AJR Am J Roentgenol* 2005; **184**: 505-510 [PMID: 15671371 DOI: 10.2214/ajr.184.2.01840505]

18 **Groszmann RJ**, Wongcharatrawee S. The hepatic venous pressure gradient: anything worth doing should be done right. *Hepatology* 2004; **39**: 280-282 [PMID: 14767976 DOI: 10.1002/hep.20062]

19 **Ripoll C**, Groszmann RJ, Garcia-Tsao G, Bosch J, Grace N, Burroughs A, Planas R, Escorsell A, Garcia-Pagan JC, Makuch R, Patch D, Matloff DS; Portal Hypertension Collaborative Group. Hepatic venous pressure gradient predicts development of hepatocellular carcinoma independently of severity of cirrhosis. *J Hepatol* 2009; **50**: 923-928 [PMID: 19303163 DOI: 10.1016/j.jhep.2009.01.014]

20 **Van Beers BE**, Leconte I, Materne R, Smith AM, Jamart J, Horsmans Y. Hepatic perfusion parameters in chronic liver disease: dynamic CT measurements correlated with disease severity. *AJR Am J Roentgenol* 2001; **176**: 667-673 [PMID: 11222202 DOI: 10.2214/ajr.176.3.1760667]

21 **Preibsch H**, Spira D, Thaiss WM, Syha R, Nikolaou K, Ketelsen D, Lauer UM, Horger M. Impact of transjugular intrahepatic portosystemic shunt implantation on liver perfusion measured by volume perfusion CT. *ActaRadiol* 2017; **58**: 1167-1173 [PMID: 28084812 DOI: 10.1177/0284185116685922]

22 **Ripoll C**, Bañares R, Rincón D, Catalina MV, Lo Iacono O, Salcedo M, Clemente G, Núñez O, Matilla A, Molinero LM. Influence of hepatic venous pressure gradient on the prediction of survival of patients with cirrhosis in the MELD Era. *Hepatology* 2005; **42**: 793-801 [PMID: 16175621 DOI: 10.1002/hep.20871]

23 **Villanueva C**, Albillos A, Genescà J, Garcia-Pagan JC, Calleja JL, Aracil C, Bañares R, Morillas RM, Poca M, Peñas B, Augustin S, Abraldes JG, Alvarado E, Torres F, Bosch J. β blockers to prevent decompensation of cirrhosis in patients with clinically significant portal hypertension (PREDESCI): a randomised, double-blind, placebo-controlled, multicentre trial. *Lancet* 2019; **393**: 1597-1608 [PMID: 30910320 DOI: 10.1016/S0140-6736(18)31875-0]

24 **Bhardwaj A**, Kedarisetty CK, Vashishtha C, Bhadoria AS, Jindal A, Kumar G, Choudhary A, Shasthry SM, Maiwall R, Kumar M, Bhatia V, Sarin SK. Carvedilol delays the progression of small oesophageal varices in patients with cirrhosis: a randomised placebo-controlled trial. *Gut* 2017; **66**: 1838-1843 [PMID: 27298379 DOI: 10.1136/gutjnl-2016-311735]

Published by **Baishideng Publishing Group Inc**
7041 Koll Center Parkway, Suite 160, Pleasanton, CA 94566, USA
Telephone: +1-925-3991568
E-mail: bpgoffice@wjgnet.com
Help Desk: https://www.f6publishing.com/helpdesk
https://www.wjgnet.com